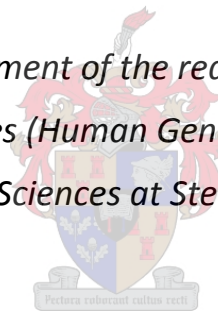# An investigation into the role of mitochondrial dysfunction in South African Parkinson's Disease patients

Celia van der Merwe

Thesis presented in partial fulfilment of the requirements for the degree Master of Science in Medical Sciences (Human Genetics (lab)) in the Faculty of Medicine and Health Sciences at Stellenbosch University

Supervisor: Assoc. Prof. Soraya Bardien

Division of Molecular Biology and Human Genetics

Department of Biomedical Sciences

Faculty of Health Science

December 2012

Declaration

I, the undersigned, hereby declare that the work contained in this thesis is my own original work and has not previously in its entirety or in part been submitted at any university for a degree

Signature……………………………………………………….. Date…………………………………………………..

Abstract

Parkinson's disease (PD) is a neurodegenerative movement disorder characterized by the loss of dopaminergic neurons in the substantia nigra of the midbrain. Although the aetiology of PD is still not fully understood, it is thought to involve a combination of environmental (such as exposure to pesticides and neurotoxins) and genetic factors. A number of PD-causing genes have been found including *SNCA*, *LRRK2*, *EIF4G1* and *VPS35* (for autosomal dominant forms of PD) and *parkin*, *PINK1*, *DJ-1* and *ATP13A2* (for autosomal recessive forms of PD – arPD). Mutations in the *parkin* gene are the predominant cause of arPD. Parkin plays a role in the ubiquitin-proteasomal system which degrades damaged and unwanted proteins in the cell and it is also thought to be involved in maintaining healthy mitochondria. Numerous studies have implicated mitochondrial function in the pathogenesis of PD. Therefore the aim of the present study was to investigate the role of mitochondrial dysfunction in PD patients with *parkin*-null mutations.

Four South African PD patients, each harbouring two *parkin*-null mutations, were recruited for this study. A muscle biopsy was performed for analysis of mitochondrial morphology using histology and transmission electron microscopy (TEM). Skin biopsies were taken, from which fibroblasts were cultured. These fibroblasts were used in i) mitochondrial morphological assessments using TEM, ii) mitochondrial network analysis, iii) functional studies via ROS measurement and iv) analysis of the proteome using a LTQ Orbitrap Velos mass spectrometer. In addition, RNA was isolated from peripheral blood samples for gene expression studies using the RT² Profiler PCR Array (SABiosciences, USA) and the RT² PCR Primer Assay (SABiosciences, USA). Heterozygous family members (carriers) and wild-type controls were also recruited for this study.

Results from the histological and TEM analysis from the muscle biopsy observed subtle mitochondrial changes including the presence of type II fibres, atrophic fibres, the presence of lipids, and wrinkling of the sarcolemmal membrane. Enlarged mitochondria were also observed in one patient. TEM analysis on the patient's fibroblasts observed an increase in the number of electron dense vacuoles, speculated to be autolysosomes. The mitochondrial network in two of the patients' fibroblasts showed fragmented and dot-like networks which are indicative of damaged mitochondria. An increase in mitochondrial ROS levels was observed in three of the four patients. Expression studies found down-regulation of 14 genes from four of the five mitochondrial complexes and a total of 688 proteins were found only in the control and not in the patient fibroblasts. Some of these proteins are known to be part of the 'mitochondrial dysfunction' pathway.

Taken together, these results indicate that the absence of parkin results in a number of mitochondrial alterations. Based on these findings, a model of PD was proposed: It is speculated that when parkin is absent, electron transport chain complex genes are down-regulated. This results in impaired oxidative phosphorylation, causing an increase in the production of mitochondrial ROS and subsequent oxidative stress. Mitochondria are then damaged; resulting in the fragmentation of the

mitochondrial network. The impaired mitochondria are thus tagged for degradation, causing the recruitment of autolysosomes which engulf the mitochondria via mitophagy. Ultimately, as the compensatory mechanisms fail, this triggers the consequential cascade of cellular apoptotic events.

This study has elucidated the effect of parkin on the mitochondria, and can act as a 'stepping stone' towards future development of therapeutic strategies and/or biochemical markers that will benefit not only patients with PD but also other neurodegenerative disorders.

Opsomming

Parkinson se siekte (PS) is 'n neurodegeneratiewe bewegings-afwyking gedefineer deur die verlies van dopaminergiese neurone in die substantia nigra van die midde brein. Alhoewel die spesifieke oorsprong van die afwyking nog nie ten volle begryp is nie, word bydraes van beide omgewings faktore (bv. blootstelling aan plaagdoders en neurotoksienes) asook genetiese faktore gespekuleer. Vanuit 'n genetiese aspek is 'n aantal gene al geassosieer met PS. Hierdie gene sluit in *SNCA, LRRK2, EIF4G1* en *VPS35* (vir outosomale dominante vorms van PS) en *parkin, PINK1, DJ-1,* en *ATP13A2* (vir outosomale resessiewe vorms van PS - orPS). Mutasies in die *parkin* geen is aangedui as die hoof oorsaak van orPS. Parkin speel 'n rol in die ubiquitine-proteasomale sisteem wat beskadige en ongewensde proteïne binne in die sel verwyder en is verdink om by te dra tot die instandhouding van gesonde mitokondria. Mitokondriese wanfunksionering is ook deur talle studies gewys as 'n bydraende faktor in die patologie van PS. Die doel van die studie is om ondersoek in te stel tot die spesifieke rol wat mitokondriese wanfunsionering speel in PS pasiënte met *parkin*-nul mutasies.

Vier Suid-Afrikaanse PS-pasiënte, elk met twee *parkin*-nul mutasies, is gebruik vir die studie. Deur middel van spierbiopsies is monsters verkry vir mitokondriese morfologiese analises met behulp van histologiese en elektron-oordrag mikroskopie tegnieke (TEM). Vel biopsies is ook geneem en fibroblaste is gekweek vir die gebruik in: i) mitokondriese morfologiese assesering; ii) mitokondriese netwerk analiese; iii) funksionele studies waar vlakke van reaktiewe suurstof spesies (ROS) gemeet is; iv) proteoom analiese met behup van 'n LTQ Orbitrap Velos massa spektrometer. RNA is ook geisoleer vanaf perifere bloedmonsters vir die gebruik in geen-uitdrukkings studies met behulp van 'n RT² Profiler PCR Array en 'n RT² Primer Assay. Selle vanaf famielie lede wat heterosigotiese draers is van die mutasie, asook normale (geen *parkin* mutasie) selle is gebruik as kontroles in die studie.

TEM resultate vanaf die spier monsters het subtiele mitokondriese veranderinge getoon. Hierdie sluit in die teenwoordigheid van tipe II vesels, atrofiese vesels, teenwoordigheid van lipiedes, assook waarnemings van rimpeling van die sarcolemmal membraan. Vergrote mitokondrias is ook in een van die pasiënte opgelet. TEM resultate vanaf die fibroblaste het toename in die aantal elektron-digte vakuole vertoon, moontlik geidentifiseer as autolisosome. Gefragmenteerde en onderbreekte mitokondria netwerke is gelet tydens netwerk analiese van die fibroblaste, 'n indikasie van beskadigde mitokondria. 'n Toename in mitokondriese ROS vlakke is gevind in drie van die vier pasiënte. Af-regulering van 14 gene, geassosieerd met vier uit die vyf mitokondria komplekse, is verneem tydens die geen-uitdrukkings studie. Saam met dit is 'n totaal van 688 proteïene geidentifiseer wat slegs teenwoordig is in die kontrole monsters en nie in die pasiënt monsters nie. Hierdie proteïene is almal uitgedruk en betrokke in die mitokondriese wanfunsionerings-weë.

Hierdie resultate dui dat die afwesigheid van parkin mitokondriese afwykings tot gevolg het wat kan lei tot die afsterwing van selle. Dit dra ook by tot die vorming van 'n beter-verstaande siekte-model

vir PS: Mutasies in *parkin* (wat lei tot die afwesigheid van parkin) kan dus moontlik lei tot die af-regulasie van gene geassosieerd met die elektron-vervoer ketting komplekse in die mitokondria. Dit lei tot gebrekkige oksidatiewe fosforilering en veroorsaak 'n toename in die vorming van ROS, wat dan 'n toename in oksidatiewe stres binne in die sel tot gevolg het. Uiteindelik lei dit dus tot die beskadiging van die mitokondria wat gepaard gaan met fragmentering van die mitokondriese netwerk. Beskadigde mitokondrias word geetiketeer vir afbraking. Hierdie etiketering aktiveer omringende autophagosome wat die beskadigde mitokondrias dan verwyder deur middel van 'n verswelgende proses genaamd mitophagy. Dit veroorsaak die aktivering van 'n aantal gekorreleerde sellulêre prosesse wat lei tot apoptose (afsterwing van die sel).

Hierdie studie dra by tot die verklaring van die spesifieke effek wat *parkin* mutasies het op die funksionering van die mitokondria. Resultate hier lê ook die grondslag vir toekomstige studies met die doel tot die ontwikkeling van terapeutiese strategeë en biochemiese merkers wat kan bydrae tot die genesing van beide pasiënte met PS, asook pasiënte met ander neurodegeneratiewe afwykings.

Acknowledgements

I would like to express my sincere gratitude to the following people and organisations:

I thank God for providing me with faith, strength and guidance.

To Assoc. Prof Soraya Bardien, I am so appreciative of the encouragement, motivation, positivity and hours of hard work you have put into this project. Thank you for all your help, effort and perseverance. A second thanks to Dr. Craig Kinnear, Dr. Ben Loos and Dr. Jonathan Carr for all the wise words and encouragement.

Thank you to everyone in the MAGIC lab for all your support and practical help.

Thank you to my family and friends that that have provided me with continued encouragement. Mom - thanks for your words of wisdom and prayers; Dad - thank you for always believing in me and motivating and supporting me; Ez - thanks for all the chats, laughs and being my best friend; Miko – I love you; thank you for our life together. I am so grateful to have such wonderful people like you in my life.

Stellenbosch University and the Department of Biomedical Sciences for the use of their facilities.

The National Research Foundation, Medical Research Council and the Harry Crossley Foundation for financial support and project funding.

Table of contents

List of abbreviations

AAD: L- Amino acid decarboxylase

AAO: Age at onset

Ab: Antibody

Acetyl CoA: Acetyl coenzyme A

AD: Autosomal dominant

ADP: Adenosine diphosphate

APS: Ammonium Peroxide Disulphate

ATP: Adenosine–5 '–triphosphate

ATP13A2: ATPase type 13A2 gene

ATP13A2: ATPase type 13A2 protein

AR: Autosomal recessive

bp: base pairs

BSA: Bovine serum albumin

CCCP: Carbonyl cyanide m-chlorophenylhydrazone

Ct: threshold cycle

DAD: Diabetes Mellitus and deafness

DBS: Deep brain stimulation

DCF: 6-carboxy-2'7'-dichlorodihydrofluoresce in diacetate, diacetoxymethyl ester

ddH_2O: double distilled water

del: deletion

dH_2O: distilled water

DJ-1: Oncogene DJ-1 gene

DJ-1: Oncogene DJ-1 protein

Drp-1: Dynamin-related protein 1 gene

Drp-1: Dynamin-related protein 1 protein

EIF4G1: Eukaryotic translation initiation factor 4 – gamma gene

EIF4G1: Eukaryotic translation initiation factor 4 – gamma protein

EOPD: Early onset Parkinson's Disease

ER: Endoplasmic reticulum

EtBr: Ethidium Bromide

ex: exon

$FADH_2$: reduced flavin adenine dinucleotide

FFT: Fast Fourier Transformation

GAPDH: glyceraldehyde–3–phosphate dehydrogenase

gDNA: genomic DNA

gel doc: gel documentation

het: heterozygous

HKG: Housekeeping genes

homo: homozygous

H_2O_2: Hydrogen Peroxide

IBR: In-between Ring

IMS: Intermembrane space

KRS: Kufor-Rakeb syndrome

LB: Lewy body

LHON: Lebers hereditary optic neuropathy

LOPD: Late onset Parkinson's Disease

LRRK2: Leucine-rich repeat kinase 2 gene

LRRK2: Leucine-rich repeat kinase 2 protein

MAD: Malondialdehyde

MALDI/TOF: Matrix assisted laser desorption/ionisation time of flight

MAO-B: Type B monoamine oxidase

MERRF: Myoclonic Epilepsy with ragged red fibres

Mfn: Mitofusin gene

Mfn: Mitofusin protein

MLPA: Multiplex ligation-dependent probe amplification

MnSOD: Manganese Superoxide Dismutase

mRNA: messenger RNA

MPP$^+$: 1–methyl-4–phenylpyridinium

MS: Mass spectrometry

mtDNA: mitochondria DNA

MPTP: 1-methyl–4–phenyl-1,2,3,6–tetrahydropyridine

MTS: Mitochondrial-targeting domain

N: Asparagine

NADH: reduced nicotinamide adenine dinucleotide

ND3: NADH dehydrogenase 3

NHLS: National Health Laboratory Service

NRF: Nuclear respiratory factor

P1: Patient 1

P2: Patient 2

P3.1: Patient 3.1

P3.2: Patient 3.2

P2het: Heterozygous 2

P3het: Heterozygous 3

PAGE: Polyacrylamide gel electrophoresis

PBS: Phosphate Buffer saline

PCR: Polymerase Chain Reaction

PD: Parkinson's disease

PINK1: PTEN – induced kinase gene

PINK1: PTEN – induced kinase protein

PGC-1α: Peroxisome proliferator-activated receptor-γ coactivator

Pi: inorganic phosphate

PPC: Positive PCR control

PVDF: Polyvinylidene fluoride

qRT-PCR: quantitative Real Time PCR

RBR: Ring Between Ring fingers

REF: reference

RER: Rough Endoplasmic Reticulum

REST: relative expression software tool

RIN: RNA Integrity Number

RNAi: RNA interference

ROS: reactive oxygen species

RQI: RNA Quality Indicator

RRF: Ragged red fibres

RTC: Reverse Transcription Control

S: Serine

SAP: Shrimp Alkaline Phosphatase

SB: Sodium Borate

SDS: Sodium dodecyl sulfate

siRNA: small interfering RNA

SNCA: α- synuclein gene

SNc: Substantia nigra pars compacta

SNP: single nucleotide polymorphism

Ta: annealing temperature

TEM: Transmission Electron Microscopy

TEMED: Tetramethylethylenediamine

TM: Transmembrane domain

Tm: melting temperature

TRG: target

tRNA: transfer RNA

Ubl: Ubiquitin-like domain

UPS: Ubiquitin-proteasome system

VPS35: Vacuolar protein sorting 35 gene

VPS35: Vacuolar protein sorting 35 protein

WBC: White blood cell

WTC1: Wild-type control 1

WTC2: Wild-type control 2

List of figures

PAGE

Chapter 1

Chapter 4

List of tables

Chapter 4

Chapter 1

INTRODUCTION

Parkinson's disease (PD) is a progressive, neurodegenerative disease caused by a loss of dopaminergic neurons in the brain. It is the second most common neurodegenerative disorder after Alzheimer's disease. In 1817, a physician in London, Dr. James Parkinson (Figure 1.1) first described the disease in the published essay "An Essay on the Shaking Palsy" and this was the first modern description of the disorder (Parkinson, 1817). Dr. Parkinson described six cases in his essay, and he noted the clinical motor symptoms including resting tremor, abnormal posture and gait, and diminished muscle strength. For one of these patients he documented the following:

Case II: "The subject of the case which was next noticed was casually met with in the street. It was a man sixty-two years of age; the greater part of whose life had been spent as an attendant at a magistrate's office. He had suffered from the disease about eight or ten years. All the extremities were considerably agitated, the speech was very much interrupted, and the body much bowed and shaken. He walked almost entirely on the fore part of his feet, and would have fallen every step if he had not been supported by his stick. He described the disease as having come on very gradually, and as being, according to his full assurance, the consequence of considerable irregularities in his mode of living, and particularly of indulgence in spirituous liquors. He was the inmate of a poor-house of a distant parish, and being fully assured of the incurable nature of his complaint, declined making any attempts for relief."

Figure 1.1: **Photograph of Dr. James Parkinson (1755 – 1825).** Taken from:
http://www.allaboutparkinsons.com/james-parkinson.html

Half a century later, Dr. Jean-Martin Charcot named the disorder in honour of Dr. Parkinson. Today, PD is characterised as the degeneration or loss of neuromelanin-containing dopaminergic neurons in the substantia nigra pars compacta (SNc), a portion of the midbrain (Figure 1.2). There are four cardinal motor symptoms which are observed in the majority of PD patients, namely *resting tremor* (trembling usually of the hands and feet that occurs only when not in motion), *bradykinesia* (slowness of movement), *rigidity* (stiffness of the muscles) and *postural instability* (loss of balance and difficulty with walking), but there are also many other non-motor symptoms including loss of smell, depression, constipation, sleep disturbances and psychosis. There are currently no proven neuroprotective or neurorestorative therapies for PD, and progression of the disease is irreversible (Dawson & Dawson, 2002)
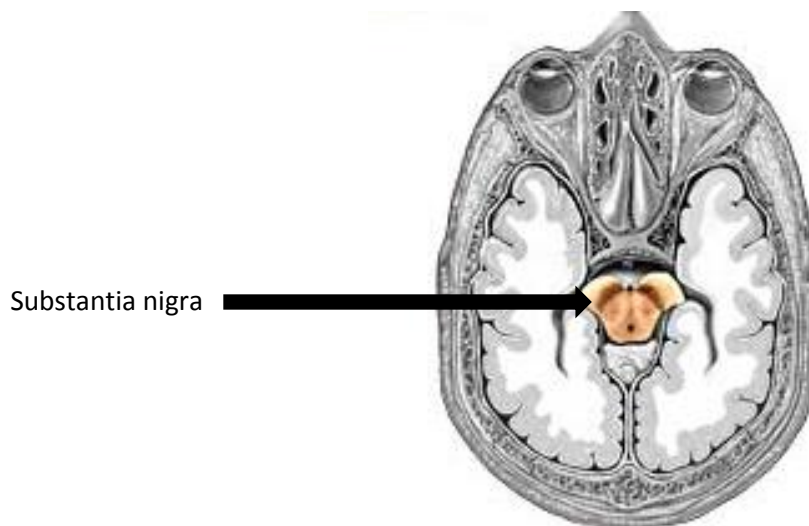
Substantia nigra

Figure 1.2: Cross-sectional cut of the mid-section of the brain showing the location of the substantia nigra pars compacta (SNc), the site of dopaminergic neurons. The SNc is the black pigmented area, indicated by the arrow (Taken from: http://health.allrefer.com/health/parkinsons-disease-substantia-nigra-and-parkinsons-disease.html).

1.1. Prevalence of Parkinson's disease (PD)

It has been observed that PD affects approximately 1-2% of the global population over the age of 65 years, and 4% over the age of 80 years (de Lau & Breteler, 2006). In a study on Western Europe's five

most and the world's ten most populous countries (including Germany, France, Nigeria and Japan) the number of PD-affected individuals was estimated to be between 4.1 and 4.6 million in 2005, and this number is expected to double by 2030 (Dorsey et al., 2007).

The most recent study recording incidence rates of PD across age, gender and ethnicity (Van Den Eeden et al., 2003) showed an overall annual incidence rate of 12.3 per 100 000, whereas individuals with an age of over 50 years had an incidence of 44.0 per 100 000, showing that the incidence of PD increases with age. Noticeably different incidence rates were observed between different ethnic groups – Hispanics had the highest age- and gender-matched incidence rate of 16.6 per 100 000, non-Hispanic Whites at 13.6 per 100 000, Asians at 11.3 per 100 000, and Blacks at 0.2 per 100 000. The reason for this difference could be due to either genetic or environmental diversity; however it may also be due to a lack of facilities and services (in underdeveloped countries) needed to diagnose the disease. Gender-specific incidence rates showed 19.0 per 100 000 in males, and 9.9 per 100 000 in females, with a male: female ratio of 1.9 (Van Den Eeden et al., 2003). Although similar ratios have been seen in other studies (Twelves et al., 2003), this is not a consistent finding and further studies are needed.

1.2. Clinical characteristics

1.2.1. Age at onset

The age at onset (AAO) in PD patients ranges from 20 years of age to over 70 years, and is categorised into three sub-groups, namely juvenile onset PD, early onset PD (EOPD) and late onset PD (LOPD). Juvenile onset PD (AAO <20 yrs.) is uncommon, and is caused by rare mutations in the genes that cause PD (Section 1.3.2). EOPD (≤40-50 yrs.) is also relatively rare with predominantly genetic causative factors. Patients with an AAO over the age of 50 fall into the LOPD category, and this is thought to be caused by a combination of genetic and environmental factors. PD is an age-related disorder, and it has been found that an increase in age is one of the strongest risk factors.

1.2.2. Neuropathology of PD

PD is characterized pathologically by the loss of 70 – 80% of the dopaminergic neurons which results in depigmentation of the SNc (Figure 1.3 A) as dopaminergic neurons also produce melanin that is responsible for the pigmentation of the SNc. This neuronal loss causes a substantial decrease in dopamine production, thus leading to the movement problems seen in PD patients. A second pathological characteristic of PD is the presence of Lewy bodies (LB) in the SNc and several other regions of the brain (Figure 1.3 B). LBs are cytoplasmic protein inclusions composed predominantly of alpha-synuclein, neurofilament proteins and ubiquitin (Figure 1.4; Spillantini et al., 1997; Wooten, 1997). It is hypothesized that the formation of LBs occurs prior to PD diagnosis in the dorsal motor nucleus, and progressively moves through the brainstem into the SNc and towards the cerebral cortex (Braak et al., 2003). Patients with EOPD caused by mutations in the *parkin* gene generally have an absence of LBs in post mortem analyses, suggesting that parkin may play a role in the formation and ubiquitylation of these inclusions.
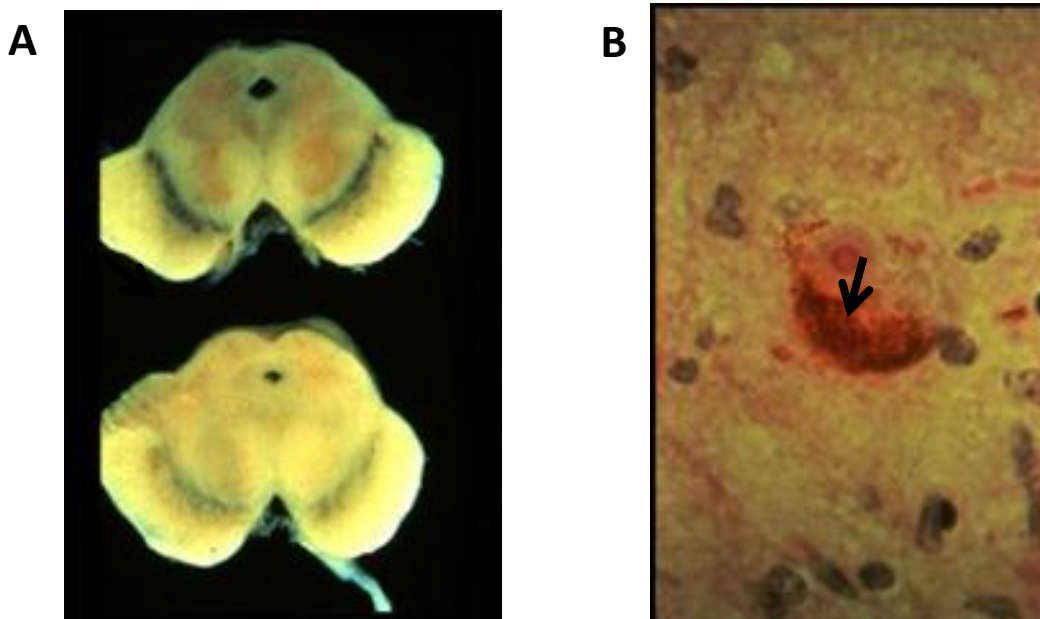
Figure 1.3: **The pathology of the substantia nigra pars compacta (SNc).** A. Unaffected (top) and PD-affected (bottom) SNc showing de-pigmentation of the neurons as a result of a loss of melanin-containing cells. B. The presence of a Lewy body (arrow) in the SNc. Taken from: Stacy et al., 2009
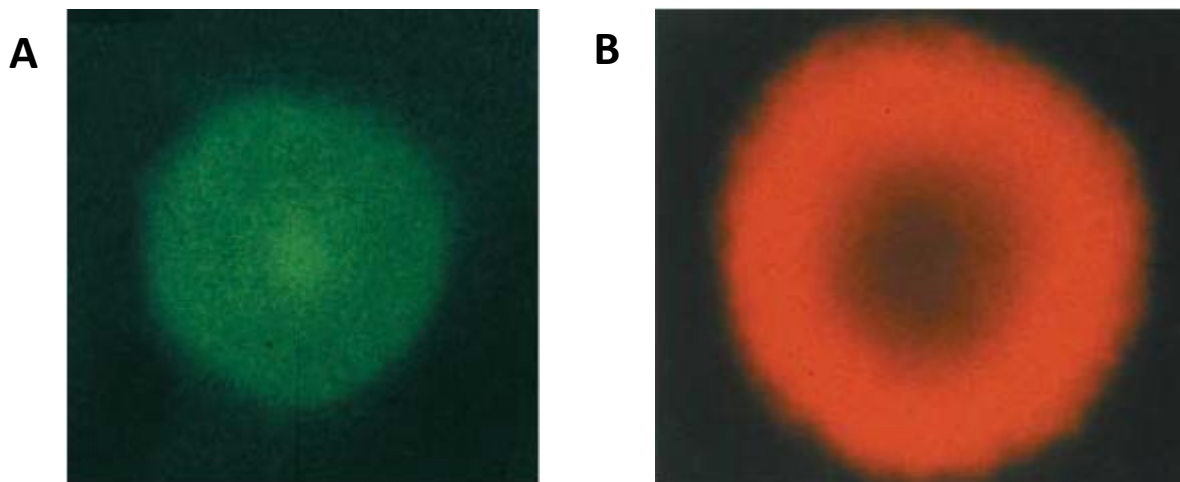
Figure 1.4: **Immunohistochemical analysis of sections from the substantia nigra pars compacta (SNc) of a patient with sporadic PD.** A. Lewy body stained with an antibody against ubiquitin (green dye). B. Lewy body stained with an antibody against α- synuclein (red dye). Taken from: Guttmacher et al., 2003

1.2.3. Symptoms of PD

Traditionally, it was believed that PD was only a motor system disorder, with little or no symptoms affecting other bodily functions. However, clinical data now show a far more complex and systemic condition with not only motor symptoms, but also neuropsychiatric and other non-motor symptoms playing a role in the early diagnosis of PD.

1.2.3.1.   *Motor symptoms*

As previously mentioned, there are four cardinal motor symptoms found in the majority of PD patients, namely resting tremor, bradykinesia, rigidity and postural instability, and these are depicted in Figure 1.5.
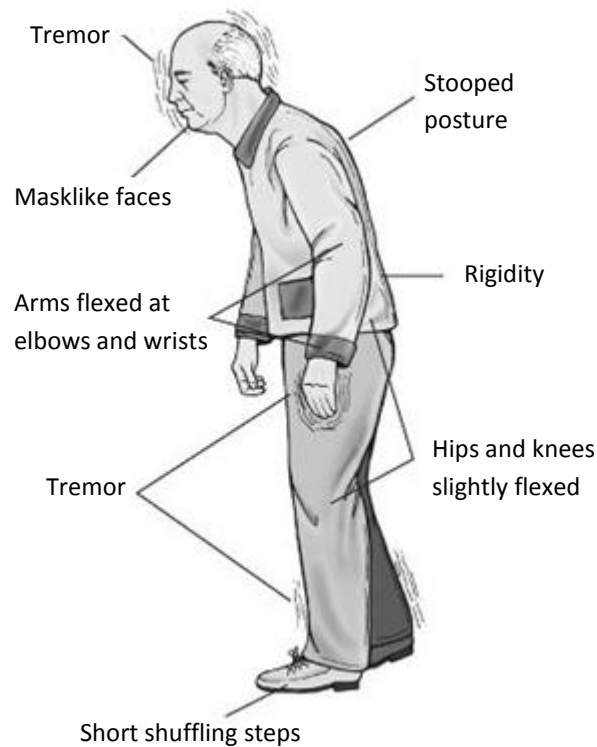
Figure 1.5: Illustration indicating the motor symptoms of Parkinson's disease. Taken from: http://schoolworkhelper.net/2011/02/parkinson.

A resting tremor is usually the first sign of the onset of PD. It can appear in the hands, feet, face or jaw and the exact cause is not known. It has been speculated that a loss of dopamine disrupts the operations of the thalamus, leading to a lack of control of movement.

Bradykinesia is defined as the slowing of movement. It is thought to result from 'a failure of basal ganglia output to reinforce the cortical mechanisms that prepare and execute the commands to move' (Berardelli et al., 2001).Other factors such as muscle weakness, rigidity, tremor, movement variability and slowing of thought can all contribute to the development of bradykinesia.

Rigidity is described as an increased resistance to passive movement about a joint. Patients suffering from PD often complain of stiffness and pain, which is the result of rigidity of the joints.

Postural instability is a symptom that causes a lack of balance or stability. It leads to a higher risk of falling in PD patients, due to a loss of 'righting reflexes' or the occurrence of freezing (Gelb et al., 1999)

1.2.3.2.   Non-motor symptoms

Several non-motor symptoms, such as loss of smell, constipation and depression, can occur up to ten years before the onset of motor symptoms. These symptoms remain under-recognized as an indication of PD, and as a result, are under-treated. Other non-motor symptoms include sleep disorders, apathy and cognitive impairment, hallucinations, dementia and psychosis (Chaudhuri et al., 2006). It has been suggested that these non-motor symptoms may be markers of a pre-clinical stage of PD. Some patients list non-motor symptoms as even more disabling than the motor symptoms (Gulati et al., 2004). A study by Whetten-Goldstein *et al* interviewed over one hundred people suffering from PD to determine the burden of the disease (Whetten-Goldstein et al., 1997). A substantial number of these patients listed non-motor symptoms such as depression and fatigue as some of the greater burdens of PD, particularly in the earlier stages of the disease. Studies such as these suggest that more effort should be made in recognizing these symptoms prior to the onset of motor symptoms, and treating them in a unified and integrated manner.

1.2.4. Treatment strategies

Currently, there are several drug treatment options available to treat for PD. Levodopa (precursor to dopamine) and dopamine agonists can both manipulate the dopaminergic system, however, these strategies only alleviate the symptoms and each drug has a wide-range of side effects that need to be carefully monitored and controlled.

Levodopa is a large aromatic amino acid which acts as a precursor to dopamine (Figure 1.6). It is absorbed from the small bowel, via amino acid transporters into the blood. It is able to cross the blood-brain barrier, where it is converted into dopamine via a chemical reaction involving the enzyme aromatic L-amino acid decarboxylase (AAD), thus increasing the concentrations of dopamine

in the central nervous system. Levodopa has a particularly short half-life (about 90 minutes); therefore sustained antiparkinsonian response is dependent on continuous delivery of Levodopa (Nutt 2010). Side effects include involuntary movements and mental status changes such as anxiety, panic and depression, specifically towards the end of a dose cycle.
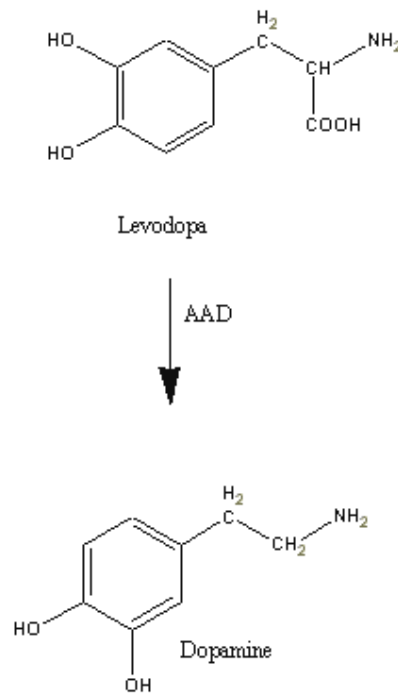
Figure 1.6: **The conversion of Levodopa into dopamine via the enzyme aromatic L-amino acid decarboxylase.** Taken from: www.ualberta.ca.htm

Two of the dopamine agonists, pramipexole and ropinirole, are agonists at the dopamine D-2 receptor family. These agents show antiparkinsonian effects, however not as effectively as Levodopa (Rascol et al., 2000), due to a limitation imposed by stimulation of only the dopamine D-2 receptor family (Nutt 2010). Side effects of dopamine agonists also include motor complications and depression, however these are to a far lesser extent than the side effects experienced by Levodopa. Other side effects include hallucinations and impulse control disorders.

Another treatment option for PD is deep brain stimulation therapy (DBS). DBS is a surgical procedure, whereby electrodes are implanted into a precise location in the brain (either the subthalamic nucleus or the globus pallidus, depending on each individual patient) within specific brain circuits, or neuronal loops, for modulation of the activity of those circuits. The electrodes are connected to an implanted pulse generator that is responsible for delivery of continuous stimulation, and the current produced then acts as either a suppressor or a driver of neuronal activity (Lozano, 2012). Risks of DBS include the small chance of a haemorrhage or stroke, depression, paraesthesias, dysarthria, motor contractions and infection. However, this treatment option is continually expanding and improving, and studies show that the clinical benefits of DBS outweigh the risks involved (Deuschl et al., 2006; Follett et al., 2010)

A major drawback of all current therapies for PD is that they only treat the symptoms and do not cure the disorder. Therefore, more intensive research is required into the underlying cause of PD for the ultimate development of a cure or neuroprotective therapy.

1.3.   Causes of PD

PD was traditionally considered to be a sporadic disease, caused by environmental factors, such as lifestyle and aging. However, the past fifteen years have been successful in proving the role of genetic factors in the cause of this condition. A positive family history is associated with a higher risk of PD and the aetiology of this disorder, although not fully understood, is considered to involve an interaction between genetic and environmental factors (Sherer et al. 2002).

1.3.1. Environmental causes

Several environmental factors have been found to influence the occurrence of PD. Current interest is focused on pesticide and neurotoxin exposure, such as rotenone, paraquat and MPTP (1-methyl-4-phenyl-1,2,3,6-tetrahydropyridine). It is thought that farming as an occupation also holds a significant risk for PD, possibly due to the greater risk of pesticide exposure (Gorell et al., 1998). A

meta-analysis examining 16 case-control studies found a positive association with rural living and the risk of PD in 11 of the studies, with the average duration of exposure being 40 years or longer (Priyadarshi et al., 2001). This could be due to a higher concentration of neurotoxins that are present in pesticides, well-water or spring water in these areas. The same study analysed the effect of well-water drinking on the onset of PD, where 11 out of the 19 studies found a positive association, although this was not significant. Reasons for the onset of PD from well-water drinking could be due to chemical or bacterial contaminations of the water from the soil and surrounding areas (Butterfield et al., 1993). Other possible environmental causes include head trauma, heavy metal exposure (manganese), as well as exposure to organic solvents, carbon monoxide and carbon disulphide; however studies have shown conflicting results (Seidler et al., 1996; Taylor et al., 1999).

Apart from the environmental risk factors for an increased risk of developing PD, there are also several factors that have been associated with a decreased risk, such as coffee drinking and cigarette smoking. A meta-analysis performed on 48 studies that have analysed the effect of these factors on the onset of PD found a 60% lower risk of PD among cigarette smokers compared to those that had never smoked, and a 30% lower risk of PD for coffee drinkers compared to non-coffee drinkers (Hernán et al., 2002). They also discovered that PD risk continues to decrease as exposure to smoking and increased coffee intake increases.

It is thought that components of cigarette smoke may decrease the activity of type B monoamine oxidase (MAO-B) in the brain. MAO-B is responsible for the breakdown of dopamine in the brain (Checkoway et al., 2002), so by decreasing the activity of MAO-B, the eventual risk of PD is decreased. Similarly, caffeine intake is thought to have neuroprotective properties, and has been shown to decrease the dopamine cell destruction in mice exposed to MPTP (Hernán et al., 2002).

1.3.1.1.   Rotenone

Rotenone is a garden pesticide with a high-affinity to inhibit mitochondrial complex I. Complex I is one of the five enzyme complexes in the electron transport chain of the mitochondria, responsible for oxidative phosphorylation (Refer to Section 1.4.2). Impaired complex I activity leads to an increase in oxidative stress, which is defined as an imbalance between production of free radicals (e.g. reactive oxygen species; ROS) and the antioxidant capacity of the cell. The increase in ROS and

the decrease in ATP (Adenosine-5'-triphosphate) production caused by the complex I dysfunction will ultimately lead to cell death via apoptosis. Exposure to rotenone in rat models showed a defect in complex I that led to behavioural, anatomical, neurochemical and neuropathological features of PD (Betarbet et al., 2000).

1.3.1.2. MPTP

MPTP is a neurotoxin capable of crossing the blood-brain barrier, resulting in its conversion to MPP$^+$ (1-methyl-4-phenylpyridinium). MPP$^+$ then enters the mitochondria of the dopamine-producing neurons and prevents the binding of complex I to electron transport particles such as electrons and hydrogen ions, thus impairing mitochondrial respiration (Tipton & Singer, 1993; Przedborski et al., 2004). This leads to cell death due to a decrease in ATP production and an increase in the production of ROS.

In America in the early 1980's, a number of heroin users presented at emergency rooms with symptoms indistinguishable to that of PD (Burns et al., 1985). It was discovered that the heroin used was from a synthetic batch that was contaminated with MPTP, causing the addicts to become mute and rigid and present with symptoms similar to PD, as the MPTP acted on the nerve cells in the substantia nigra. These patients were described by Dr. JW Langston in his paper "The Case of the Tainted Heroin" (Langston, 1985).

Primates treated with MPTP showed motor disturbances such as bradykinesia, rigidity and postural instability, almost indistinguishable to the motor symptoms seen in patients with PD (Jenner, 2003). Biochemically, these primate models have decreased release of dopamine and serotonin, as well as nerve cell loss in the SNc (Burns et al., 1985; Russ, et al., 1991). These animal models have provided critical insight into the understanding of the possible pathophysiology of PD.

1.3.1.3. Paraquat

Due to the similarity in structure of paraquat (1,1'-dimethyl-4,4'-bipyridinium) and MPP$^+$ (McCormack et al., 2002), it is hypothesized that paraquat plays a similar role in the cell. However,

animal models have produced contradicting results (Uversky, 2004; Ossowska et al., 2005), thus it is still questionable as to whether this pesticide has a significant effect on causing PD.

1.3.2. Genetic causes

Thus far, at least 17 loci and 11 genes have been linked to inherited forms of PD. Of these, eight genes (*SNCA, LRRK2, parkin, PINK1, DJ1, ATP13A2, EIF4G1* and *VPS35*) have shown conclusive evidence to cause the condition (Lesage & Brice, 2009; Vilariño-Güell et al., 2011; Chartier-Harlin et al., 2011). These genes can be divided into either autosomal dominant (AD) or autosomal recessive (AR) inheritance forms of PD. Approximately 5-10% of PD patients are thought to have a genetic cause of the disorder. Table 1.1 shows a summary of the genes involved in PD.

1.3.2.1. *Genes involved in autosomal dominant forms of PD*

To date, the dominant forms of PD arise from mutations in the *α-synuclein (SNCA)*, and *leucine-rich repeat kinase 2 (LRRK2)* genes, and in the last year two additional genes have been found - *eukaryotic translation initiation factor 4-gamma (EIF4G1)* and *vacuolar protein sorting 35 (VPS35).*

<u>*SNCA*</u>

SNCA was the first gene to be identified as a cause for AD PD (Polymeropoulos et al., 1997). The gene comprises six exons and encodes a 140 amino acid protein. Human α-synuclein protein is made up of an amphipathic region, a NAC domain (highly amyloidogenic) and an acidic tail (Appendix I). Seven imperfect repeats (KTKEGV) are found in the amino end of the protein. The α-synuclein protein is expressed abundantly throughout the brain, and is the major component of Lewy bodies, however little is known about its biological function. Mutations in *SNCA* range from missense mutations (PARK1-linked PD) to whole-gene multiplications (duplications and triplications; PARK4-linked PD), and are extremely rare forms of familial PD. Three missense mutations have been reported, namely A53T, A30P and E46K (Polymeropoulos et al., 1996; Zarranz et al., 2004).

<u>Table 1.1:</u> Summary of Parkinson's disease genes and loci

PARK Loci	Gene	Map position	Inheritance	Disease onset	AAO (yrs.)	Mutations
PD-associated loci and genes with conclusive evidence						
PARK1/PARK4	*SNCA*	4q21	AD	EOPD	20-85	A30P, E46K, A53T, genomic duplications/triplications
PARK2	*Parkin*	6q25 – q27	AR	Juvenile, EOPD	16-72	Point mutations, exonic rearrangements
PARK6	*PINK1*	1p35-p36	AR	EOPD	20-40	Point mutations, rare large deletions
PARK7	*DJ-1*	1p36	AR	EOPD	20-40	Point mutations, large deletions
PARK8	*LRRK2*	12q12	AD	LOPD	32-79	80 missense variants, 7 of them pathogenic, including the common G2019S
PARK9	*ATP13A2*	1p36	AR	EOPD, Juvenile Kufor-Rakeb syndrome (KRS)	11-16	Point mutations
PARK18	*EIF4G1*	3q26-q28	AD	LOPD	57-80	R1025H, A502V, 8 coding variants, 4 missense mutations
Not assigned	*VPS35*	16p12.1-q12.1	AD	LOPD	37-72	D620N, P316S
PD-associated loci and genes with unknown relevance						
PARK3	unknown	2p13	AD	LOPD	60-69	Not identified
PARK5	*UCHL1*	4p14	AD	LOPD	55-58	One mutation in a single PD sibling pair
PARK10	unknown	1p32	unclear	LOPD	50-60	Not identified
PARK11	*GIGYF2*	2q36-q37	AD	LOPD	33-68	Seven missense variants
PARK12	unknown	Xq21-q25	unclear	unclear	-	Not identifies
PARK13	*Omi/HTRA2*	2p13	unclear	LOPD	49-77	Two missense variants
PARK14	*PLA2G6*	22q12-q13	AR	Juvenile levodopa-responsive dystonia-parkinsonism	18-26	Two missense variants
PARK15	*FBXO7*	22q12-q13	AR	Early-onset parkinsonism-pyramidal syndrome	10-19	Three point mutations
PARK16	unknown	1q32	unclear	unclear	-	Not identified
Not assigned	*SNCAIP*	5q23	Unclear	LOPD	63-69	R621C, various SNPs with association
Not assigned	*MAPT*	17q21	AD	FTDP, O, CBS	25-76	Haplotype H1, various SNPs with association
Not assigned	*SCA2*	12q24.1	AD	EOPD	45-59	Low-range interrupted CAG expression in SCA2
Not assigned	*GBA*	1q21	AR	EOPD	40-50	Point mutations

CBS: corticobasal syndrome, FBXo7: F-box only protein 7; FTDP: frontotemporal dementia with parkinsonism; GBA: β glucocerebrosidase; GIGYF2: GRB10 interacting GYF protein 2; MAPT: microtubule associated protein tau; O: ocular signs; HTRA2: HtrA serine peptidase 2; SCA2: spinocerebellar ataxia type 2; UCHL1: ubiquitin carboxyl-terminal esterase L1. Adapted from: Lesage & Brice, 2009

Duplications and triplications of the PARK4 locus are more common than missense mutations, and result in an increase in the amount of protein produced, leading to a more rapid progression of PD. Early onset, marked dementia and frequent dysautonomia (disorder of the autonomic nervous system) are found in patients expressing triplications of the gene (Ross et al., 2008).

LRRK2

LRRK2 mutations (PARK8-linked PD) present with LOPD at a mean age at onset of 60 years, and are present in up to 10% of AD familial PD cases (Paisán-Ruíz et al., 2008). The majority of mutations in the *LRRK2* gene are missense variants, of which seven mutations thus far are considered pathogenic. The most common of these is the G2019S mutation, which occurs in three to six percent of familial cases of PD in persons from European descent (Di Fonzo et al., 2005). This mutation is predominantly prevalent in North African Arabs, where 7 of 17 familial cases were observed (Lesage et al., 2005) . The frequency of mutations among Arabs was found to be 37 percent in familial cases and more surprisingly, 41 percent in sporadic cases (Lesage et al., 2006). Similarly, this frequency is also high in the Ashkenazi Jewish population, reaching 29.7 percent in familial cases and 13.3 percent in sporadic cases (Ozelius et al., 2006) due to founder effects.

LRRK2 has 2527 amino acids and contains a combination of motifs and several conserved domains (Appendix I). The function of LRRK2 is unknown, although it is thought to play a role in kinase activity and protein-protein interactions due to the functional domains of the protein (Dächsel et al., 2007). It is suggested that the kinase activities of LRRK2 are increased by the PD-associated mutations, hence the hypothesis of a gain-of-function pathogenic mechanism. LRRK2 is considered to interact with α-synuclein however little is known regarding the mechanism of this occurrence (Lin et al., 2009).

EIF4G1

A genome-wide linkage analysis of a French family with a positive family history of AD PD discovered a missense mutation R1025H in the *EIF4G1* gene (Chartier-Harlin et al., 2011). Further analysis found the mutation present in families from Ireland, Italy and the US. It is suggested that the mutation originates from a common ancestral founder (Sundal et al., 2012). A second novel missense

mutation – A502V - has also been found in 3 PD individuals (Tucci et al., 2012). PD caused by the R1025H mutation presents at a relatively late AAO, between 57 and 80 years of age. *EIF4G1* encodes for a scaffold protein eIF4G1, which plays a role in the regulation of translation in response to development or environmental stressors in the cell.

VPS35

Whole exome sequencing of a Swiss family with 11 affected members with AD LOPD was performed (Vilarińo-Güell et al., 2011). The D620N mutation in the *VPS35* gene was discovered; and an independent study done on a family from the US and Tunisia confirmed the presence of the PD-causing D620N mutation (Zimprich et al., 2011). The gene encodes for the VPS35 protein, which is a critical component of the retromer cargo-recognition complex. The role of this complex is recycling membrane proteins between endosomes and the trans-Golgi network.

1.3.2.2. Genes involved in autosomal recessive forms of PD

The recessive forms of PD arise from mutations in four genes – namely *parkin, PTEN-induced kinase (PINK1), oncogene DJ-1 (DJ-1)* and *ATPase type 13A2 (ATP13A2)*. The pathogenic mechanism of recessive forms of PD is a loss-of-function, due to the resulting absence or inactivation of protein.

Parkin

Parkin (PARK2-linked PD) mutations range from missense and nonsense mutations, to exonic deletions (most common), rearrangements and duplications. PARK2-linked PD is a common cause of juvenile and EOPD, although there are cases where LOPD occurs. It is estimated that *parkin* mutations are responsible for up to 50% of recessive familial cases of PD in some studies (Lucking et al., 2000). *Parkin* encodes a 465 amino acid ubiquitin E3 ligase protein. The protein is comprised of a C-terminal 'ring between ring fingers' (RBR) domain consisting of 2 RING fingers (R1 and R2) linked by a cysteine-rich 'in-between-RING" (IBR) motif. The N-terminal is an ubiquitin-like domain (Ubl) (Appendix I).

The role of parkin in the cell is the targeting of other cellular proteins for degradation via the ubiquitin-proteasome system (UPS). This is performed by the RBR domain and several ubiquitin enzymes (e.g. E1 and E2), catalysing the attachment of ubiquitin to proteins (ubiquitylation), thus tagging these proteins for destruction (Further discussed in Section 1.4.5). Parkin possibly links ubiquitylation with mitophagy (autophagy which is selective for degradation of mitochondria). *Parkin* knockout studies in the fruit fly *Drosophila melanogaster* and mice have resulted in mitochondrial abnormalities (Greene et al., 2003; Palacino et al., 2004), suggesting possible mitochondrial dysfunction in patients with PD (Further discussed in Section 1.4.5).

PINK1

PINK1 (PARK6-linked PD) is a form of early onset AR PD. The protein has been shown to localize in the matrix and intermembrane space of the mitochondrion. Mutations in the *PINK1* gene include missense and nonsense mutations (most common), frameshifts and truncating mutants. *PINK1* encodes for a 581 amino acid protein which has a protein kinase domain; a mitochondrial-targeting domain (MTS) and a transmembrane domain (TM; Appendix I; Corti et al., 2011). Although the function of PINK1 is unknown, it is thought to play a neuroprotective role against mitochondrial dysfunction. Studies on human cells with *PINK1* mutations have shown that a deficiency of PINK1 can lead to swelling of the mitochondria and loss of mitochondrial complex I activity (Section 1.4.5; Exner et al., 2007; Grünewald et al., 2009).

Interestingly, PINK1 and parkin appear to work in the same pathway to prevent oxidative stress and regulate mitochondrial morphology. In *Drosophila*, *parkin* overexpression supresses *PINK1* mutant phenotypes tested, whereas *PINK1* overexpression does not compensate for loss of function in *parkin* mutant phenotypes (Clark et al., 2006; Park et al., 2006). Therefore *PINK1*'s role in the pathway is thought to be situated upstream of *parkin*, as *parkin* can rescue *PINK1* but the inverse does not occur (Dagda et al., 2009; Park et al., 2006). Both genes affect the same pathway, so the interactions are thought to occur in the mitochondria (Shimura et al., 1999; Silvestri et al., 2005). Interaction of these proteins has been speculated to occur via three mechanisms – i) by direct binding and phosphorylation of PINK1 to parkin; ii) by phosphorylation of an intermediate protein by PINK1, which would then form a signal to alter the activity of parkin or iii) both proteins act on the same target. Parkin and PINK1 also seem to play roles in mitochondrial quality control and disposal (Narendra et al., 2010), which will be further discussed in sections 1.4.4 and 1.4.5.

DJ-1

DJ-1 mutations constitute an extremely rare early onset AR EOPD, and consist of missense mutations, frameshift and splice-site mutations, and exonic deletions. The protein is made up of 189 amino acids (Appendix I) and expressed in most mammalian tissues. DJ-1 is a cytoplasmic protein and part of a family of molecular chaperones, and can act as an anti-oxidant as well as a ROS scavenger in high levels of oxidative stress. Studies have shown a deficiency of DJ-1 results in increased apoptosis due to oxidative stress levels, whereas *DJ-1* overexpression has protective effects on the cell under oxidative conditions (Abeliovich & Flint Beal, 2006). Currently, the mechanism of these effects is unknown.

ATP13A2

ATP13A2 is a large protein, made up of 1180 amino acids and 10 transmembrane domains (Appendix I). The protein is a lysosymal membrane protein, and although the function is relatively unknown, it is thought to be involved in the transport of inorganic cations and other substrates. High levels of ATP13A2 are found in the SNc. *ATP13A2* (PARK9-linked PD) mutations were first recognized in Jordanian and Chilean families (Ramirez et al., 2006) with Kufor-Rakeb syndrome (KRS), which is a form of recessively inherited atypical parkinsonism, characterized by very early or juvenile AAO (11 – 16 yrs.). The mutations found in these families are thought to induce degradation of ATP13A2 in the endoplasmic reticulum (ER; Ramirez et al., 2006)

1.3.2.3.   *Heterozygous mutations in recessive genes*

In AR EOPD, mutations that cause PD are either homozygous or compound heterozygous (heterozygous for two different mutations). It has been reported in several studies that individuals who are heterozygous carriers of mutations (have only one mutation) in *parkin* and *PINK1* can also present with PD (West et al., 2002; Bonifati et al., 2005; Hedrich et al., 2006). However there is much debate as to whether these individuals have mild signs of parkinsonism but not PD per se. Parkinsonism is the term for nervous disorders similar to PD, marked by muscular rigidity, tremor and impaired motor control. However, not all studies have shown that heterozygous individuals present with parkinsonism features and symptoms (Chien et al., 2006; Chishti et al., 2006),

suggesting that further research is essential in deciphering the role of heterozygous mutations in causing PD.

Identification of the PD-causing genes have shed light on a number of pathways thought to be underlying the disorder, which include oxidative damage, abnormal protein accumulation, defective protein phosphorylation, defective cell signalling and mitochondrial dysfunction (Cookson & Bandmann, 2010). The next section will elaborate on the mitochondrial dysfunction hypothesis as this has received much attention over the last three years (Grünewald et al., 2009; Grünewald et al., 2010; Zheng et al., 2010; Pacelli et al., 2011)

1.4.   Mitochondrial dysfunction and PD

As stated in previous sections, mitochondrial dysfunction has been implicated in the development of PD through studies on pesticides and neurotoxins that disrupt complex I (e.g. MPTP, rotenone) and various genes that play a role in mitochondrial function (*parkin*, *PINK1* and *DJ-1*). The following section will briefly discuss the structure, function, genome and dynamics of this organelle and will also focus on *parkin* and *PINK1*'s possible roles in the maintenance of healthy mitochondria.

The mitochondrion is a vital intracellular organelle found in all tissue types and it is responsible for one of the cell's key survival functions – the production of energy in the form of ATP. Mitochondria are also responsible for several other secondary functions, including regulation of cellular metabolism and respiration, signalling, cellular differentiation, cell death, control of the cell cycle and cell growth, and storage of calcium ions.

1.4.1. Structure of the mitochondria

Mitochondria are approximately 0.5-1µm in diameter, and are elongated, cigar-shaped organelles. The structure of the mitochondria is divided into the outer membrane, the intermembrane space,

the inner membrane, and the matrix (Figure 1.7). The mitochondrial structure facilitates efficient functional capacity of the organelle. If there is swelling of the mitochondria or fragmentation of the mitochondrial network, this generally leads to mitochondrial dysfunction and a decrease in the ATP levels.

A
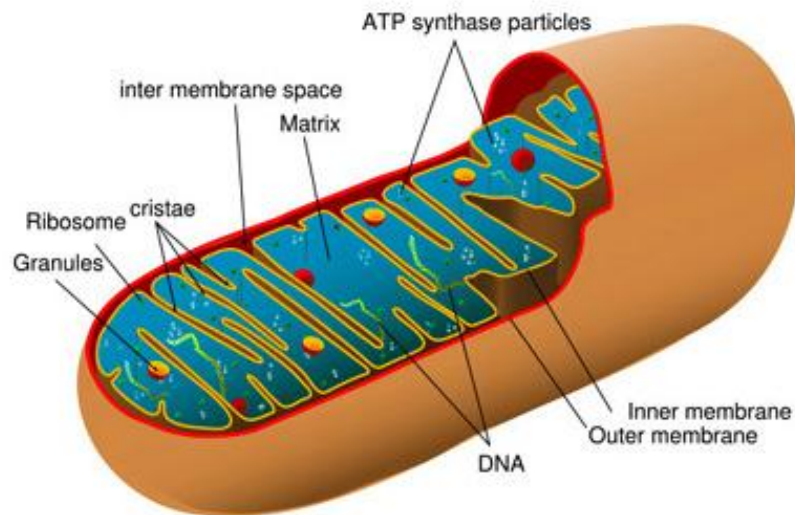
B
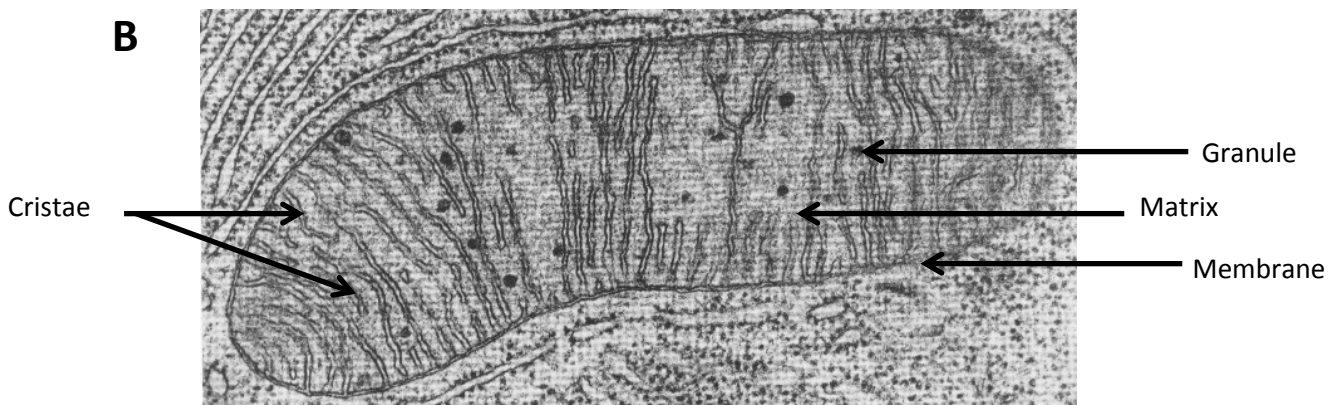
Figure 1.7: **Images to show the structure of the mitochondria.** A. Schematic diagram and B. Electron micrograph of a mitochondrion. Taken from: http://www.tutorvista.com

1.4.1.1.   Outer membrane

The outer mitochondrial membrane encloses the entire organelle, and is composed of phospholipids and proteins. Large channels called porins allow for the diffusion of larger proteins from one side of the membrane to the other.

1.4.1.2.   Intermembrane space

Separating the outer membrane from the inner membrane is a space known as the intermembrane space (IMS). The IMS is made up of the same composition of the cytosol of the cell, and houses enzymes such as cytochrome c, which is important for oxidative phosphorylation and cell apoptosis (Finsterer, 2004)

1.4.1.3.   Inner membrane

The inner membrane is less permeable than the outer membrane, but far more complex. Situated here are all four respiratory chain complexes and the ATP synthase (also known as complex V) of the electron transport chain, which is the site of oxidative phosphorylation in mitochondrial respiration. Cristae (Figure 1.7) are folds formed by the inner membrane in order to increase the surface area, and are vital for rapid and efficient energy production. Other membrane proteins situated in the inner membrane include metabolites and ion carriers that aid in linking the metabolism of the cytoplasm with the IMS (Sherwood, 2012).

1.4.1.4.   Matrix

The matrix is situated inside the inner membrane and is the site of the Krebs cycle. It is a gel-like solution, composed of enzymes involved in other processes such as the urea cycle and fatty acid oxidation. Also found in the matrix are ribosomes, messenger RNAs (mRNAs), transfer RNAs (tRNAs) and multiple copies of the mitochondrial genome.

1.4.2. Function of the mitochondria

The mitochondrion is involved in a variety of functions but for the purpose of the present study, the focus will be on the production of energy via mitochondrial respiration.

1.4.2.1.   *Mitochondrial respiration and ATP production*

Mitochondrial respiration is defined as the series of metabolic processes by which all living cells produce energy through the oxidation of organic substances. Glycolysis is the first step of the process and occurs in the cytosol of all cells. It involves the breakdown of one molecule of glucose into two three-carbon molecules of pyruvate via a series of enzyme-controlled reactions. In glycolysis, a net yield of two ATP molecules for one molecule of glucose is produced (Figure 1.8). In comparison, oxidative phosphorylation produces 36 ATP molecules per molecule of glucose (assuming that for each molecule of NADH three ATP is produced, and each molecule of FADH2 produces two ATP). This is notably higher than the amount produced during glycolysis, signifying that glycolysis is less efficient in energy production than oxidative phosphorylation. Should oxidative phosphorylation be dysfunctional, then glycolysis assumes the role of the primary source for ATP. An example of when this occurs is in the absence of oxygen (when the cells are undergoing anaerobic respiration), oxidative phosphorylation cannot proceed, and glycolysis is then responsible for ATP production.

$$C_6H_{12}O_6 + 2HPO_4{}^{2-} + 2ADP^{3-} + 2NAD^+ \longrightarrow$$

$$2Pyruvate + 2NADH + 2H^+ + 2H_2O + \textbf{2ATP}$$
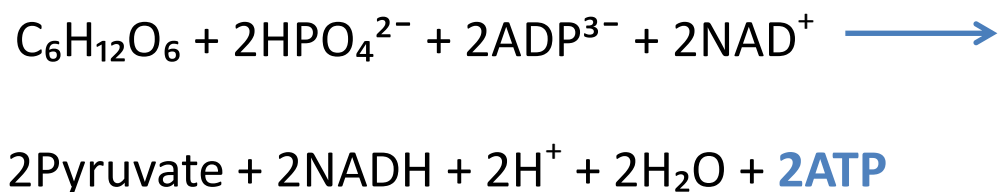
Figure 1.8: Equation of cellular glycolysis producing a net yield of two ATP molecules

The two pyruvate molecules produced by glycolysis are transported into the matrix of the mitochondria and converted to acetic acid, which combines with coenzyme A to form a compound, acetyl coenzyme A (acetyl CoA). Acetyl CoA then enters the eight-step Krebs cycle (also known as the Citric Acid Cycle), resulting in the production of electron donors NADH (reduced nicotinamide adenine dinucleotide) and $FADH_2$ (reduced flavin adenine dinucleotide) as well as two ATP molecules.

The final step of mitochondrial respiration is that of oxidative phosphorylation, which is the synthesis of ATP from adenosine diphosphate (ADP) and inorganic phosphate (Pi). This process occurs on the inner membrane of the mitochondria via five enzyme complexes (complex I, complex II, complex III, complex IV and ATP synthase/complex V; Figure 1.9). NADH and $FADH_2$ act as carrier molecules, transporting hydrogen ions from the matrix to the inner membrane. NADH releases the hydrogen protons at complex I, whereas $FADH_2$ releases the protons at complex II. Once the protons are released, high energy electrons are extracted from the hydrogen. The hydrogen ions then move through the complexes and into the IMS, whilst the electrons move through the electron transport chain via ubiquinone and cytochrome c and other specific electron carriers. When the electrons reach complex IV, they are passed to O_2, the final acceptor, and H_2O is formed.

As the electrons move, energy is released which aids in the movement of more hydrogen ions into the IMS. The high concentration of hydrogen ions in the IMS then leads to a density gradient from the IMS to the matrix, forcing the hydrogen ions to move from the IMS into the matrix through the ATP synthase complex. This leads to the activation of ATP synthase, which drives the conversion of ADP and Pi into ATP (Figure 1.9).
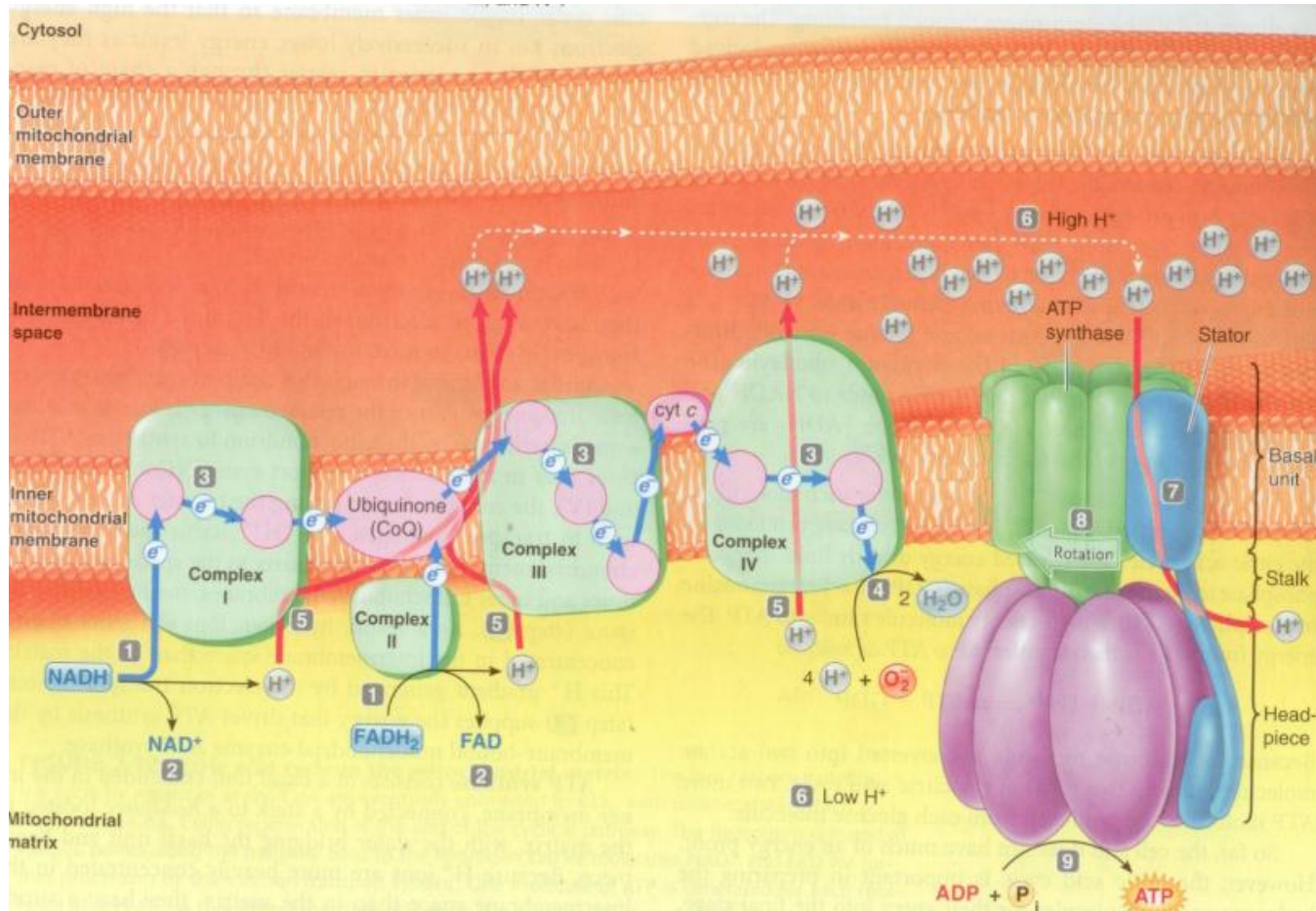
Figure 1.9: Oxidative phosphorylation at the mitochondrial inner membrane, shown in steps 1-9. This process involves the movement of electrons from the electron donors NADH and FADH₂ through a series of complexes, resulting in the movement of proton's to the IMS. This creates a high proton gradient, which in turn forces the hydrogen ions to move from the IMS into the matrix through the ATP synthase complex which drives the conversion of ADP and Pi into ATP

e⁻, electron; NADH, reduced nicotinamide adenine dinucleotide; FADH₂, reduced flavin adenine dinucleotide; IMS, Intermembrane space; H⁺, proton; ADP, adenosine diphosphate; Pi, inorganic phosphate; ATP, adenosine triphosphate

Taken from: Sherwood, 2012

Figure 1.10 represents the final equation of mitochondrial respiration, whereby the substrates glucose and oxygen are converted into carbon dioxide, water and energy in the form of ATP.

$$C_6H_{12}O_6 + 6O_2 \longrightarrow 6CO_2 + 6H_2O + \textbf{ENERGY (38ATP)}$$

Figure 1.10: Equation of mitochondrial respiration producing a net yield of 38 ATP molecules

1.4.2.2.   *Mitochondrial ROS*

Mitochondria are the main producers of ROS in the cell as a by-product of respiration. ROS are part of the free radical family, which are molecules that have a shortage of electrons in their outer orbital. An example of such a molecule is oxygen, because it has two unpaired electrons in its outer orbital. ROS are scavengers, because in order to find stability they need to extract electrons from neighbouring molecules to complete their own outer orbital (Beal, 2003). This leads to oxidation of neighbouring molecules.

For example, when oxygen adds an extra electron, it becomes the superoxide anion ($O_2^{\cdot-}$), which is also a free radical. When there is a complex I deficiency or any other deficiency in the respiratory chain, the amount of electrons lost to oxygen significantly increases, resulting in an increase in the levels of ROS. A cell undergoes oxidative stress when there is an imbalance between the production of ROS and the cells ability to detoxify or neutralize the changes with antioxidants. Excessive ROS production, and oxidative stress, is toxic to the cell as they cause protein, lipid and DNA damage. For example guanosine can be oxidized to form 8-hydroxy-deoxyguanine which can lead to the incorrect pairing of these bases in the DNA molecule. Concentrations of 8-hydroxy-deoxyguanine have been shown to be significantly increased in the substantia nigra of patients with PD (Sanchez-Ramos et al., 1994; Alam et al., 1997).

1.4.3. Mitochondrial genome

The mitochondrial genome is a small, circular double-stranded DNA molecule consisting of 16 569 base pairs (Figure 1.11), far smaller than the nuclear genome. Each human cell contains hundreds of mitochondria and thousands of copies of the mitochondrial genome. It is also more compact than the nuclear genome, as there are no introns present. It encodes for 37 genes – specifically 13 polypeptides, 22 tRNAs and 2 rRNAs (Figure 1.11). The 13 polypeptides are all involved in the respiratory chain, and make up subunits of the five enzyme complexes. Mutations in the mitochondrial DNA (mtDNA), such as point mutations and rearrangements, can cause several diseases that typically affect the organs with high-energy requirements such as the brain, eyes and liver. These disorders include diabetes mellitus and deafness (DAD), myoclonic epilepsy with ragged red fibres (MERRF), and Leber's hereditary optic neuropathy (LHON).
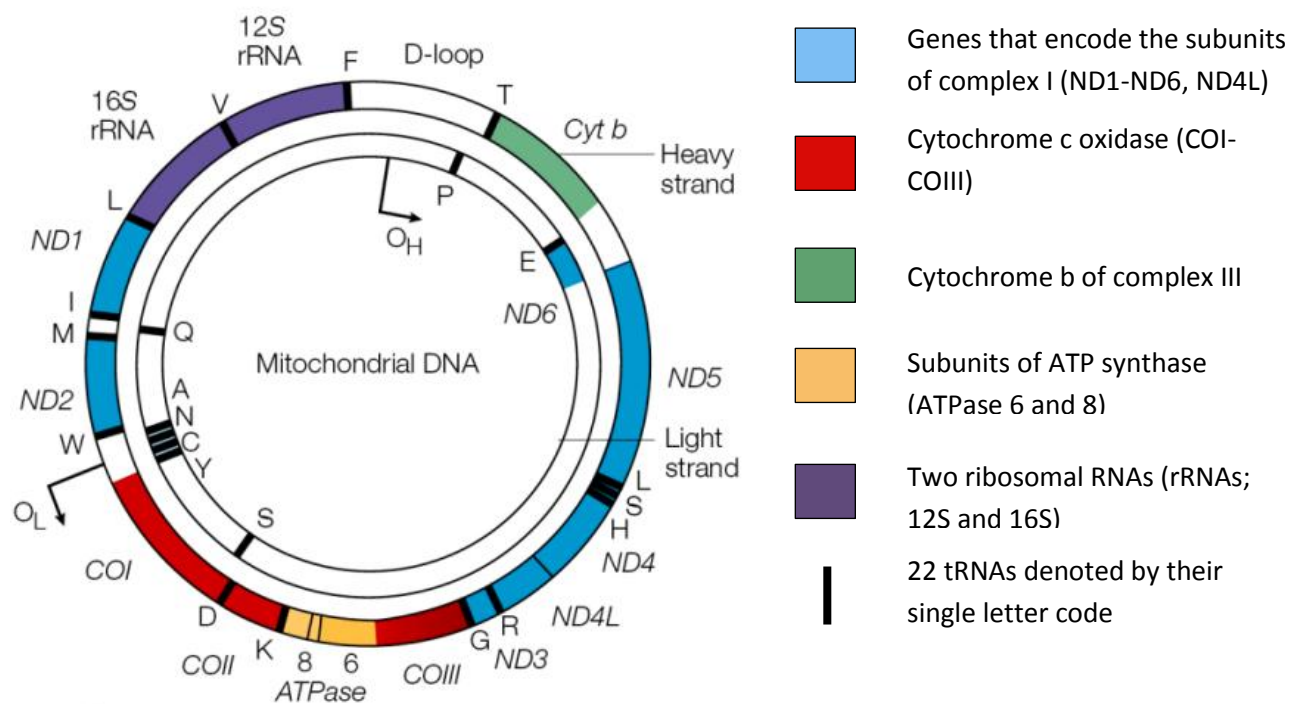
Figure 1.11: A map of the human mitochondrial genome. The legend indicates the mtDNA genes encoding each specific complex, as well as the position of the rRNAs and tRNAs. The D-loop, also known as the displacement loop, is a non-coding region with sequences vital for the initiation of mtDNA replication and transcription. The origin of the heavy stand is indicated as O_H and the origin of light-strand replication is shown as O_L. Taken from: Taylor & Turnbull, 2005

Several studies have been done to investigate whether mutations in mtDNA may cause PD through a complex I defect. This is difficult to determine due to the fact that as one ages, large mtDNA deletions accumulate, causing complex I activity to decrease (Beal, 1995). Therefore, as PD is also associated with old age, distinguishing between the two causes has proven to be difficult. One study showed that although there was a high proportion of deleted mtDNA in age matched controls, there was a higher proportion of deleted mitochondria in parkinsonian cases (Bender et al., 2006). Furthermore, although specific mitochondrial sequence variants have been found in patients with PD there has not been a common finding in all studies (Kösel et al., 2000; Shoffner et al., 1993; Vives-Bauza et al., 2002).

The definition of a mitochondrial haplogroup is 'an individual group characterized by the presence of a particular set of polymorphisms' (Domínguez-Garrido et al., 2009). Human mitochondria can be subdivided into 36 different haplogroups which are all labelled by a letter of the alphabet, ranging from haplogroup A – N, P – Z, and subgroups of several of these haplogroups, such as HV, JT and L0 – L6. A study done by van der Walt and colleagues analysed 609 unrelated PD patients of European ancestry and compared them to age-matched controls (Van der Walt et al., 2003). It was found that the frequencies of haplogroup J and haplogroup K were lower in the PD cases compared to the control cases. This was due to single nucleotide polymorphism (SNP) 10398G in the *NADH dehydrogenase 3 (ND3)* gene in both haplogroups. It is thought that this SNP protects against development of PD compared to haplogroup H due to a possible increase in the performance of complex I in the brain and other tissues (Van der Walt et al., 2003). It has also been suggested that SNP 4216C which defines the haplogroup cluster JT is more frequent among Irish patients with PD than controls (Ross et al., 2003). This was also observed by Autere and colleagues when analysing the JTIWX supercluster (Autere et al., 2004) . However, it is currently unknown as to whether the decreased or increased risk of PD is due to a single polymorphism or a combination of polymorphisms.

1.4.4. Mitochondrial dynamics

Recent studies have shown that mitochondria are not only static organelles with primary and secondary functions, but are highly dynamic, and are involved in processes such as movement, fusion, fission and mitophagy (Detmer & Chan, 2007). In most tissues, but especially in neuronal tissue, healthy mitochondria are transported towards areas with a high energy demand. In contrast, damaged or dysfunctional mitochondria move away from these areas into less demanding spaces of the cell. Movement can also promote morphological transitions in the mitochondria depending on the cell type. This is controlled by fusion and fission. Fusion and fission play major roles in maintaining the mitochondria, which is done by controlling the integrity of the mitochondria, the electrical and biochemical connectivity, the turnover of the mitochondria, and the protection of mtDNA (Berman et al., 2008)

Fusion is the merging of the double membranes of two mitochondria, resulting in a larger single organelle (Figure 1.12). Subsequently, fission may occur, which is the division of one mitochondrion into two smaller mitochondria, a healthy one and an 'impoverished one', which is tagged for degradation whilst the healthy mitochondrion remains in the cell. The balance of both of these processes is vital in the maintenance of functional mitochondria and cellular requirements (Burbulla et al., 2010) and an imbalance can lead to autophagy and cellular apoptosis. Any type of disequilibrium of this system results in increased fission for fragmentation and removal of damaged mitochondria.

There is tight regulation of these process via the action of the GTPases – namely Mitofusin 1 (Mfn1) and Mitofusin2 (Mfn2) which are situated in the mitochondrial outer membrane, and Opa1 which resides in the intermembrane space. These three GTPases are responsible for the process of mitochondrial fusion (Figure 1.12), and it is thought that the carboxy-terminal coils secure the two organelles undergoing fusion (McBride et al., 2006). Mitochondrial fission is controlled by a large GTPase called dynamin-related protein 1 (Drp1), with the aid of mitochondrial protein Fis1 and cytoplasmic endophilin B1/Bif-1 (Santel & Frank, 2008). Drp1 is recruited to the surface of the mitochondria (Figure 1.12); however the exact mechanism of fission remains unclear.
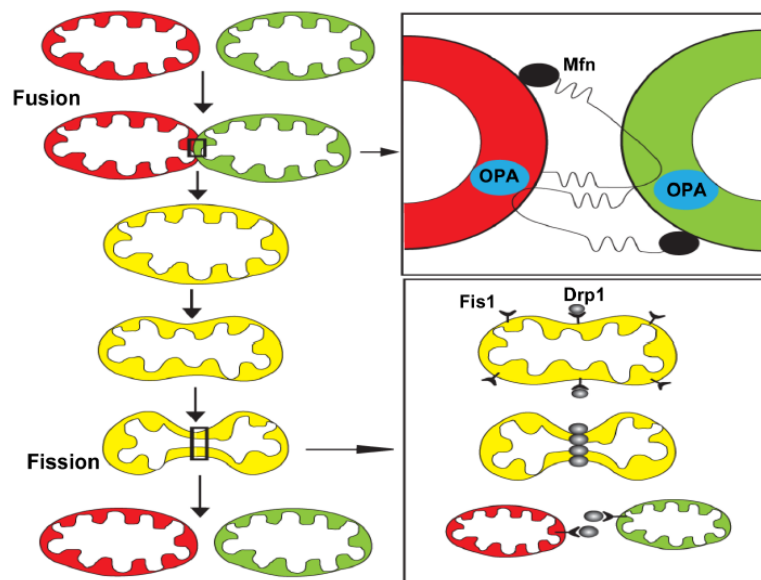
Figure 1.12: **Mitochondrial fusion and fission mechanisms.** Taken from: Mattson et al., 2008

Detection of mitochondrial fusion or fission in cells is done via analysis of the mitochondrial network. These organelles form tubular networks (Legros et al., 2002) and when they are predominantly undergoing fusion, they appear joined together, resulting in a highly connected network. Conversely, when the majority of the mitochondria are undergoing fission to rid the cell of damaged mitochondria, the network appears fragmented and broken up. Defects in both processes are shown in Figure 1.13. The mitochondria are stained using fluorescent probes in order to observe the networks within the cells.
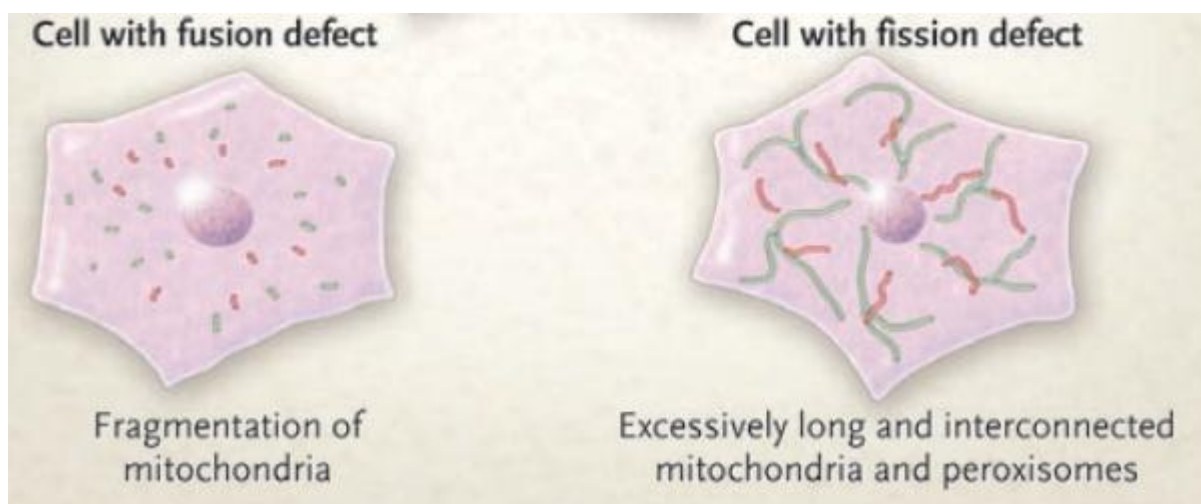
Figure 1.13: **Diagram illustrating defects in mitochondrial fusion and fission.**

A study performed on *Drosophila* models used RNA interference (RNAi) to knockdown and over express the genes involved in fusion (*Mfn1/2* and *Opa1*) and fission (*Drp1* and *Fis1;* Ziviani et al., 2010). They found that the knockdown of *Opa1* and *Mfn* resulted in fragmented mitochondria, as no fusion was occurring (Figure 1.14A). In contrast, knockdown of *Fis1* and *Drp1* caused a highly connected mitochondrial network, as no fission was occurring. The opposite was seen to occur when *Opa1* and *Mfn* were overexpressed – resulting in a high level of mitochondrial connectivity. When over expressing *Fis1* and *Drp1,* a fragmented network was observed, similar to the knockdown of *Mfn* and *Opa1* (Figure 1.14B). The normal state of the cells should show a balance of both fusion and fission.
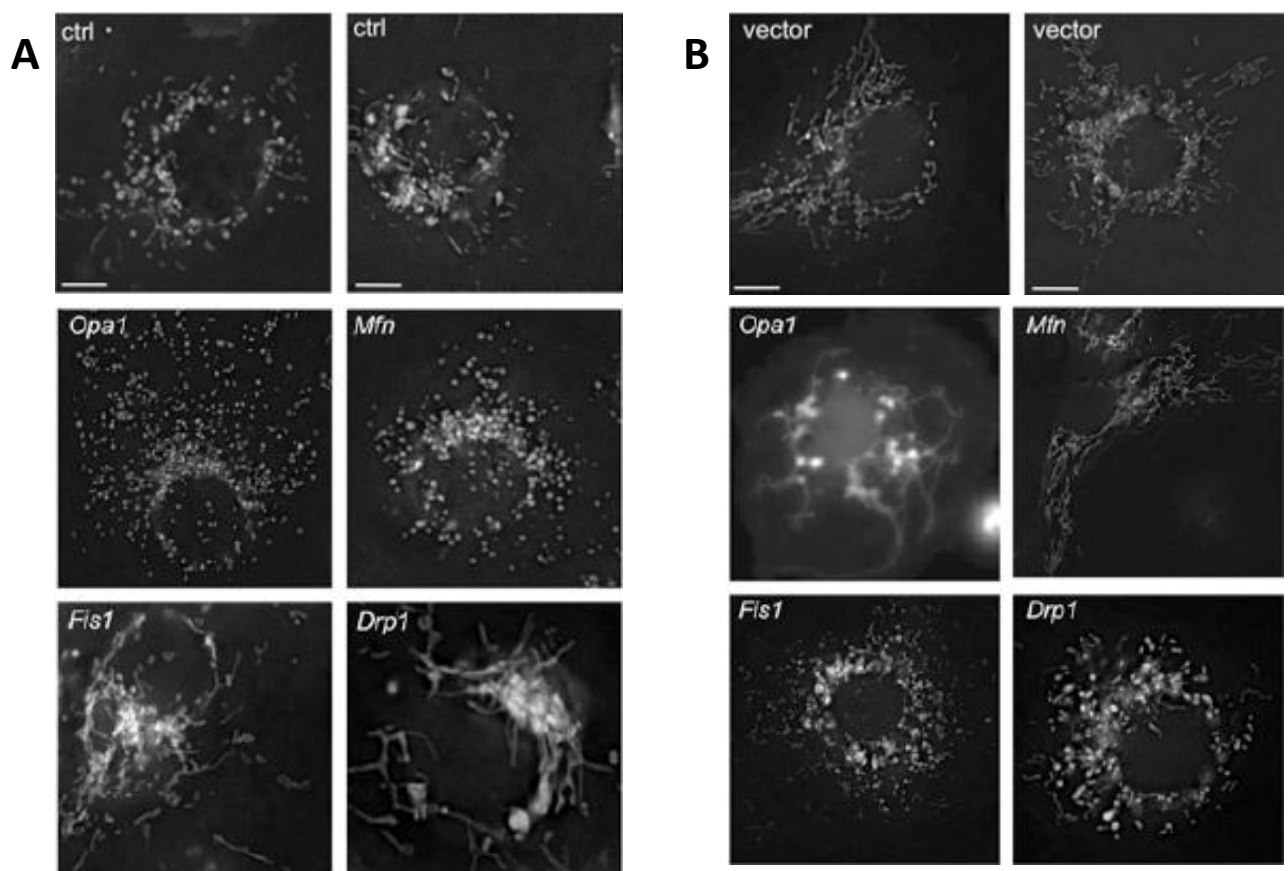
Figure 1.14: Under- and over-expression of the genes responsible for fusion (*Opa1* and *Mfn*) and fission (*Fis1* and *Drp1*). A. Control cells exhibit a balanced network, knockdown of *Opa1* and *Mfn* show fragmented mitochondria, whereas knockdown cells of *Fis1* and *Drp1* show a high connectivity of mitochondria. B. Control cells indicate a healthy mitochondrial network, over-expression of *Opa1* and *Mfn* show fused mitochondria, whereas over-expressed *Fis1* and *Drp1* have a fragmented network. Taken from: Ziviani et al., 2010

Damaged mitochondria are thought to be degraded via the process of mitophagy, which is defined as autophagy specifically selected for degradation of mitochondria. Mitochondria are especially susceptible to damage due to the relatively high levels of ROS produced during oxidative phosphorylation. Increased ROS can lead to ATP depletion, a higher mutation rate of mtDNA (Yakes & Van Houten, 1997) and ultimately cell death (Lemasters et al., 1998). Mitophagy is therefore essential in removing dysfunctional mitochondria to prevent cell death (Kim et al. 2007).

1.4.5. Mitochondrial-associated PD genes

The three PD genes known to be associated with mitochondrial function are *parkin, PINK 1* and *DJ-1*. The autosomal dominant gene *LRRK2* has also been associated with mitochondrial membranes. However, since most of the work has been done on *parkin* and *PINK1*, these genes will be the focus of the next section. Both genes have been implicated in causing mitochondrial structural defects such as an alteration in mitochondrial morphology (Grunewald et al., 2009; Pacelli et al., 2011), as well as functional defects such as an increase in ROS production, a decrease in the levels of ATP and a decrease in respiratory complex activity (Piccoli et al., 2008; Grunewald et al., 2009; Grunewald et al., 2010; Pacelli et al., 2011). Mitochondrial function can also be affected by changes in the expression levels of genes within the mitochondrial energy metabolism pathway.

1.4.5.1. Parkin

Parkin forms part of the UPS system whereby cystolic, secretory and membrane proteins undergo degradation (Dawson & Dawson, 2003). It is specifically involved in the removal of degraded, unwanted or short-lived proteins in the cell. The process is initiated by the activation of the carboxyl group of ubiquitin, resulting in its transfer to specific E2 ubiquitin-conjugating enzymes. This then causes conjugation of ubiquitin to the ε-amino group of lysine residues of the protein substrate (Ye & Rape, 2009). This process is aided and catalysed by three specific enzymes – E1 ubiquitin-activating enzyme, E2 ubiquitin-conjugating enzyme and E3 ubiquitin-protein ligases. The attachment of ubiquitin to the lysine residue of the substrate leads to the formation of a

polyubiquitin chain, and thus the protein is 'tagged' for degradation. Parkin acts as an E3-ubiquitin-protein ligase, and absence or inactivation of parkin is thought to lead to abnormal accumulation of the proteins selected for degradation (Kahle & Haass, 2004). Also, due to the presence of LBs (partially made up of ubiquitin) in PD patients, failure of the UPS might also play an important role in the pathology of the disease.

Animal studies

Animal knockout models of *parkin* show several changes in the mitochondria in comparison to the wild-type controls. A study on a *Drosophila* knockout model revealed that mitochondrial defects were a common characteristic of pathology (Greene et al., 2003). They found severe morphological differences in the knockout models – such irregular & dispersed myofibrillar arrangements and swollen and malformed mitochondria with disintegration of cristae (Figure 1.15). In mice knockout models, a decrease in the number of proteins involved in mitochondrial function or oxidative stress, a decrease in respiratory capacity of striatal mitochondria, as well as decreased serum antioxidant capacity were found (Palacino et al., 2004). In contrast to the Drosophila model however, the mitochondrial morphology in the mouse model was similar between the knockouts and the control.
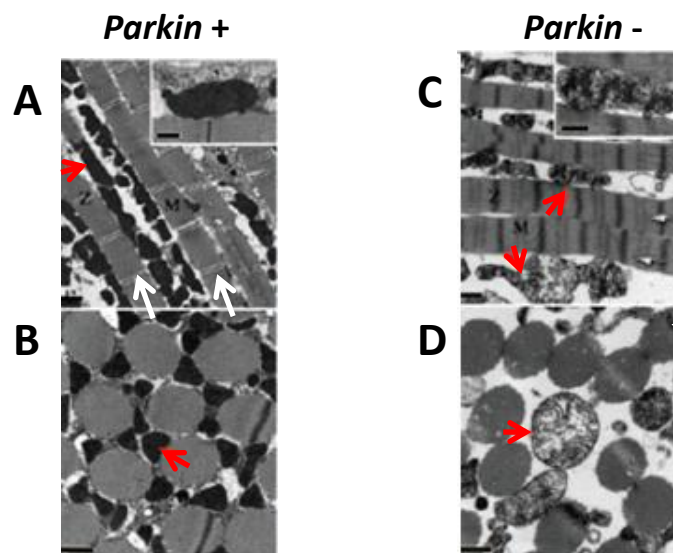
Figure 1.15: **Sections through *parkin* wild-type (*parkin* +) and *parkin* knockout (*parkin* -) *Drosophila* muscle fibres.** A & B. Regular and compact myofibril arrangement (white arrow) with electron dense areas (red arrow) in *parkin* + cells. C & D. Irregular and dispersed myofibrillar arrangement (white arrows) with swollen mitochondria and disintegration of cristae in *parkin* – cells (red arrows). Taken from: Greene et al., 2003

Human studies

In humans, loss-of-function mutations of *parkin* should result in no parkin protein being produced (Mortiboys et al., 2008; Pacelli et al., 2011). This is thought to lead to the accumulation of critical substrates, resulting in the initiatory events that induce changes in mitochondrial structure and function. Studies done on mitochondrial morphology in fibroblasts from patients with *parkin* mutations show an increase in mitochondrial mass (Grünewald et al., 2010) which is suggestive of swollen mitochondria. This is supported by analysis of ultrastructural changes in the mitochondria from fibroblasts of patients with *parkin* mutations where irregular shaped, swollen mitochondria with few remaining cristae were observed (Figure 1.16). It has been shown that impaired mitochondrial fusion is common in *parkin*-null mutants (Deng et al., 2008; Poole et al., 2008) and this is indicated by a fragmented mitochondrial network (Figure 1.17; Pacelli et al., 2011), although this particular finding has not been observed in other studies (Grünewald et al., 2010; Mortiboys et al., 2008). Further morphological studies need to be conducted on parkin-null fibroblasts, as the current findings are contradictory.
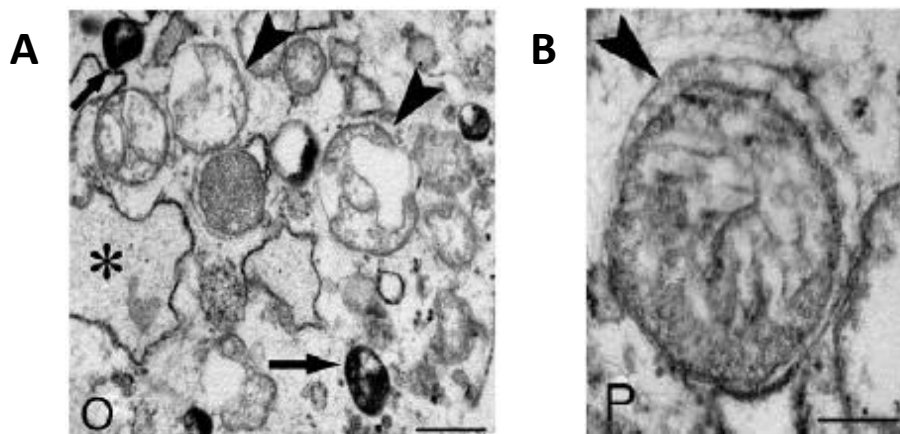
Figure 1.16: **Electron microscopy analysis of fibroblasts obtained from PD patients with *parkin* mutations.** Swollen mitochondria with disorganized membrane compartments and few remaining cristae (indicated by arrow heads in A and B), electron dense vacuoles (arrow in A), and enlarged rough endoplasmic reticulum (RER) cisternae (asterisk in A) were found. Taken from: Pacelli et al., 2011
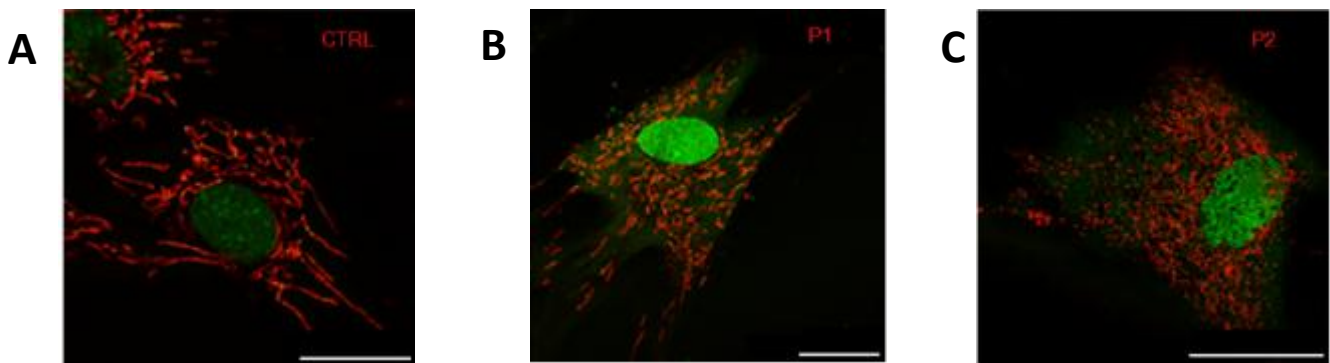
Figure 1.17: **Mitochondrial network analysis of A. control and B & C. two *parkin*-mutant patients.** The red dye indicates the mitochondrial network and the green dye shows the nucleus. Note the highly fragmented network in the patients compared to the control, indicating dysfunctional mitochondria. Taken from: Pacelli et al., 2011

Further evidence of a dysfunctional mitochondrion is via analysis of the respiratory capacity in the electron transport chain complexes of the inner membrane of the mitochondria. The majority of studies performed on fibroblasts to detect complex I activity in patients with *parkin* mutations have found a significant decrease in activity in comparison to age-matched controls (Mortiboys et al., 2008; Pacelli et al., 2011; Winkler-Stuck et al., 2004) . Muftuoglu and colleagues analysed complex I activity in leukocytes from *parkin*-null patients and also found a significant decrease (Müftüoglu et al., 2004). However, the activities of the other respiratory enzyme complexes remain unchanged in *parkin* mutant patients compared to controls (Grünewald et al., 2010). In some studies, complex IV activity has been found to be decreased in patients with *parkin* mutations, but this is not a consistent finding (Mortiboys et al., 2008; Müftüoglu et al., 2004; Pacelli et al., 2011), suggesting that further analysis needs to be done in order to determine which complexes are affected by *parkin*-null mutations and the mechanisms involved. Another indication of mitochondrial dysfunction in a cell is the amount of ROS present. An increased amount of cellular ROS levels is indicative of faulty oxidative phosphorylation, as more electrons are lost to oxygen than should be. Various studies on *parkin*-null patients have shown significantly increased concentrations of intracellular ROS (Grünewald et al., 2010; Pacelli et al., 2011), although to date no studies have analysed generic and mitochondrial ROS as separate entities.

1.4.5.2.   PINK1

Animal studies

Several animal knockout models of *PINK1,* specifically in *Drosophila*, have shown mitochondrial dysfunction, as well as muscle and dopamine-producing neuron degeneration. Studies on *Drosophila* are important, as the structure and localisation of PINK1 in flies is similar to that of humans (Park et al., 2006). Results from loss-of-function *PINK1* mutant flies showed locomotion defects in flight ability and climbing speed. Furthermore, abnormal muscle structure was observed. When analysing mitochondrial morphology, mutant flies had swollen, enlarged mitochondria with a loss of the mitochondrial outer membrane and fragmented cristae (Figure 1.18). The number of dopaminergic neurons was also notably decreased. Functionally, energy depletion was noted due to a decrease in ATP levels of mutant flies. In all cases, phenotypes were rescued by *PINK1* expression, suggesting that PINK1 is a critical factor in the normal functioning of the mitochondria (Clark et al., 2006; Park et al., 2006; Yang et al., 2006). In *Drosophila* models, mitochondrial dynamics such as the fusion and fission machinery play a large role in cell survival and overall plasticity of neurons. When *PINK1* is over-expressed, fission appears to be promoted, however when under-expressed fusion appears to take over (Yang et al., 2006).
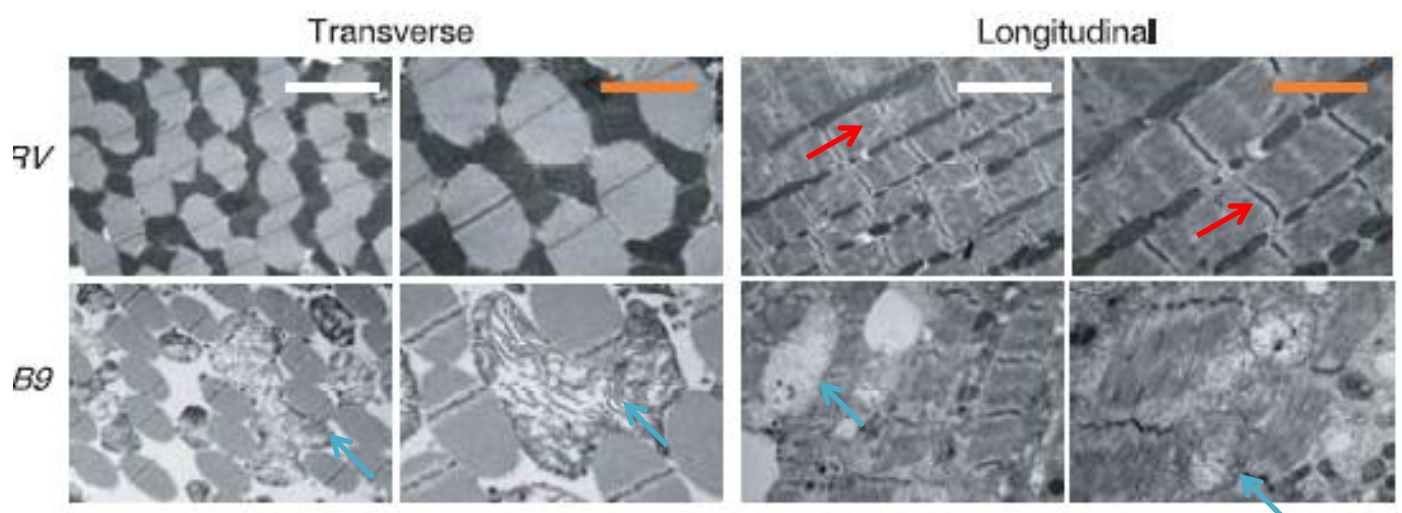
Figure 1.18: **Transverse and longitudinal sections of the flight muscle in two *PINK1* knockout *Drosophila* models - RV and B9.** Irregular arrangement of myofibrils (**red arrow**) and swollen mitochondria lacking an outer membrane (**blue arrow**) are observed. Taken from: Park et al., 2006

Human studies

A study was performed on human HeLa cells transfected with small interfering RNA (siRNA) to cause *PINK1* silencing and thus create a *PINK1* knockout model (Exner et al., 2007). This down-regulation of *PINK1* expression resulted in an increase in the number of cells with swollen, ruptured mitochondrial morphology with altered degraded cristae compared to the control cells. The same study also looked at mitochondrial network analysis and found that exposure to *PINK1* siRNA caused more cells to have a fragmented mitochondrial network (Figure 1.19; Exner et al., 2007). Grunewald and colleagues also noted swollen mitochondria with enlarged cristae in fibroblasts of patients with missense *PINK1* mutations, whereas no structural changes were observed in patients with nonsense mutations (Grünewald et al., 2009).
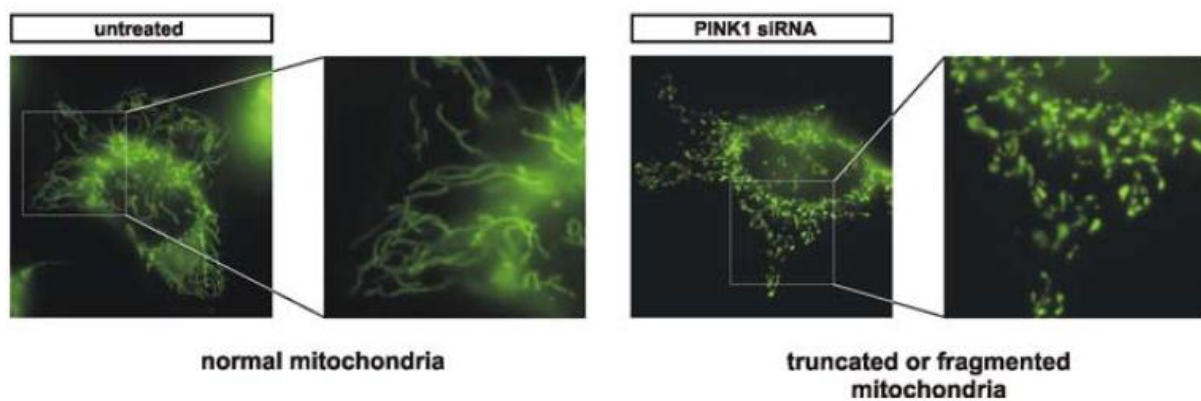
Figure 1.19: **Representative examples of normal or altered (truncated or fragmented) mitochondrial morphologies in HeLa cells following down-regulation of *PINK1* using siRNA.** Taken from: Exner et al., 2007

As ROS generation is thought to underlie the degeneration of neurons with dopaminergic neurotransmission, it is vital to detect levels of ROS in patients, as well as levels of antioxidants, to determine the extent of the damage as well as the degree of activation of the defence mechanisms. Analysis of mitochondrial dysfunction in *PINK1* null mutant patients shows accumulation of hydrogen peroxide (H_2O_2) in the mitochondria (Piccoli et al., 2008). H_2O_2 is a ROS formed by the addition of one electron to the outer orbital of the superoxide anion. This is thought to occur due to the decrease in the content of cytochrome c, which is a scavenger of ROS.

A second study on fibroblasts of mutant *PINK1* patients showed an increase in the levels of malondialdehyde (MAD), which is a marker for oxidative stress and is formed by the degradation of polyunsaturated lipids by ROS (Hoepken et al., 2007). This indicates an increase in the levels of ROS. Levels of 8-oxo-2'deoxyguanosine (indicates DNA damage) and protein carbonyls (indicate protein damage) remained unchanged, suggesting that mutant *PINK1* results in a peroxidation effect on lipids, but has no effect on DNA and proteins (Petit et al., 2005). The levels of the antioxidant manganese superoxide dismutase (MnSOD) were increased in the patients, implying that oxidative stress induces significant damage which results in the activation of the cellular defence mechanisms.

Analysis of respiratory activity on mutant *PINK1* fibroblasts has shown varied results in both complexes I and IV which is dependent on the type of mutation present in the patients – either nonsense or missense. In terms of complex I activity, results showed a significant decrease in activity in patients with a G309D missense mutation (Grünewald et al., 2009; Hoepken et al., 2007), but unchanged levels of activity in patients with a W437X nonsense mutation (Piccoli et al., 2008; Grünewald et al., 2009) Investigation of complex IV activity showed a decrease in the activity of patients with missense mutations, and no changes in the activity of patients with nonsense mutations (Grünewald et al., 2009).

1.5.   Gene and protein expression analysis

Altered gene or protein levels may be an important contributory factor in the pathobiology of a disorder. In contrast to studying one gene at a time, analysis of all mRNA transcripts or proteins in a cell can potentially identify the global biological pathways that are causally, reactively or independently involved with the disorder. This data could be used to generate hypotheses about disease mechanisms and analyses of the transcriptomes and proteomes of PD patients could potentially also provide insights into the processes underlying other forms of neurodegeneration such as Alzheimer's disease and Huntington's disease.

Gene expression levels can be analysed from tissue from an individual using a technique known as quantitative real-time PCR (qRT-PCR). qRT- PCR is a gene expression tool used to quantitate the target gene, and involves the production of identical copies of parts of cDNA that are fluorescently measured after each cycle of PCR to produce a threshold cycle (Ct) number once a certain amount of product has been formed. It requires the analysis of the change in levels of PCR product over time in both patient and control samples. Quantification allows one to detect the signals on a response curve graph. As the amount of product increases, the signal of the fluorescence increases exponentially and this is known as the exponential growth phase. When the reaction has completed, a plateau is reached called the plateau phase (Figure 1.20). A response curve enables one to distinguish between a positive sample (e.g. cDNA) where visible exponential growth and plateau phases are present, and a negative sample (e.g. gDNA or dH_2O) where no product is amplified and thus no curve is produced.
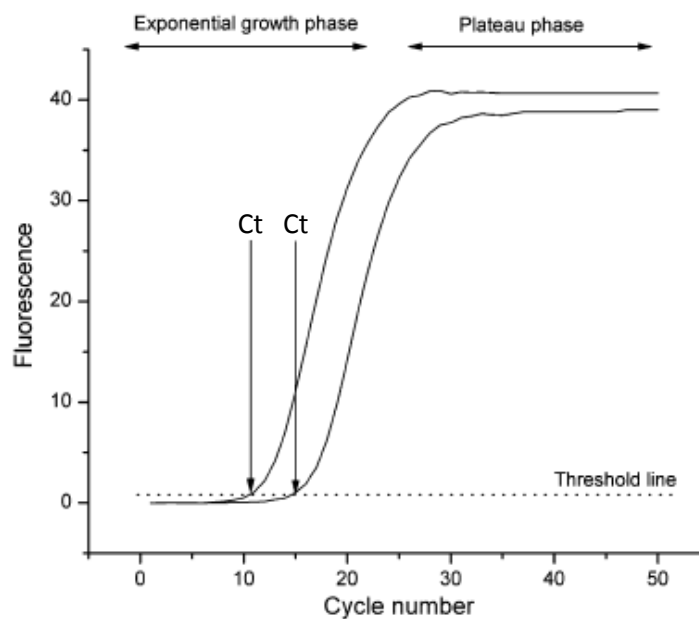
Figure 1.20: **RT-PCR response curve of fluorescence vs. cycle number indicating the growth phase and the plateau phase, the threshold line and the point where the number of cycles to reach threshold is registered (Ct).** Taken from: Kubista et al., 2006

The Ct value is the number of amplification cycles required to obtain a particular amount of DNA, or in other words, to reach the threshold (Kubista et al., 2006). The threshold value is subject to change, and can be done so to allow the response curves to be parallel in the growth phase (Kubista et al., 2006). Therefore, although the individual Ct values are changed by an increase or decrease in

the threshold value, the overall differences in the product of each samples will remain the same. The more copies of cDNA there are in a sample, the fewer cycles of amplification are required to generate the number of amplicons that can be detected reliably, and thus the Ct number will be lower (Bustin et al., 2005).

It is essential to normalize the expression level of a target gene to the expression level of a reference or housekeeping gene (HKG; Bower et al., 2007), such as glyceraldeyde-3-phosphate dehydrogenase (GAPDH) or β-actin. Normalisation accounts for differences in quality and quantity of the starting RNA and efficiencies of the reverse transcription reaction, as well as controls for errors between samples. Due to the lack of knowledge that there is one reference gene that is expressed in all tissue types (Dheda et al., 2004) it is vital that more than one HKG is used in expression studies. In order to ensure that normalization has occurred, expression levels of the HKGs should differ by no more than one Ct value between patient and control samples.

Data obtained from qRT-PCR is commonly analysed by relative quantification, which describes the change in expression of the gene of interest relative to a reference group such as an untreated control (Livak & Schmittgen, 2001). Relative quantification enables one to determine the fold increase or decrease of expression levels of a particular gene. The method used to determine this fold change number is known as the Delta-Delta Ct method (or $2^{-\Delta\Delta Ct}$). This is calculated by the change in Ct values of the target gene for the control and the target gene for the patient, subtracted from the change in Ct values of the reference gene for the control and the reference gene for the patient. The value obtained is the relative up – or down-expression of the gene of interest in the patient compared to the control.

1.5.1. Gene expression studies in PD

When using microarrays in expression studies on PD patients, the genes involved in mitochondrial energy metabolism and cell quality control have shown expression changes in tissue from the SNc (Mandel et al., 2005; Moran et al., 2006). Simunovic and colleagues found down-regulation of a large

number of genes involved in mitochondrial function when analysing data from microarrays of SNc tissue from patients and controls (Simunovic et al., 2009).

Sherzer and colleagues isolated RNA from the blood of 50 PD patients and 55 age-matched controls, and performed a real-time PCR on specific genes of interest (Scherzer et al., 2007). This study showed 22 differentially expressed genes in PD patients, including genes involved in the UPS (e.g. *ST13*), apoptosis-related genes (e.g. *BCL11B*) as well as mitochondrial genes (e.g. *LRPPRC*). Also, qRT-PCR analysis performed on two *parkin*-mutant PD patients found significant down-regulation of the genes involved in mitochondrial biogenesis (*NRF-1, NRF-2, TFAM*) and fatty acid metabolism (*MCAD*) (Pacelli et al., 2011).

As individual studies with small sample sizes often produce contrasting results, genome-wide expression meta-analysis studies are essential in creating a greater understanding of PD pathobiology. A meta-analysis was performed on the data sets of 17 independent genome-wide expression studies (Zheng et al., 2010). Nine studies had been conducted on laser-captured dopamine neuron and SNc post-mortem tissues, one on blood, one on a lymphoblastoid cell line and the remainder on various brain tissue. This analysis revealed significant defects in mitochondrial electron transport, as well as defects in glucose utilization and glucose sensing. Notably, this was found in the brain tissues as well as in the blood and lymphoblastoid cells. The majority of nuclear-encoded electron transport chain genes showed under expression in PD patients (Figure 1.21). Zheng and colleagues also specifically analysed the expression of peroxisome proliferator-activated receptor-γ coactivator (PGC-1α) – responsive genes. PGC-1α is a transcriptional coactivator and a master regulator of mitochondrial biogenesis and oxidative metabolism. They found under-expression of PGC-1α – responsive genes in patients with PD (Figure 1.21). Activation of PGC-1α resulted in up-regulation of nuclear subunits of all complexes in the mitochondrial respiratory chain.
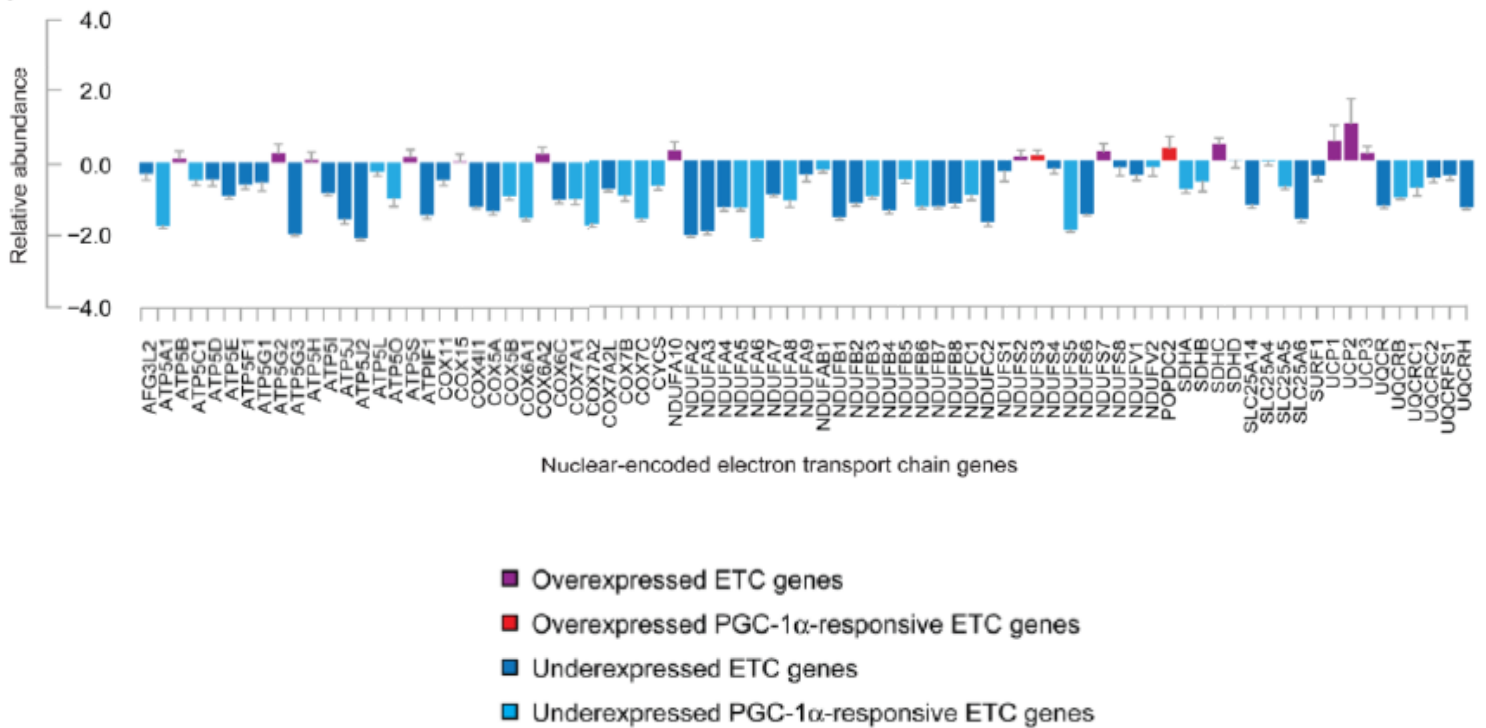
Figure 1.21: qPCR analysis shows under-expression of specific electron transport chain (ETC) genes in SNc of patients with PD. Taken from: Zheng et al., 2010

1.5.2. Proteome analysis in PD

Proteome analysis involves the identification and measurements of levels of the entire protein complement of a cell or tissue in order to give insights into alterations associated with specific protein pathways. Due to the high level of complexity and vast number of proteins in a single cell, the detection and analysis of proteins has proven to be a complicated and intricate process. Several methods have been developed for detection of protein complexes, protein-protein interactions, and protein levels in the cells as well as identification of post-translationally modified proteins.

Mass spectrometry (MS) is the most widely used technique to study proteomics, and involves the measurement of a mass-to-charge ratio of charged particles as they are eluted through a system. However, due to the surge in the reports of genomics, metabolomics and proteomics over the past decade, high performance instruments are vital in the understanding of these 'omic' studies. One such instrument known as the LTQ Orbitrap Velos spectrometer (ThermoFisher Scientific Inc., USA)

uses quantitative mass spectrometric analysis to capture and measure ion frequencies which can, through intricate physics calculations, determine the mass/charge ratios of each individual amino acid in the sample (Hu et al., 2005).

A study performed on healthy human fibroblasts analysed the proteome of the mitochondria to detect the protein levels responsible for mitochondrial stress response and unbalanced metabolism (Palmfeldt et al., 2009). They cultivated the cells in both glucose and galactose – which is a medium that induces cellular stress. Using the Orbitrap, they found an increased level of respiratory chain proteins when cells were grown in the galactose medium. By using the Mascot database, they grouped all the proteins detected into different mitochondrial pathways, such as citric acid cycle, fatty acid oxidation, respiratory chain and apoptosis and mitochondrial morphology, and were able to determine the specific mechanisms occurring in the cells. This study is just one example of many that show the impact of the results of quantitative proteomics.

To date, only a handful of studies on proteomic analysis on PD patients have been performed, typically using mass spectrometry techniques such as 2D electrophoresis and matrix assisted laser desorption/ionisation time of flight (MALDI-TOF). One study identified 44 proteins using these techniques, of which nine were differentially expressed in PD SNc tissue (Basso et al., 2004). A second study focusing on large scale protein detection used MALDI-TOF and detected 16 differentially expressed proteins involved in ion and redox regulation as well as novel metabolic and structural functions (Werner et al., 2008). However, despite the success of these techniques, detection of hundreds of proteins is only possible when making use of a mass spectrometer such as the Orbitrap.

In knockout *parkin* mice models, 2D electrophoresis was performed to separate the proteins and thereafter MALDI-TOF was used as a mass spectrometer procedure (Palacino et al., 2004). This revealed a decrease in the abundance of a number of proteins involved in mitochondrial function and oxidative stress. In a second study using *parkin*-expressing HeLa S3 cells, the proteome changes in response to parkin activity were analysed after a 2 hour treatment with carbonyl cyanide m-chlorophenylhydrazone (CCCP), which aids in the recruitment of parkin to the mitochondria (Chan et al., 2011). A total of 2979 unique proteins were quantified, of which 766 were mapped in the MitoCarta inventory, which is a database of 1013 human genes encoding proteins specifically

localized to the mitochondria. K48-linked proteins were detected, which targets proteins for degradation via the UPS. The study also observed degradation of mitochondrial outer membrane proteins which is thought to precede mitophagy. This result suggests that the UPS and mitophagy are functionally linked, and stresses the importance of proteome studies in determining disease mechanisms for PD.

1.6.   The present study

Increasing evidence has linked PD with mitochondrial dysfunction, but there is still much debate on the exact mechanisms leading to dopaminergic cell death, and whether mitochondrial dysfunction is a cause or an effect. It is therefore important to conduct further comprehensive and conclusive studies to investigate the pathophysiology of this disorder. Ultimately, this may lead to the development of improved treatment modalities and neuroprotective strategies for individuals with PD and their at-risk family members.

In the present study we investigated South African PD patients with *parkin*-null mutations using a number of different approaches to determine whether these individuals exhibit evidence of mitochondrial dysfunction. There have been a limited number of studies on *parkin*-null patients and these have shown conflicting results. Previous studies also have limitations such as (1) not including heterozygous carriers to compare with the patients and wild-type controls (Müftüoglu et al., 2004; Mortiboys, et al., 2008; Grünewald et al., 2010); (2) not including analysis of muscle tissue from patients; and (3) not including analysis of the proteome. The present study was based on previous work but attempted to overcome these various shortcomings.

1.6.1. Hypothesis

It is hypothesized that mitochondrial dysfunction plays a major role in the development of PD in South African patients with null alleles of *parkin*. We would expect to detect a down-regulation in mitochondrial gene expression and also differences in the proteome between patients and controls.

In addition, it is hypothesized that these patients would exhibit mitochondrial structural defects and functionally show an increased mitochondrial ROS production.

1.6.2. Aims & Objectives

The aim of the present study was to determine whether mitochondrial dysfunction plays a role in the development of PD in specific South African patients who harbour two null alleles in the *parkin* gene (and therefore produce no functional parkin).

There are three South African families who harbour mutations in the *parkin* gene, and these were all recruited for this study. Also, family members who have a heterozygous *parkin* mutation (carriers) were included, and this will enable a comparison to be made between the carriers, the patients and the wild-type controls.

The objectives of this study were as follows:

1. To obtain peripheral blood samples, muscle biopsies and skin biopsies for culturing of fibroblasts from patients and carriers of three PD families with null mutations in *parkin*.
2. To analyse mitochondrial morphology in fibroblasts and muscle tissue.
3. To determine ROS levels in fibroblasts.
4. To analyse mitochondrial gene expression levels in peripheral blood samples.
5. To investigate expression of parkin protein in fibroblasts.
6. To investigate the proteome in fibroblasts.

*Initially, we had wanted to include patients with *PINK1*-null mutations for comparison with the *parkin*-null patients. However, we were unable to recruit the *PINK1*-null patients for this study.
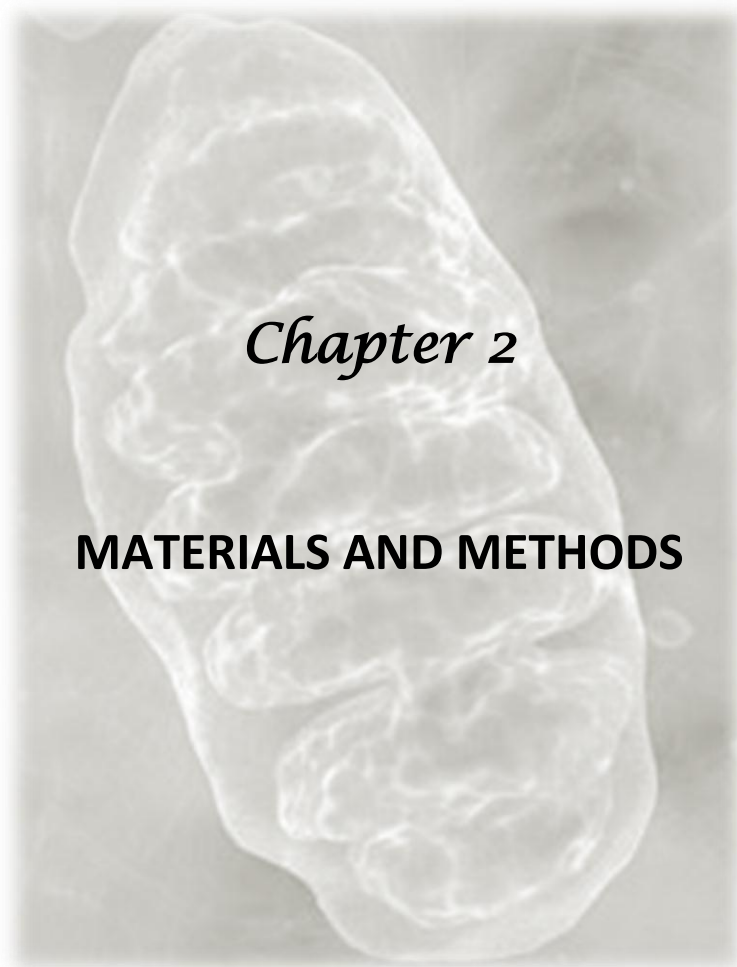
Chapter 2

MATERIALS AND METHODS

49

2.1.   Summary of methodology

Four PD patients with *parkin*-null mutations from three families were recruited for this study. Three tissue types were obtained from the patients – a peripheral blood sample, a skin biopsy and a muscle biopsy (Figure 2.1). Family members (unaffected carriers) and wild-type controls were recruited and from these skin biopsies and blood samples were obtained.

A muscle biopsy was performed on the probands for histological and transmission electron microscopy (TEM) mitochondrial morphology analysis. Muscle is the best tissue to observe mitochondrial morphological defects but the muscle biopsies were performed only on the three probands as part of their clinical work up. Due to the invasiveness of this procedure and the risks associated with it, muscle biopsies were not performed on the other study participants.

A skin biopsy was performed and fibroblasts were cultured which were then used in both structural experiments via TEM and mitochondrial network analysis, and functional (ROS measurement) experiments. A western blot was performed to confirm the absence of parkin in patient fibroblasts and proteome analysis was conducted in order to assess the effect that the lack of parkin has on fibroblast protein content, thus elucidating alterations in specific protein pathways associated with mitochondrial function.

A blood sample was obtained from each patient, and RNA was extracted for use in the two gene expression qRT-PCR studies – the PCR Array and the Primer Assay. Due to the high cost of the PCR Arrays only the three probands and a wild-type control were analysed using this technique.
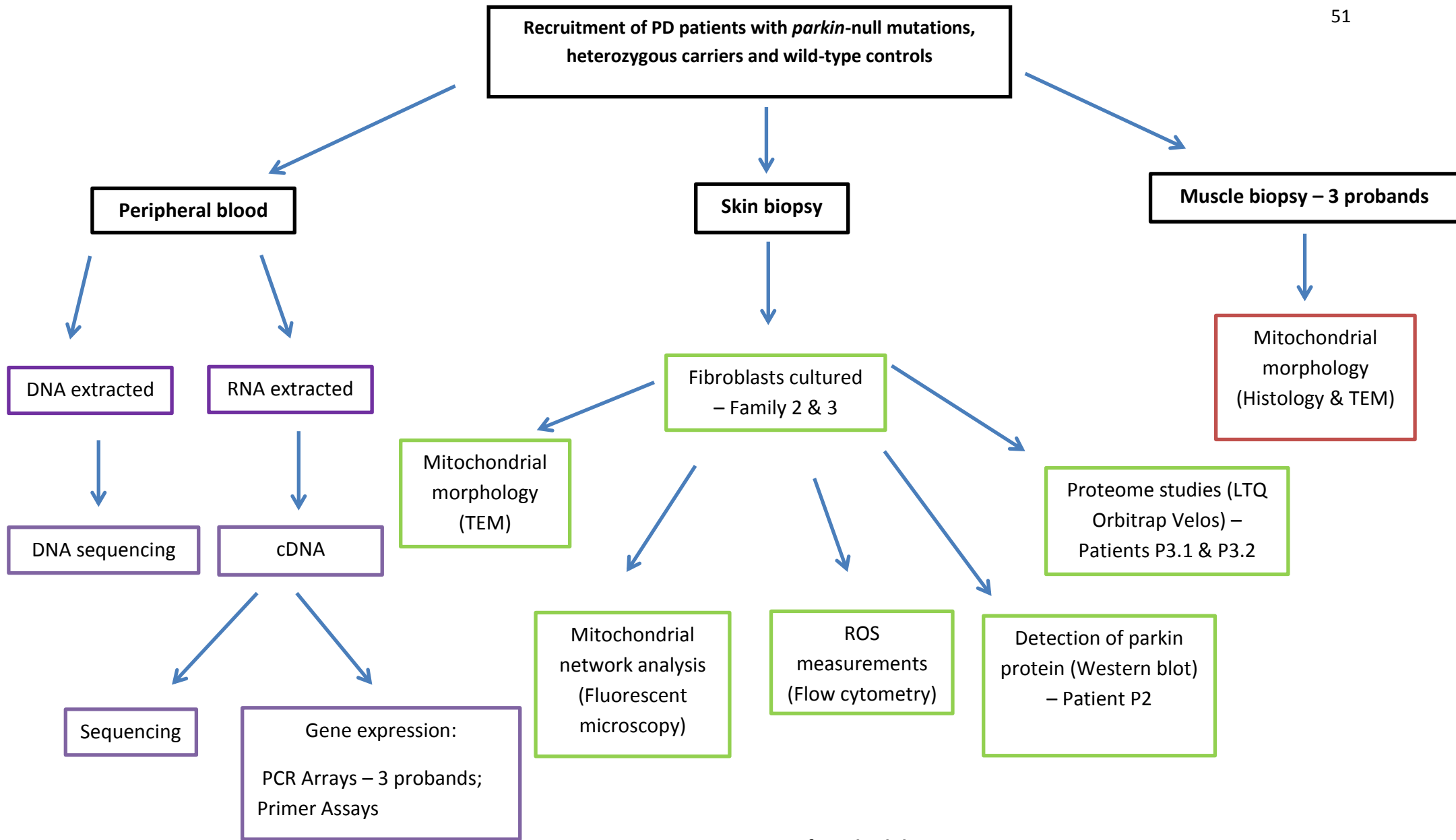
Figure 2.1: Summary of Methodology

2.2.   Ethical approval

This study was approved by the Committee for Human Research at Stellenbosch University (Protocol number: 2002/C059). The approval is renewed annually. All study participants were recruited with informed written consent.

2.3.   Patient and control selection

Over the past six years, patients suffering from PD have been recruited from the Movement Disorder clinic at Tygerberg Hospital, as well as the Parkinson's Association of South Africa. The patients were examined by a movement disorder specialist, Professor Jonathan Carr, and met the UK Parkinson's Disease Society Brain Bank Research criteria for diagnosis of PD (Gibb & Lees, 1988). Four patients that each have two null *parkin* mutations were selected for the study (designated P1, P2, P3.1 and P3.2, Table 2.1). Inclusion criteria were individuals with two *parkin* mutations, with familial PD and who had provided consent for a blood sample as well as muscle and skin biopsies. The mutations had been identified in previous studies using multiplex ligation-dependent probe amplification (MLPA) and DNA sequencing (Bardien et al., 2009; Keyser et al., 2010). Patient P1 has a 40bp deletion in exon 3 of one allele of *parkin*, and a whole exon 3 deletion on the other allele and patient P2 is homozygous for exon 3 and exon 4 deletions. Patients P3.1 and P3.2 are siblings, and are both homozygous for an exon 4 deletion. In effect, all these patients resemble 'knock out' models of *parkin*. For each patient recruited, a heterozygous carrier from the patient's family was also included (Table 2.1). Incorporated in the analysis, were two wild-type controls, WTC1 and WTC2. The control for the muscle biopsy was supplied by National Health Laboratory Service (NHLS) Histopathology Laboratory at Red Cross Children's Hospital.

Table 2.1: **List of patients, family members and controls included in the study.**

Family	Patient/ control	Status	Age and Gender	AAO	Length of disease	*Parkin* mutations
1	P1	PD patient – proband	38 years Male	25 years	13 years	• Het 40bp exon 3 del • Het exon 3 del
	P1het	Heterozygous mutation carrier - unaffected	71 years Female	-	-	• Het exon 3 del
2	P2	PD patient - proband	37 years Female	27 years	10 years	• Homo exon 3 and ex 4 del
	P2het	Heterozygous mutation carrier - unaffected	65 years Female	-	-	• Het exon 3 and ex 4 del
3	P3.1	PD patient - proband	50 years Female	27 years	23 years	• Homo exon 4 del
	P3.2	PD patient	52 years Female	27 years	25 years	• Homo exon 4 del
	P3het	Heterozygous mutation carrier - unaffected	54 years Female	-	-	• Het exon 4 del
	WT C1	Wild-type control	39 years Male	-	-	-
	WT C2	Wild-type control	36 years Male	-	-	-

*AAO, age at onset; het, heterozygous; homo, homozygous; del, deletion

2.4.   RNA extraction

After obtaining patient consent, 20ml blood was drawn into two PAXgene Blood RNA tubes
(PreAnalytix, Qiagen, Germany). The PAXgene Blood RNA Kit (PreAnalytix, Qiagen, Germany) was
used for isolation and purification of intracellular RNA from whole blood. The first step of
centrifugation (Centrifuge 5810 R, eppendorf, Germany) was performed to pellet nucleic acids.

Thereafter, the pellet was washed and resuspended, followed by manual RNA purification according to the manufacturer's instructions.

2.4.1. RNA Quality determination

2.4.1.1. *NanoDrop® N1000-UV-Vis Spectrophotometer (NanoDrop Technologies Inc., USA)*

The RNA quality was determined using the NanoDrop® N1000-UV-Vis Spectrophotometer (NanoDrop Technologies Inc., USA) and verified by the Experion StdSens Analysis Kit (BioRad, USA). The NanoDrop is made up of a spectrophotometer and linked to computer-based software. To blank the machine, 1.5µl of sterile water (EuroMed Inc., Denmark) was pipetted onto the sensor and read by the software. Thereafter, the sensor was wiped clean and 1.5µl of the RNA sample was pipetted onto it. The software then reads the concentration of the RNA. As efficient as the NanoDrop may be, it is not accurate enough for RNA studies. Thus, the Experion StdSens Analysis Kit was used to verify the results of the NanoDrop.

2.4.1.2. *Experion StdSens Analysis Kit (BioRad, USA)*

This kit involves the use of a 16-well chip and equipment whereby a virtual gel is run using the Experion machine. The reagents used were an RNA gel, RNA StdSens stain, RNA StdSens loading buffer and RNA ladder. All the equipment was calibrated and run according to the manufacturer's specifications. The Experion automatically measures the total RNA concentration, ratio of 28S/18S rRNA and the RQI (RNA Quality Indicator) value. The ratio 28S/18S is the ratio of two rRNA species that are derived from the same precursor molecule. Figure 2.2 indicates an example of the difference between a good quality RNA sample and a bad quality sample, based on the individual 28S/18S ratio. This ratio serves as an indication of RNA integrity. The RQI values are the equivalent to RIN (RNA Integrity Number) values, whereby a result out of ten is given that rates the quality of the RNA. The higher the result, the better the quality of the RNA. RNA with a value of 8 and above was used for all RNA-based experiments.
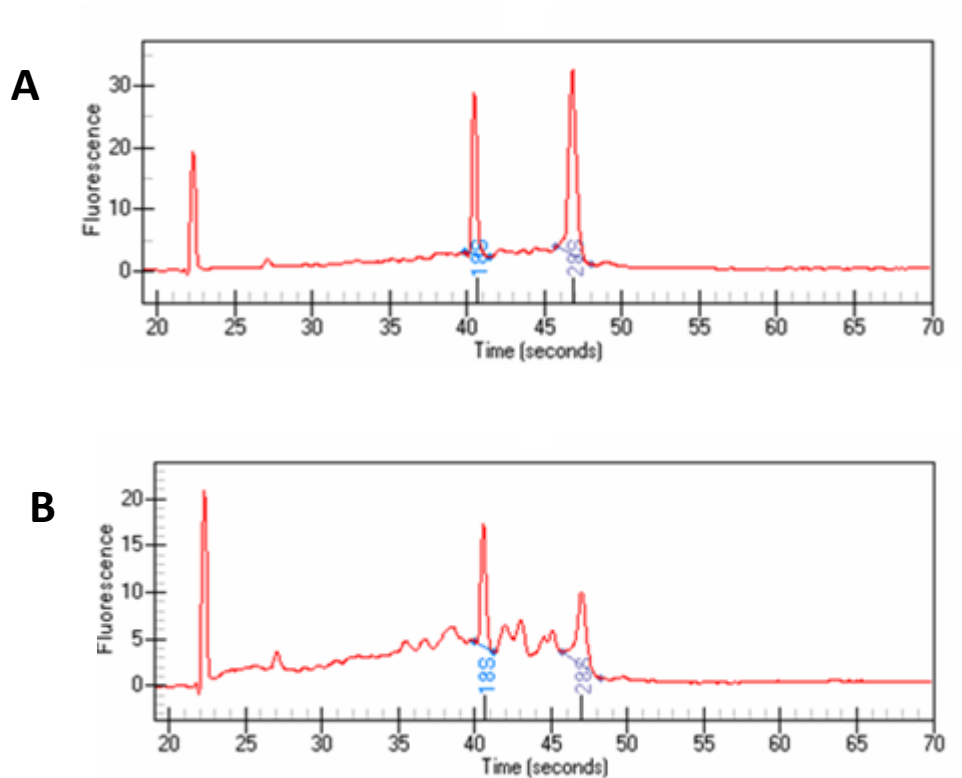
Figure 2.2: **Total RNA separation using Experion StdSens Analysis**. A. Example of a high quality RNA sample with a high 28S/18S ratio. B. Example of a low quality RNA sample with a lower 28S/18S ratio.

2.4.2. cDNA synthesis

RNA conversion into cDNA was carried out using the Quantitect Reverse Transcription Kit (Qiagen, Germany) in a two-step process. This kit provides a convenient procedure for effective reverse transcription as well as effective genomic DNA (gDNA) elimination. The first reaction involves the removal of gDNA by the gDNA wipeout buffer, and the second step is a reverse transcription reaction prepared by the addition of reverse transcriptase (Qiagen, Germany), RT buffer (Qiagen, Germany) and RT primer mix (Qiagen, Germany). The result is high yields of cDNA template for use in subsequent real-time PCR reactions.

2.5.   Polymerase Chain Reaction (PCR)

2.5.1.   Using cDNA as a template

All PCR primers (Table 2.2, Figure 2.3) were designed using Primer 3 software (Rozen & Skaletsky, 2000) and the sequences available from the GenBank database (http://www.ncbi.nlm.nih.gov/Entrez). The accession number used for PARK2 was NT_007422. Integrated DNA Technologies (IDT, USA) synthesized all primers. Calculation of the melting temperature was conducted using the following formula:

$$Tm = 4(G + C) + 2(A + T)$$

Table 2.2: PCR primers used for amplification of the PARK2 cDNA between exons 2 and 5

PCR primer orientation	Primer name	Primer Sequence	%GC	Primer Tm (°C)	Ta (°C)	Product size
Forward	PARK2 2i	5'-GGA GCT GAG GAA TGA CTG GA-3'	55%	56.4	60	555bp
Reverse	PARK2 5i	5'-ATC ATC CCA GCA AGA TGG AC-3'	50%	54.7		

*Tm, melting temperature; Ta, annealing temperature

GCAGCCGCCACCTACCCAGTGACCATGATAGTGTTTGTCAGGTTCAACTCCAGCCATGGTTTCCCAGT
GGAGGTCGATTCTGACACCAGCATCTTCCAGCTCAAGGAGGTGGTTGCTAAGCGACAGGGGGTTCCGG
CTGACCAGTTGCGTGTGATTTT   Exon 2

PARK2 2i FORWARD primer

CGCAGGGAAGGAGCTGAGGAATGACTGGACTGTGCAGAATTGTGACCTGGATCAGCAGAGCATTGTTC
ACATTGTGCAGAGACCGTGGAGAAAAGGTCAAGAAATGAATGCAACTGGAGGCGACGACCCCAGAAAC   Exon 3
GCGGCGGGAGGCTGTGAGCGGGAGCCCCAGAGCTTGACTCGGGTGGACCTCAGCAGCTCAGTCCTCCC
AGGAGACTCTGTGGGGCTGGCTGTCATTCTGCACACTGACAGCAGGAAGGACTCACCACCAGCTGGAA
GTCCAGCAGGTAGATCAATCTACAACAGCTTTTATGTGTATTGCAAAGGCCCCTGTCAAAGAGTGCAG
CCGGGAAAACTCAGGGTACAGTGCAGCACCTGCAGGCAGGCAACGCTCACCTTGA   Exon 4

PARK2 5i REVERSE primer

CCCAGGGGTCCATCTTGCTGGGATGATGTTTTAATTCCAAACCGGATGAGTGGTGAATGCCAATCCCCA   Exon 5
CACTGCCCTGGGACTAGTGCAGAATTTTTCTTTAAATGTGGAGCACACCCCACCTCTGACAAGGAAAC
ATCAGTAGCTTTGCACCTGATCGCAACAAATAGTCGGAACATCACTTGCATTACGTGCACAGACGTCA   Exon 6

```
GGAGCCCCGTCCTGGTTTTCCAGTGCAACTCCCGCCACGTGATTTGCTTAGACTGTTTCCACTTATAC     Exon 7
TGTGTGACAAGACTCAATGATCGGCAGTTTGTTCACGACCCTCAACTTGGCTACTCCCTGCCTTGTGT
GGCTGGCTGTCCCAACTCCTTGATTAAAGAGCTCCATCACTTCAGGATTCTGGGAGAAGAGCAGTACA     Exon 8
ACCGGTACCAGCAGTATGGTGCAGAGGAGTGTGTCCTGCAGATGGGGGGCGTGTTATGCCCCCGCCCT
GGCTGTGGAGCGGGGCTGCTGCCGGAGCCTGACCAGAGGAAAGTCACCTGCGAAGGGGGCAATGGCCT     Exon 9
GGGCTGTGGGTTTGCCTTCTGCCGGGAATGTAAAGAAGCGTACCATGAAGGGGAGTGCAGTGCCGTAT     Exon 10
TTGAAGCCTCAGGAACAACTACTCAGGCCTACAGAGTCGATGAAAGAGCCGCCGAGCAGGCTCGTTGG
GAAGCAGCCTCCAAAGAAACCATCAAGAAAACCACCAAGCCCTGTCCCCGCTGCCATGTACCAGTGGA     Exon 11
AAAAAATGGAGGCTGCATGCACATGAAGTGTCCGCAGCCCCAGTGCAGGCTCGAGTGGTGCTGGAACT     Exon 12
GTGGCTGCGAGTGGAACCGCGTCTGCATGGGGGACCACTGGTTCGACGTGTAGCCAGGGCGGCCGGGC
GCCCCATCGCCACATCCTGGGGGAGCATACCCAGTGTCTACCTTCATTTTCTAATTCTCTTTTCAAAC
ACACACACACACGCGCGCGCGCGCACACACACTCTTCAAGTTTT
```

Figure 2.3: **Representation of the 555kb fragment of *parkin* generated by PCR-amplification.** The blue and black font separates each exon in the 12 exon PARK2 gene

The cDNA synthesised from patient RNA was used as a template for PCR amplifications. PCR reactions were all performed on the GeneAmp® PCR system 2720 Thermal Cycler (Applied Biosystems, USA). The PCR reagents added included 20pmol of the forward and the reverse primers (Table 2.2), 75µM dinucleotide triphosphates (dATP, dGTP, dCTP, dTTP; Bioline Ltd., UK), 0.5 Units BIOTAQ™ DNA Polymerase (Bioline Ltd., UK), 1 X NH4 Buffer (Bioline Ltd., UK), 1.5mM MgCl2 (Bioline Ltd., UK) and ddH$_2$O (Euro Med, Denmark) to a final volume of 25µl.

PCR cycling conditions comprised of an initial denaturation step of 94°C for 5 min, followed by 30 cycles of denaturation at 94°C for 30s, annealing at 60°C for 1 min, extension at 72°C for 2 min 30 s and a final extension step of 72°C for 10 min. The PCR products were then run on a 2% Agarose (SeaKem®, USA) or PAGE gels (Section 2.6). After amplification, all PCR products were stored at -4°C until further use.

2.5.2. Using genomic DNA (gDNA) as a template

Total gDNA was isolated from blood samples by Mrs. Ina le Roux using an in-house method (Appendix III). The gDNA of two samples used as wild-type controls in this study (WTC1 and WTC2) underwent PCR amplification to screen for pathogenic mutations in each of the 12 exons of PARK2. PCR primers had been designed previously and Table 2.3 shows the PCR conditions and primer

sequence for each exon. PCR reactions and cycling conditions were as described in section 2.5.1. The PCR amplicons were electrophoresed on agarose gels (to determine whether they were the correct size) and then sequenced.

Table 2.3: **Primers designed to amplify the exonic regions of the PARK2 gene**

Region	Primer Sequence (number of bps)	Tm	%GC	PCR Ta	bp	PCR conditions
Exon 1	For: gaa cta cga ctc cca gca g (19)	60°C	58	55	300	5% Formamide
	Rev: ccc gtc att gac agt tgg (18)	56°C	56			
Exon 2	For: cac cat tta agg gct tcg ag (20)	60°C	50	55	313	5% Formamide
	Rev: tca ggc atg aat gtc aga ttg (21)	60°C	43			
Exon 3	For: tct cgc att tca tgt ttg aca (21)	58°C	39	55	364	No additives
	Rev: gca gac tgc act aaa caa aca (21)	62°C	43			
Exon 4	For: gct ttt aaa gag ttt ctt gtc (21)	56°C	33	55	299	No additives
	Rev: ttt ctt ttc aaa gac ggg tga (21)	58°C	38			
Exon 5	For: gga aac atg tct taa gga gt (20)	56°C	40	55	223	No additives
	Rev: ttc ctg gca aac agt gaa ga (20)	58°C	45			
Exon 6	For: cca aag aga ttg ttt act gtg (21)	58°C	38	55	276	No additives
	Rev: ggg gga gtg atg cta ttt tt (20)	58°C	45			
Exon 7	For: cct cca gga tta cag aaa ttg (21)	60°C	43	55	280	No additives
	Rev: gtt ctt ctg ttc ttc att agc (21)	58°C	38			
Exon 8	For: ggc aac act ggc agt tga ta (20)	60°C	50	55	232	No additives
	Rev: ggg gag ccc aaa ctg tct (18)	58°C	61			
Exon 9	For: tcc cat gca ctg tag ctc ct (20)	62°C	55	55	297	No additives
	Rev: cca gcc cat gtg caa aag c (19)	60°C	58			
Exon 10	For: caa gcc aga gga atg aat at (20)	56°C	40	53	272	No additives
	Rev: gga act ctc cat gac ctc ca (20)	62°C	55			
Exon 11	For: ccg acg tac agg gaa cat aaa (21)	62°C	48	55	300	No additives
	Rev: ggc acc ttc aca cag ct (20)	62°C	55			
Exon 12	For: tct agg cta gcg tgc tgg tt (20)	62°C	55	55	296	No additives
	Rev: gcg tgt gtg tgt gtg ttt ga (20)	60°C	50			

*bp, base pair; Tm, melting temperature

2.6.   Gel electrophoresis

2.6.1. Agarose gel electrophoresis

PCR products were run on a 2% agarose (SeaKem®, USA) gel. For a 100ml gel plate, 2grams of agarose was weighed out and dissolved in 100ml sodium borate (SB) buffer (Appendix II) in an Erlenmeyer flask. This was placed in the microwave and heated for approximately 2 min until the agarose was completely dissolved. It was then cooled down and 7μl of 1μg/μl ethidium bromide (EtBr) was added to the gel solution, which enables visualisation of the DNA fragments under a UV light. The gel solution was then poured into a gel tray and a well-forming comb was firmly placed in the gel.

Once the gel was set (15 min), the comb was removed and the samples were loaded. Approximately 2μl of Bromophenol Blue (Appendix II) loading dye was mixed with 8μl of the PCR product, and this was loaded into the first well of the gel. Each product was then loaded into separate wells of the gel, and 1.5μl of the 100bp or 200bp DNA ladder (Promega, USA) was loaded as a size marker to determine the size of the PCR fragments. The gel plate was attached to two electrodes, covered with SB buffer and electrophoresis was run at 240 volts for approximately 20 min. The gel was analysed under a UV light in the gel documentation (gel doc) system using the G: Box (Syngene, UK). The gel was placed under the Transilluminator and a live image was captured by the software (GeneSnap Image Acquisition Software).

2.6.2. Polyacrylamide gel electrophoresis (PAGE)

PAGE gels were used in order to detect PCR fragments that could not be resolved on an agarose gel, specifically fragments that had a small size difference (<50bp) between them.

Two 100mm x 80mm plates and two 80mm x 10mm x 1mm spacers were cleaned with 70% ethanol sprayed onto the surface and wiped with a paper towel. The spacers were placed on either side of the two plates in order to make room for the comb once the gel had been poured. The two plates were then sealed together at the bottom and the sides with gel-sealing tape (Sigma, Germany) and then clamped tight on both sides and the bottom. This is done to ensure that none of the gel solution will leak out whilst setting.

A 12% gel solution was then prepared with the following reagents: 6ml 40% acrylamide (Promega, USA), 120µl 10% APS (Ammonium-Perox-Disulphate), 45µl TEMED (Tertramethylethylenediamine; (Sigma, Germany), 1.5ml 10x TBE buffer (Appendix II) and 7.5µl ddH$_2$O. Immediately after the solution was made, it was poured between the two plates and the well-forming comb was placed in the gel between the two plates. This was then left to set for approximately 45 minutes.

Once the gel had set, the tape was removed from each side of the gel, and the comb was extracted using a spatula to avoid disrupting the wells. The plates were then added to an electrophoresis apparatus ensuring the plates were tightly clipped on using clamps. A dilution of 1 X TBE buffer (Appendix II) was then poured into the buffer chambers of the apparatus. Thereafter, 1.5µl of the 20bp, 100bp, 200bp or 500bp DNA ladder (Promega, USA) was loaded into the first well of the gel, depending on the size of the PCR fragment. A second size marker, Pst1-digested lambda DNA (Promega, USA), was loaded as a secondary DNA ladder so that a more accurate reading of the size fragments could be made. A minimum of 6µl of the PCR products was then mixed with 3µl Bromophenol Blue and loaded into the remaining wells. The cables were then connected to the voltage power and the gel underwent electrophoresis for approximately 1 hour to at 150V at room temperature.

Once the gel had run, it was removed from the plates and placed in a clean plastic trasdy. A solution of 50ml SB buffer and 5µl EtBr was made up and poured over the gel. This was placed on the orbital shaker SSL1 (Stuart®, UK) for 20 minutes. The solution was removed and ddH$_2$O was poured over the gel and left to shake for an additional 5 minutes. The gel was then visualised using the 6: Box gel doc system.

2.7.   DNA Sequencing

2.7.1. Purification of PCR products

Sequencing was performed to verify the DNA sequence of the PCR fragments. A volume of 8µl of each PCR product was pipetted into a 0.2ml microcentrifuge PCR tube (Sigma-Aldrich, USA), and this was purified with 5U of both *Exonuclease I* (USN Corporation, USA) and *SAP* (Shrimp Alkaline Phosphatase; Promega, USA). The samples were mixed and spun in the Hermle Z100M microcentrifuge (Labnet, USA) and then incubated at 37°C for 15 minutes followed by 80°C for 10 minutes to deactivate the enzymes. The concentration of each sample (ng/µl) was then read by the NanoDrop® ND1000-UV-Vis spectrophotometer (NanoDrop Technologies Inc., USA; Section 2.4.1). Each product was diluted down to 30ng/µl for the sequencing reaction.

2.7.2. Automated sequencing analysis

The primers used for sequencing were the same primers used during the PCR amplification and these were diluted to 1.1µM. All automated sequencing reactions of the PCR products were performed at the Central Analytical Facility of the Department of Genetics, Stellenbosch University using the BigDye terminator V3.1 Ready reaction kit on the ABI 3130xl ® Genetic analyser (Applied Biosystems, USA). Analysis of sequencing data was performed using the BioEdit Sequence Alignment Editor version 7.0.5 software (Hall, 1999).

2.8.   Culturing of skin fibroblasts

Skin biopsies were performed by Dr. Willie Visser (Department of Dermatology, Tygerberg Hospital) and these were taken from the inside of the upper arm. The 2mm x 2mm skin piece was suspended in a solution of DMEM with 10% fetal calf serum and 1% penicillin streptomycin and immediately transported to the Unistel Medical Laboratories (Pty) Ltd. at Tygerberg, Stellenbosch University for the culturing of skin fibroblasts (Appendix III).

2.8.1. Culture conditions

The fibroblasts cultured at Unistel Medical Laboratories used collagenase treatment in Chang D. and Amniochrome II media (1:1 ratio) at 37°C (Appendix III). Once the cells had reached confluency, they were used in various experiments for mitochondrial morphology analysis (TEM and mitochondrial network analysis), ROS measurement, Western blots and proteome analysis on the LTQ Orbitrap Velos spectrometer. Aliquots of fibroblast cells were frozen down in liquid nitrogen by Mrs. Ina le Roux (Appendix III) for use when needed.

2.9.   Mitochondrial morphology analysis from both muscle and skin biopsies

2.9.1. Analysis of mitochondrial morphology on muscle cells

A muscle biopsy was performed on patients P1, P2 and P3.1 by Dr. Franclo Henning at the Division of Neurology, Tygerberg Hospital. The biopsies were analysed by Dr. Komala Pillay at the NHLS Histopathology Laboratory at Red Cross Children's Hospital using histopathological and TEM analysis. This is a diagnostic service; therefore all patient samples were compared to the standard muscle pathology. Data was obtained in the form of reports and this was analysed and summarised.

2.9.2. Analysis of mitochondrial morphology on fibroblasts

After skin fibroblasts were cultured, the morphology of the fibroblasts was analysed using TEM by Dr. Nolan Muller from the NHLS, Electron Microscopy laboratory in the Division of Anatomical Pathology at Tygerberg Hospital. Images were loaded onto a CD-ROM and studied for morphological changes.

In addition, mitochondrial network analysis was performed by Dr. Ben Loos (Department of Physiological Sciences, Stellenbosch University) using fluorescence microscopy. Fibroblasts were stained using Mitotracker Red (Invitrogen, Life Technologies, USA) for the mitochondrial network and Hoeschst 3343 (Thermo Scientific, Pierce Biotechnology, USA) for the nucleus. They were plated on chambered coverglass (Nunc™, Denmark) and observed on an Olympus Cell^R system attached to an IX-81 inverted fluorescence microscope equipped with an F-view-II cooled CCD camera (Soft Imaging Systems). Using a Xenon-Arc burner (Olympus Biosystems GMBH, Germany) as light source, images were excited with the 360nm, 492nm or 572nm excitation filters. Emission was collected using a UBG triple-bandpass emission filter cube. For the image frame acquisition, an Olympus Plan Apo N 60x/1.4 oil objective and the Cell^R imaging software was used. Images were processed and background-subtracted using the Cell^R software.

2.10. Reactive oxygen species measurements using flow cytometry

In collaboration with Dr. Ben Loos (Department of Physiological Sciences, Stellenbosch University) ROS analysis was performed on the cultured fibroblasts.

All flow cytometric analyses were performed on a FACSAria flow cytometer (Becton Dickinson Biosciences, USA) equipped with a 488nm Coherent Sapphire solid state laser (13-20mW), 633nm JDS Uniphase HeNe air-cooled laser (10-20mW) and 407nm Point Source Violet solid state laser (10-25mW). Generic and mitochondrial ROS was assessed by using DCF and mitoSOX Red mitochondrial superoxide indicator respectively, according to manufacturer's protocol. In brief, relative ROS generation was evaluated with the aid of 6-carboxy-2'7'-dichlorodihydrofluoresce in diacetate, diacetoxymethyl ester (DCF, Molecular Probes, D399) and MitoSOX (M36008). Unfixed cells were incubated with 50µmol/l DCF in PBS for 20 min at 37°C, and then washed in PBS and immediately analysed at room temperature. Similarly, cells were incubated for 10 min at 37°C with 5 µM MitoSox reagent, and gently washed with warm buffer. A concentration of 100µmol/l H_2O_2 was used as a positive control. Samples were analysed on the flow cytometer (BD FACSAria I, BD Biosciences, USA) and a minimum of 50 000 events were collected. Fluorescence intensity signal was measured using the geometric mean on the intensity histogram.

2.11. Quantitative PCR using PCR Arrays and Primer Assays

2.11.1. RT² Profiler PCR Array (SABiosciences, USA)

The RT² Profiler PCR Array (SABiosciences, USA) was used to determine whether the expression levels of the genes involved in mitochondrial respiration are significantly different between PD patients and wild-type controls. A catalogued, 96-well plate for Mitochondrial Energy Metabolism (PHS-008) was chosen (Figure 2.4). In 84 wells of this plate (A1 – G12) are preloaded validated real-time PCR primers, each coding for a different gene in the mitochondrial energy metabolism pathway. Genes in this array include ATP synthases, cytochrome c oxidases and NADH dehydrogenases (Appendix IV). Five HKGs are also included on the PCR array as controls, namely GAPDH, actin-β, B2M, HPRT1 and RPL13A in wells H1 – H5. The plate also includes controls for gDNA contamination (H6), RNA quality/Reverse Transcription Control (RTC, H7 - H9) and general PCR performance/Positive PCR Control (PPC, H10 – H12).
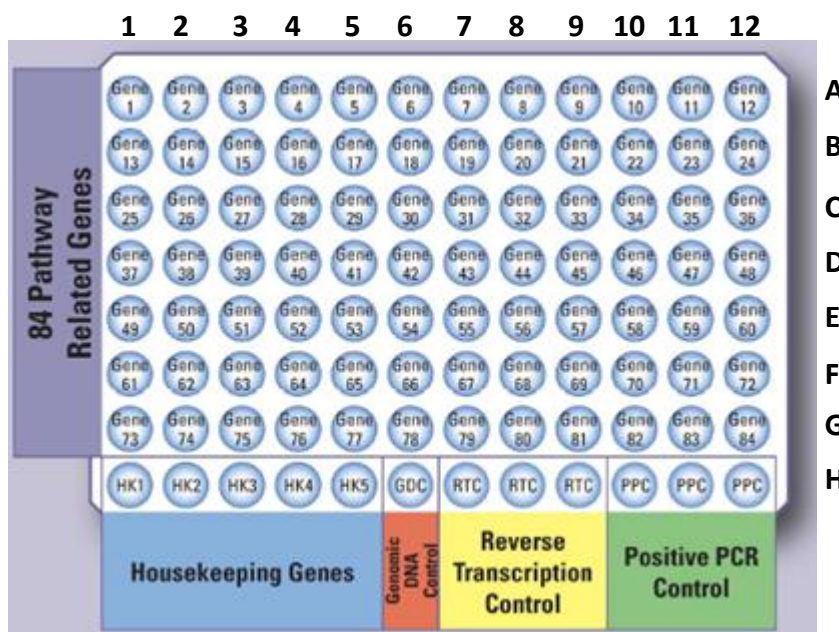
Figure 2.4: Standard PCR Array layout for a 96-well plate

Using the RT² First Strand Kit (SABiosciences, USA), 5µg patient and control RNA was separately converted to cDNA according to the manufacturer's user guidelines. A total of 102µl of the cDNA reaction was added to 1350µl RT² qPCR Master Mix (SABiosciences, USA) and RNase-free H_2O to a final volume of 2700µl. The master mix formulation enables the PCR Array to amplify 96 different gene-specific products simultaneously under uniform cycling conditions. This combination provides the PCR Array with the specificity and the high amplification efficiencies required for accurate real-time SYBR Green results.

Once the cocktail was made, 25µl was then added to each well of the 96-well plate by the EpiMotion (eppendorf, Germany). This was performed on patient and control samples. After centrifugation of each plate for 1 min at 1000xg on the Centrifuge 5810R (eppendorf, Germany), the 'patient' plate was placed in the ABI 7900HT (Applied Biosystems, USA), a fast real time PCR system, situated at the Central Analytical Facility's satellite laboratory at Tygerberg. The 'control' plate remained in the freezer for the duration of the first plates run. The system was run for 1 cycle at 95°C for 10 min, and 40 cycles at 95°C for 15s and 60°C for 1 min, and a dissociation melting curve was included at 1 cycle at 95°C for 15s, 60°C for 15s and 90°C for 15s. The 'patient' plate was then removed, covered in aluminium foil and stored at -20°C. The real time PCR conditions were repeated for the 'control' plate. After both plates were run, the threshold value was manually set so that the Ct values in the PPC wells were 20 ± 2, as per manufacturer's instructions. Automatic ΔΔCt based fold-change calculations were then performed using the raw threshold cycle data via the software provided (http://sabiosciences.com/pcrarraydataanalysis.php).

2.11.2. RT² Primer Assay (SABiosciences, USA)

The RT² Primer Assay (SABiosciences, USA) was utilized as a confirmation for the results obtained from the RT² Profiler PCR Array (SABiosciences, USA).

The first step in the RT² Primer Assay gene expression protocol is the elimination of gDNA and subsequent reverse transcription of RNA to produce cDNA. This was performed by the RT² First Strand Kit (SABiosciences, USA). The cDNA was then added to the RT² qPCR mastermix, the RT² qPCR

Primer assay and RNase-free H_2O. The gene of interest selected was *CYC1*, and the two house-keeping genes chosen were *HPRT1* and *RPL13A*. A standard curve was conducted for each gene so as to determine the efficiency value (should be approximately 1) which was calculated by REST-2009© gene quantification software (http://www.gene-quantification.de/rest.html). All reactions were performed in triplicate and gDNA was included as a negative control. The final volume was pipetted into each well in a 96-well plate (Lasec, SA). The run was performed on an ABI 7900HT (Applied Biosystems, USA) for 1 cycle at 95°C for 10 minutes, and 40 cycles at 95°C for 15 seconds and 60°C for 1 minute. A dissociation melting curve was added for 1 cycle at 95°C for 15s, 60°C for 15s and 90°C for 15s. Data was analysed using REST (relative expression software tool) gene-quantification software.

2.12. Protein analysis

2.12.1.   Cell lysis procedure

Prior to cell lysis, a cell lysis buffer was made (Appendix II).This was stored on ice until future use. Once the fibroblast cells in the culture flasks were trypsinized and concentrated in a 50ml tube, the supernatant was removed and the pellet was suspended in 200μl PBS (Appendix II). This solution was added to 2ml tubes and centrifuged at 7000rpm for 30s in the PRISM microcentrifuge (Labnet, USA). The supernatant was removed and an additional 500μl PBS was added to the pellet. This solution was then mixed in order to disrupt the pellet and re-centrifuged under the above conditions. Thereafter, 200μl of cell lysis buffer was added to the newly formed pellet, and this was kept on ice for 30min. The tubes were then centrifuged (UEC13, United Scientific, USA) for a further 10 minutes at 120rpm at -20°C. The supernatant was removed and stored in 2ml tubes at -20°C for future use.

2.12.2.   Bradford protein concentration determination

In order to calculate a standard curve of protein concentrations, 10µl of a dilution range of bovine serum albumin (BSA) standards ranging from 0 - 1000µg/µl was loaded into the wells of a luminometer plate (Nunc™, Denmark) in duplicate. A volume of 1µl of cell lysate samples were also added to the plate in duplicate. Thereafter, 200µl of Bradford reagent (Appendix II) was added to each standard and lysate sample. The protein concentration of each well was determined by a Synergy HT luminometer (BioTek Instruments Inc., USA). Using the KC4™ v 3.4 software (BioTek Instruments Inc., USA), a standard curve was set up and each sample's protein concentration was calculated.

2.12.3.   Western Blot

The Western Blot technique is a procedure for the identification and measurement of the amount of a specific protein in a cell. Proteins isolated from fibroblasts are separated by gel electrophoresis (SDS-PAGE) and then transferred to a nitrocellulose membrane which in turn is subject to immunodetection. A primary and secondary antibody is then added for detection and labelling of a specific protein, which in this case was parkin. All equipment and apparatus used in the Western blot procedure were supplied by BioRad, USA.

2.12.3.1.   Gel casting

Two 100mm x 74mm glass plates were sprayed with 70% ethanol and wiped down using a paper towel. Once the plates were clipped together, an Agarose (SeaKem®, USA) solution was heated up in the microwave and pipetted onto the bottom of the plates using a Pasteur pipette. This is done to avoid leakage out of the plates when the gel solution is left to set. A 12% resolving gel solution (Appendix II) was first prepared and poured between the two plates, leaving about a 20mm space from the top of the plates. One layer of Isopropanol was then added to the top of the resolving gel solution. This was left to set for 20 minutes.

Once the resolving gel had set, the stacking gel solution (Appendix II) was made up. Prior to addition of the stacking gel, the isopropanol was poured out and absorbed by filter paper. The stacking gel was then added to the top of the plates, and a well-forming comb was slid in between the plates. This was left for 20 minutes to set.

2.12.3.2.   Running gel

Once the gel was set, the plates were placed in a holding apparatus, with the shorter plate facing inwards. When only one gel was being run, a second makeshift plate known as the Buffer Dam was added for balance. The holding apparatus was then placed in a container. A 1x SDS Running Buffer was made up from 10x SDS Running Buffer (Appendix II), and this was poured into the container first between the two plates and then filled up to the level labelled '2 gels'. The comb was then removed from the gel.

Samples were denatured for 5 minutes at 95°C in the GeneE Thermal Cycler (Techne Inc., USA). After spinning down the samples in the Hermle Z100M microcentrifuge (Labnet, USA), the calculated amount of sample was mixed with 5µl SDS loading dye (Appendix II) and loaded into each well of the gel. A volume of 10µl of the Spectra Broad Range protein ladder (Fermentas, Lithuania) was loaded into a separate well. A lid was placed on the container with electrodes that attached to the voltage power source and the gel was run for approximately one hour at 100V.

2.12.3.3.   Transferring gel

Transfer Buffer was freshly prepared (Appendix II). Six 85mm x 5mm pieces of filter paper were cut, as well as one 8.5mm x 5mm polyvinylidene fluoride (PVDF) nitrocellulose transfer membrane (Amersham Biosciences, USA). The membrane was soaked in pure methanol (Merck, Germany) for 15 seconds and then transferred to a container with ddH$_2$O and placed on the orbital shaker SSL1 (Stuart®, UK) for 5 minutes. It was then removed from the ddH$_2$O and placed in a container with Transfer Buffer and placed on the shaker for 20 minutes. The 6 pieces of filter paper and 2 sponges were left to soak in a container with Transfer Buffer for 20 minutes.

A sandwich was made with all the elements needed for the transfer. The two sponges were placed on the outside, 3 pieces of the filter paper on the inside of each of the sponges, and lastly the gel and membrane in the middle. A roller was used to ensure no bubbles were present. This was then placed in a transfer container (BioRad, USA) next to a block of ice, and was positioned on a magnetic stirrer with a magnet placed in the centre of the container. The apparatus was then filled with Transfer Buffer. It was connected to the voltage power and ran for 1 hour at 100V.

2.12.3.4. Membrane blocking

Following the transfer of proteins from the SDS PAGE gel onto the PVDF membrane, the membrane was removed from the transfer apparatus and rinsed with ddH$_2$O for 5 minutes on the shaker. The membrane was then either blocked with 5% fat free milk (Elite, Weigh-Less) dissolved in TBST (Appendix II) or in BSA in order to determine optimal blocking medium for the antibodies used. This was placed in the shaker for 1 hour to eliminate non-specific binding of the antibodies.

2.12.3.5. Addition of Primary antibody

Following the membrane blocking, the PVDF membrane was briefly rinsed twice with TBST. Thereafter, the primary antibody was added to milk in TBST according to the optimal ratio (Table 2.4). Initially, a polyclonal goat antibody against parkin (Abcam, UK) was used at a dilution of 1:2000, however due to lack of success, the primary antibody was changed to a monoclonal mouse antibody against parkin (Cell Signalling Technology, USA). The membrane was then incubated overnight with the antibody-milk mixture on the shaker (Labcon, USA) at 4°C.

2.12.3.6. Addition of Secondary antibody

Following the incubation period, the membrane was briefly rinsed twice with TBST, followed by a 20 minute wash with TBST on the orbital shaker. The TBST was then replaced and three additional wash steps of 5 minutes each ensued, with fresh changes of TBST in between. The appropriate ratio of secondary antibody (Santa Cruz Biotechnology, USA) to milk in TBST (Table 2.4) was then added to the membrane and placed on the orbital shaker at room temperature for 1 hour. Thereafter, the membrane was washed with the same washing protocol used after the primary antibody incubation.

Table 2.4: Antibodies and antibody concentrations used in the Western blot assays

ANTIGEN	PRIMARY Ab AND MANUFACTURER	OPTIMUM RATIO	SECONDARY Ab	OPTIMUM RATIO	PRODUCT SIZE
Parkin	ab7295 Goat polyclonal Ab to parkin (Abcam, Biocom Biotech)	1:5000	Donkey anti-goat	1:5000	65kDa
	Parkin (PARK8) Mouse monoclonal Ab (Cell Signalling Technology)	1:500	Donkey anti-mouse	1:2000	50kDa

*Ab, Antibody

2.12.3.7. *Chemiluminescent visualization of membrane proteins using the SuperSignal® West Pico Chemiluminescent Substrate kit*

After all excess secondary antibody was removed from the PVDF membrane; all reagents needed for processing of the film were taken to the dark room (FISAN building, Faculty of Medicine and Health Sciences, Stellenbosch University). The two substrate components of the SuperSignal® West Pico Chemiluminescent Substrate kit (Thermo Scientific, Pierce Biotechnology, USA), viz. the SuperSignal West Pico Luminol/Enhancer solution and the SuperSignal West Pico Stable Peroxide solution, were mixed in a 1:1 ratio. The membrane was subsequently incubated in this solution for 5 minutes under the red light in the dark room. The excess solution was removed from the membrane by lightly tapping the corner of the membrane onto a dry paper towel. The membrane was then placed inside an autoradiography cassette and covered with a transparent plastic sheet. Two glow-in-the-dark stickers were placed in each top corner in the cassette to aid in orientation of the film once processed. Autoradiography film (Eastman Kodak Company, USA) was placed over the membrane and the cassette was closed. Exposure time varied from 10 seconds to 10 minutes, depending on the strength of the signal. The film was processed by the Hyperprocessor™ automatic autoradiography film processor (Amersham Pharmacia Biotech UK Ltd., UK). The size of the protein was determined when placing the film against the protein ladder on the membrane. Dr. Chrisna Swart from the Division of Molecular Biology and Human Genetics, Stellenbosch University, assisted with optimisation and protein detection in the western blot procedure.

2.12.4.   Proteome analysis

Proteome analysis was performed on fibroblasts from patients P3.1 and P3.2, unaffected control WTC2 and heterozygous carrier P3het in collaboration with Dr. Salome Smit at the Central Analytical Facility (Faculty of Medicine and Health Sciences, Stellenbosch University). This was performed on the LTQ Orbitrap Velos mass analyser (ThermoFisher Scientific Inc., USA), which is able to detect thousands of proteins from one tissue type. The Orbitrap (Figure 2.5) employs electric fields to capture and confine ions. The ions move from the linear ion trap into the C-trap, and converge on the entrance into the Orbitrap. Ions of each mass-to-charge ratio arrive at the entrance of the Orbitrap and begin coherent axial oscillation. By Fast Fourier Transformation (FFT) of the amplified current, the instrument obtains the frequencies of these axial oscillations and therefore mass-to-charge ratios of the ions by calculation. Because every peptide oscillates at a different speed, the peptides can be fragmented and the amino acid sequence can be detected.

Thermo Proteome Discoverer 1.3 software (Thermo Scientific, Germany) was used to identify proteins via automated database searching (Mascot, Matrix Science, UK and Sequest) of all tandem mass spectra against the IPI Human database (downloaded July 2011). Carbamidomethyl cysteine was set as fixed modification, and oxidized methionine, N-acetylation and deamidation (NQ) was used as variable modifications. The precursor mass tolerance was set to 10ppm, and fragment mass tolerance set to 0.8Da. Two missed tryptic cleavages were allowed. Proteins were considered positively identified when they were identified with at least two tryptic peptides per proteins, a Mascot or Sequest score of more that $p < 0.05$ as determined by Proteome Discoverer 1.3. Percolator was also used for validation of search results. In Percolator a decoy database was searched with a FDR (strict) of 0.02 and FDR (relaxed) of 0.05 with validation based on the q-value. Proteins identified in the fibroblasts were analysed using IPA software (Ingenuity Systems, USA) to find pathways that are associated with various cellular networks and disorders.
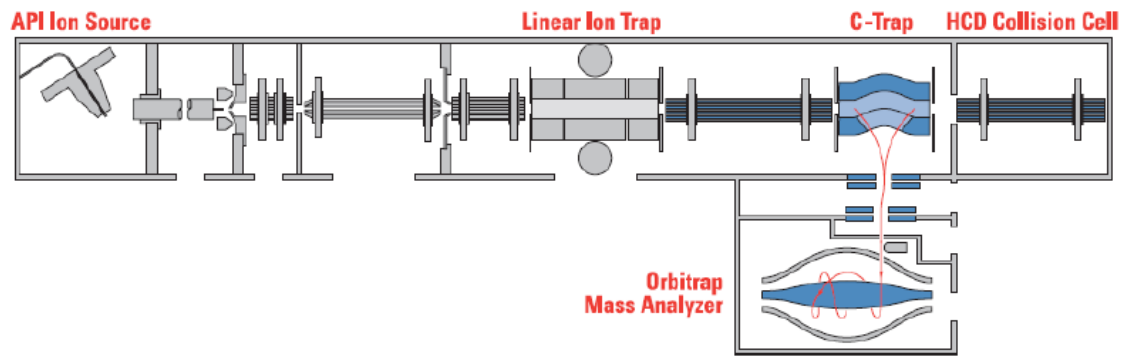
Figure 2.5: Diagram of the LTQ Orbitrap Velos spectrometer

Chapter 3

RESULTS

3.1. Sampling of PD patients and controls

3.1.1. Biological samples obtained from patients and controls

In the present study, we attempted to identify evidence for mitochondrial dysfunction at the morphological, functional, as well as gene and protein expression levels of PD patients. For these experiments, we needed to obtain a range of biological specimens from the patients and controls (Table 3.1). Four *parkin*-null PD patients from three separate families were recruited for this study, namely patients P1 (family 1), P2 (family 2), and P3.1 and P3.2 (family 3). From the wild-type control WTC1, only a blood sample had been obtained and this was used as a control for the gene expression studies whereas from wild-type control WTC2 we were able to obtain a skin biopsy, and this was used as a control for the morphological, functional and protein expression studies.

Table 3.1: **List of biological samples obtained from PD patients, heterozygotes and wild-type controls**

Patient / carrier/ control	Muscle biopsy	Skin biopsy / fibroblasts cultured	Peripheral blood sample for RNA studies
P1	✓	✗	✓
P1het	✗	✗	✓
P2	✓	✓	✓
P2het	✗	✓	✓
P3.1	✓	✓	✓
P3.2	✗	✓	✓
P3het	✗	✓	✓
WTC1	✗	✗	✓
WTC2	✗	✓	✗

✓, sample obtained; ✗, sample not obtained

The fibroblasts cultured from the skin biopsies were used for the majority of the experiments in this study. Biopsies of the substantia nigra would have been an ideal tissue to use, but fibroblasts have been used as a proxy tissue in many similar studies (Auburger et al., 2012) and parkin has previously been shown to be expressed in this particular cell type (Mortiboys et al., 2008; Pacelli et al., 2011). Fibroblasts were successfully cultured from all the patients and carriers except for patient P1 and P1het. In their case, a skin biopsy had been taken from patient P1 and his spouse (intended for use as a wild-type control at the time); however the samples were mistakenly sent to the wrong laboratory and subsequently did not grow. Since patient P1 and his spouse had travelled from another Province down to Cape Town to donate the samples, we were unable to repeat the procedure. Therefore in this case, the ROS functional analysis was performed using leukocytes, or white blood cells (WBC), and the proteome analysis was performed on cultured lymphocytes obtained from these individuals. Lymphocytes are T- and B- cells that account for 25-35% of the WBCs.

3.1.2. Confirmation of *parkin* deletions

Sequencing of the cDNA from these PD patients confirmed the presence of the deletions in *parkin* (Figure 3.1).

C
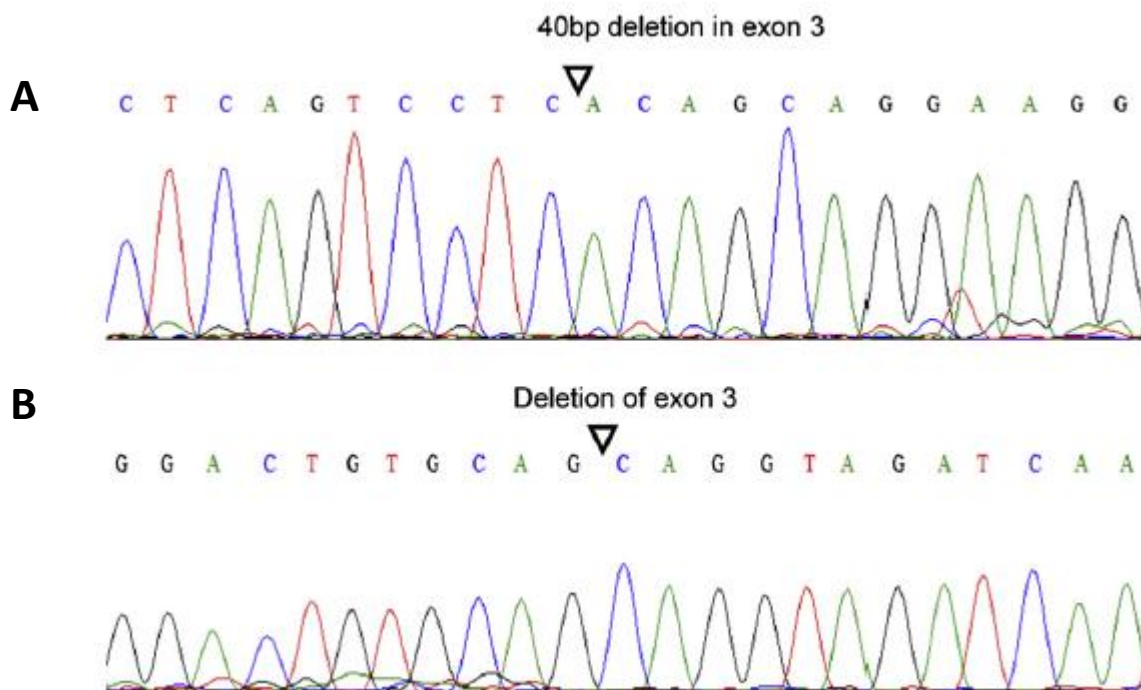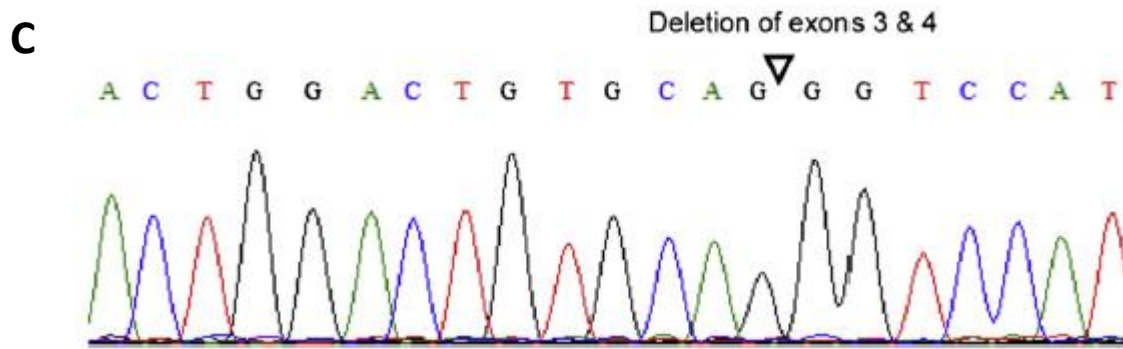
Figure 3.1: **Representative results of deletions present in parkin in patients recruited for this study.** The positions of the deletions are indicated. A. 40bp deletion in exon 3; B. Whole exon 3 deletion; C. Whole exons 3 & 4 deletion. Taken from: Haylett et al., 2011

3.1.3. Exclusion of *parkin* mutations in wild-type control samples

Sequencing of the *parkin* gene in both wild-type controls (WTC1 and WTC2) was performed to ensure that there are no mutations in the gDNA of these individuals. All 12 exons were screened and the results confirmed that both controls did not harbour any non-synonymous or nonsense pathogenic mutations, small indels or homozygous exonic deletions in *parkin* (Table 3.2). An intronic variant was found in both controls, with a G to A base pair change in intron 7 (IVS7 – 35G>A). A second intronic variant was found in WTC2, with a T to C base pair change in intron 2 (IVS2 + 25T>C). In addition, an exonic variant was present in exon 4 of WTC2 (S167N), causing an amino acid change from serine (S) to asparagine (N). The frequency of the A allele is 0.042 (n = 4550 chromosomes) indicating that this variant is a common polymorphism. All these variants are non-pathogenic polymorphisms according to dbSNP and Ensembl (http://www.ncbi.nlm.nih.gov/snp; www.ensembl.org)

Table 3.2: **Results from sequencing of *parkin* for WTC1 and WTC2**

Exon	WTC1	WTC2
1	No variants; wild-type	No variants; wild-type
2	No variants; wild-type	IVS2 +25 T>C
3	No variants; wild-type	No variants; wild-type
4	No variants; wild-type	S167N rs1801474
5	No variants; wild-type	No variants; wild-type
6	No variants; wild-type	No variants; wild-type
7	No variants; wild-type	No variants; wild-type
8	IVS7 -35 G>A	IVS7 -35 G/G>A/A
9	No variants; wild-type	No variants; wild-type
10	No variants; wild-type	No variants; wild-type
11	No variants; wild-type	No variants; wild-type
12	No variants; wild-type	No variants; wild-type

3.2.   Analysis of mitochondrial morphological changes

Mitochondria that are dysfunctional typically present with gross morphological defects including swollen, enlarged mitochondria, with disorganized membrane compartments and degenerating electron dense matrices. As parkin is thought to play a role in maintaining healthy mitochondria, we sought to determine whether there was any evidence for defective or misshapen mitochondria in the PD patients with two null mutations in *parkin*.

3.2.1. Mitochondrial morphology in muscle biopsies

The muscle biopsies of the three probands were analysed using histology and TEM to examine mitochondrial morphology. The findings suggested subtle changes in the morphology among all three patients; however the extent of mitochondrial damage differed across the three individuals.

Histological analysis showed little similarity across patients, with the exception of the absence of ragged red fibres found in all three patients (Table 3.3). Ragged red fibres are irregular skeletal muscle fibres associated with mitochondrial disease. These fibres accumulate in damaged mitochondria, thus acting as a universal indicator of mitochondrial abnormality. However, despite the absence of these fibres, several other fibre-based indicators of morphological differences are apparent. Although patient P2 showed no indication of atrophic fibres, patient P1 presented with scattered atrophic fibres, and patient P3.1 exhibited scattered elongated atrophic fibres. Grouping of type II fibres were observed in two patients (P2 and P3.1) and a predominance of these fibres were observed in patient P3.1. These are fast twitch muscle fibres that utilize anaerobic metabolism to produce energy. They have a much faster rate of fatigue, and contain less mitochondria than type I fibres. The ATP generation of type II fibres is predominantly through glycolysis, not via oxidative phosphorylation, suggesting a noticeable metabolic change within these patient cells.

Interestingly, there appeared to be a correlation between the defects and the duration of the disease – patient P2 had a shorter duration (10 years) than patients P1 (13 years) and P3.1 (23 years). Both patients P1 and P3.1 exhibited scattered atrophic fibres as well as variation in muscle fibre size which has been associated with the ageing process (Brunner et al., 2007). Sarcolemmal accentuation of enzymes also correlated with the length of the disorder – from normal in patient P2, mild in patient P1, and extensive accentuation in patient P3.1. This could also explain why patient P3.1 shows the presence of cytochrome oxidase, an oxidizing enzyme that acts at the end terminal of the respiratory chain, with the main function of electron transport. This increased presence may be suggestive of a possible compensatory mechanism by the damaged mitochondria. Results from patient P3.1 also suggest that her muscle portrays features of a possible neurogenic aetiology, which is due to the large extent of focal grouping of type II fibres. However patients P1 and P2 fibre

analysis did not appear to suggest such a cause. This result further indicates the more severe morphological changes observed in patient P3.1 in comparison to patients P1 and P2.

The results from the electron microscopy analysis (Table 3.3) also suggest subtle features of mitochondrial abnormality in both patients P1 and P3.1. All three patients' mitochondria illustrate wrinkling of the sarcolemmal membrane that is indicative of muscular atrophy, sub-sarcolemmal aggregates of mitochondria and the absence of inclusions. Both patients P1 and P3.1 exhibit an increase in the glycogen and lipid content of these mitochondrial aggregates, and an increase in these substrates was also observed in the histological analysis of patient P2. Patient P3.1 also exhibits the presence of lipofuscin, which are involved in protein storage and have lipid-containing residue. These granules are indicative of protein degradation and mitochondrial damage, and are known to accumulate with age. Most notable, however, are that in both the histological and TEM analysis more prominent and enlarged mitochondria were observed in patient P3.1. Although not grossly oversized, this is a clear indication of mitochondrial dysfunction.

Table 3.3: Results from the muscle biopsy analysis of mitochondrial morphology in terms of histology and transmission electron microscopy in patients P1, P2 and P3.1

Histological analysis of muscle cells			
Patients	**P1**	**P2**	**P3.1**
Muscle fibres	No ragged red fibres	No ragged red fibres	No ragged red fibres
	Scattered **atrophic fibres**	No atrophic fibres	Scattered elongated **atrophic fibres**
	No predominant fibre type	No predominant fibre type	**Predominantly type II fibres**
		Focal grouping of type II fibres	**Focal grouping** of type II fibres
	Mild variation in muscle size	Minimal variation in muscle size	Predominantly small muscle fibres with mild variation in size and shape

			Mitochondria appear slightly more prominent
Cell cytoplasm content	Sarcoplasmic **lipid mildly increased** in static fibres	Small amount of **intraplasmic lipid present**	No increase in sarcoplasmic lipid
	Mild sarcolemmal accentuation of enzymes	Normal sarcolemmal accentuation of enzymes	Extensive sarcolemmal accentuation of enzymes
			Cytochrome oxidase present
Conclusions	Focal isolated markedly **atrophic cells present**	Muscle biopsy within normal limits	Subtle features of **neurogenic aetiology**
	Subtle mitochondrial changes of uncertain insignificance		**Primary or secondary subtle mitochondrial changes**
Transmission Electron Microscopy of muscle cells			
Muscle fibres	**Wrinkling of sarcolemmal membrane** (indicative of atrophy)	**Wrinkling of sarcolemmal membrane** (indicative of atrophy)	**Wrinkling of sarcolemmal membrane** (indicative of atrophy)
Cell cytoplasm content	Sub-sarcolemmal **aggregates** of normal mitochondria	Sub-sarcolemmal **aggregates** of normal mitochondria	Sub-sarcolemmal and inter myofibrillar **accumulations** of normal mitochondria
	Aggregates associated with **increased lipid and glycogen**	No increased lipid or glycogen	Scattered **lipid droplets and lipofuscin**
	No inclusions	No inclusions	No inclusions
			Slightly enlarged mitochondria
Conclusions	Features suggestive of **primary or secondary mitochondrial abnormality**	Biopsy within normal limits	**Subtle mitochondrial abnormality**
Patient details			
Length of disease	13 years	10 years	23 years
Current age	38 years old	37 years old	50 years old

3.2.2. Mitochondrial morphology in cultured fibroblasts from skin biopsies

Morphological analysis was also performed on fibroblasts obtained from the patients (P2, P3.1, and P3.2), the heterozygous mutation carriers (P2het, P3het) and the wild-type control (WTC2). Previous studies on fibroblasts of *parkin*-mutant patients found gross morphological changes, with one particular study reporting on swollen mitochondria with disorganized membrane compartments as well as lysosomal vacuoles filled with electron dense material possibly indicative of degenerating mitochondria (Pacelli et al., 2011). As the mitochondrial abnormalities observed in the muscle tissues had been subtle, it was necessary to determine whether the extent of the defects in the fibroblasts were similar to that found in the muscle tissues of these patients.

 The morphology, using TEM, of the wild-type control fibroblasts is shown in Figure 3.2. The nucleus (Figure 3.2 B), ER (Figure 3.2 B) and round, rod-shaped mitochondria (Figure 3.2 A, B) are clearly visible. Analysis of the mitochondria show normally arranged cristae (Figure 3.2 B) that are very dark in colour, which is indicative of a highly electron dense matrix, suggesting that the mitochondria are healthy and undergoing constant oxidative phosphorylation. Many autophagic vacuoles (autophagosomes) are also present in the fibroblasts (Figure 3.2 B). The few vacuoles that are darker in colour (Figure 3.2 C) indicate activity and possible fusion of a lysosome with an autophagosome to form an autolysosome; however this activity is normal in healthy cells at a low level. Figure 3.2 C shows an example of mitochondrial fusion. The purpose of mitochondrial fusion is to protect mitochondrial function by preventing the accumulation of damaged mtDNA and to respond more efficiently with the metabolic demands of the cell.

A, WTC2
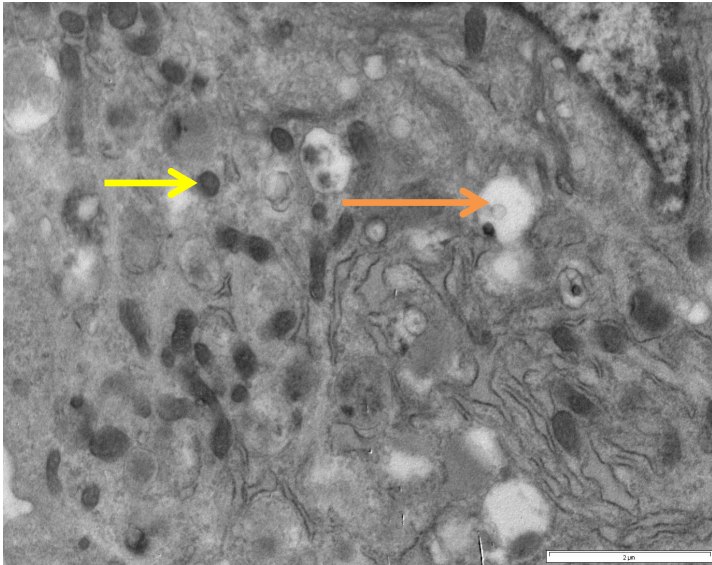
B, WTC2
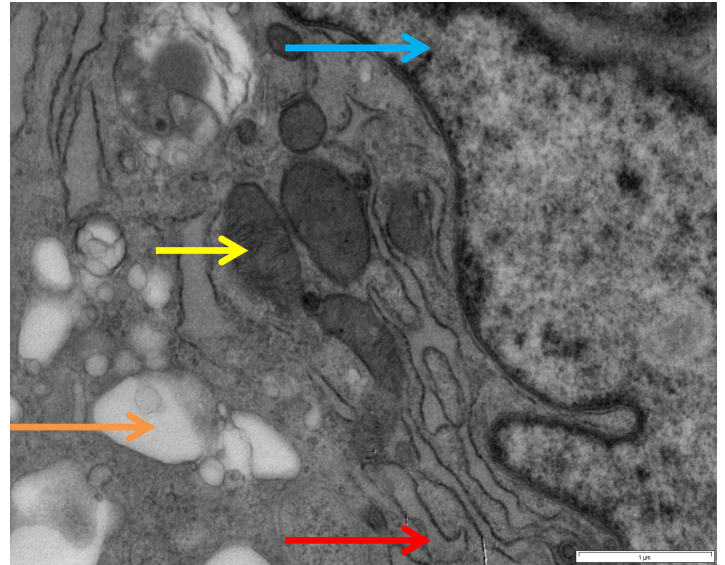
C, WTC2
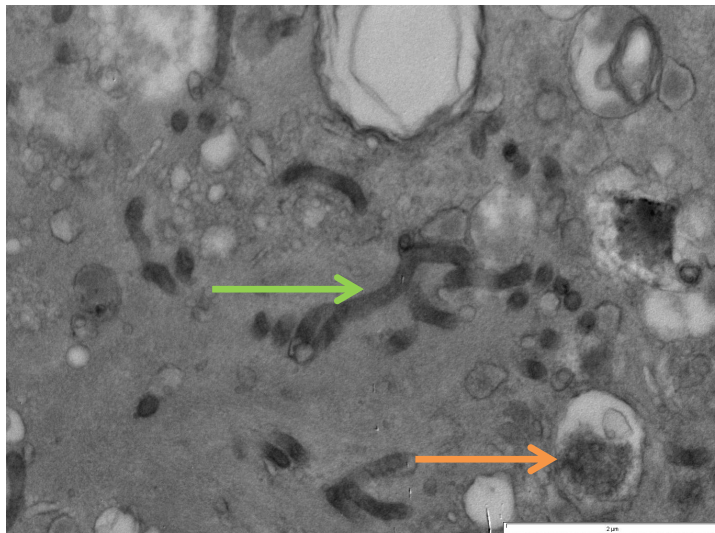
Figure 3.2: **Wild-type control (WTC2) fibroblasts analysed using transmission electron microscopy.**
A & B: nucleus (**blue arrow**), endoplasmic reticulum (**red arrow**), mitochondria (**yellow arrow**) and
lysosomal vacuoles (**orange arrow**). C: The process of mitochondrial fusion occurring within the cell
(**green arrow**); a vacuole or autophagosome in the process of lysosomal digestion (**orange arrow**).

Results from the TEM performed on patient P2 and carrier P2het can be seen in Figure 3.3. In terms of the mitochondrial morphology, the mitochondria in the patient appear rod-shaped with intact membranes and cristae (Figure 3.3 A), however several mitochondria appear circular and slightly swollen (Figure 3.3 C). Fusion is observed in the mitochondria that appear to be joined (Figure 3.3 A, B). Most notable in the patient is the appearance numerous electron dense (dark) vacuoles which suggest that they are filled with some kind of cellular material (Figure 3.3 B, C, and D). These vacuoles may be lysosomes undergoing fusion with autophagosomes for the process of autophagy. It is not clear what the material is, but it could be speculated that it is proteins targeted for degradation or dysfunctional mitochondria that are in the process of mitophagy. Whatever the content of these vacuoles, it is obvious that due to their large number, a mechanism is occurring within these cells that may be trying to remove large amounts of possibly toxic material. When comparing these patient cells to that of the control (Figure 3.2) and P2het (Figure 3.3 E, F), these vacuoles appear markedly different in terms of their size, number and colour. In P2het, the mitochondria (Figure 3.3 E, F) are well-formed and look similar to that of the mitochondria in the wild-type control WTC2. There are a number of large vacuoles, but they are predominantly light in colour. Fusion is also visible but to a lesser degree than the control.

A, P2
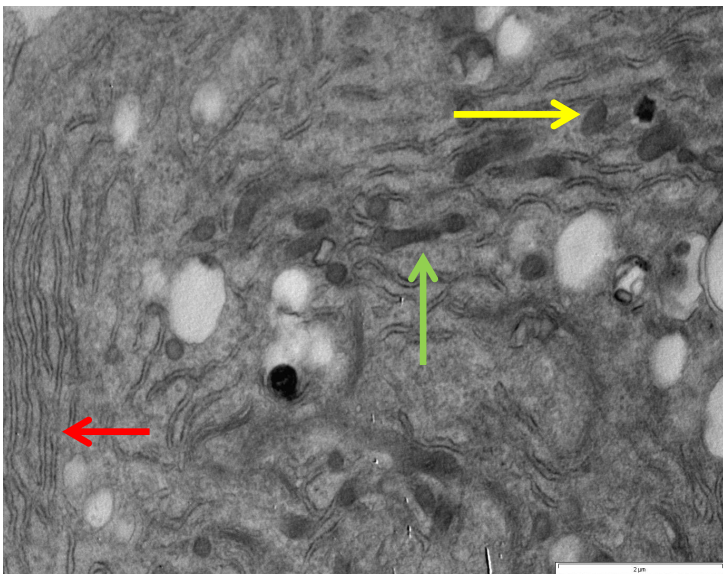
B, P2
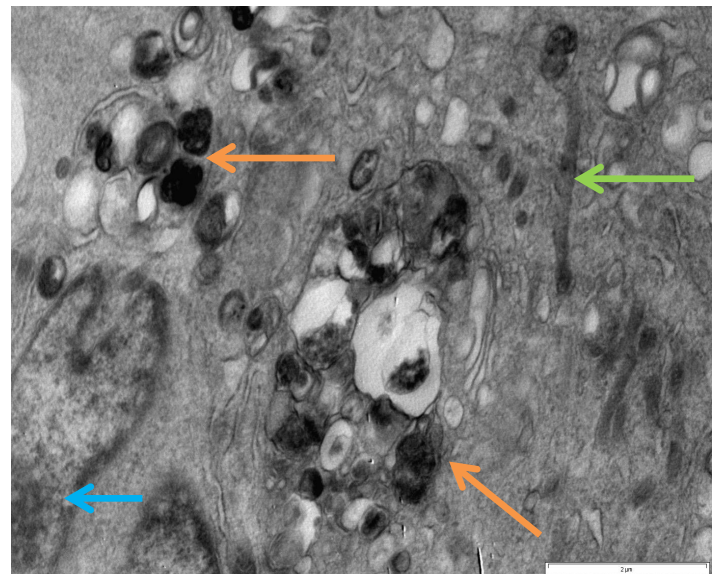
C, P2
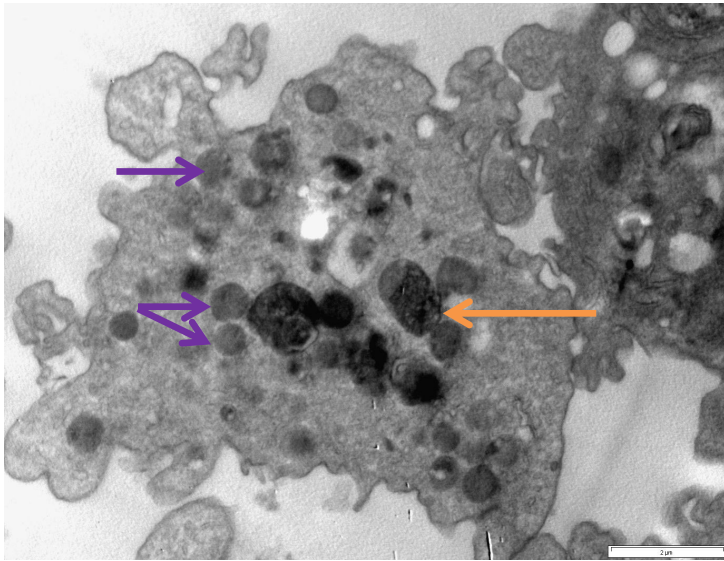
D, P2
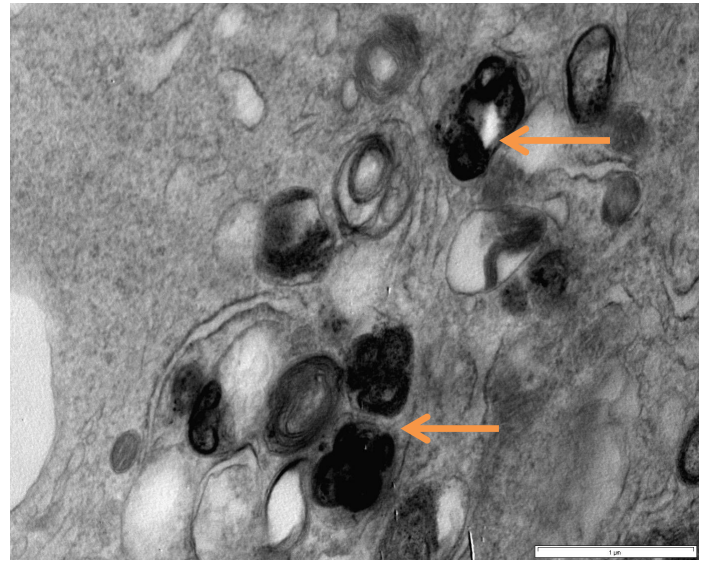
E, P2het
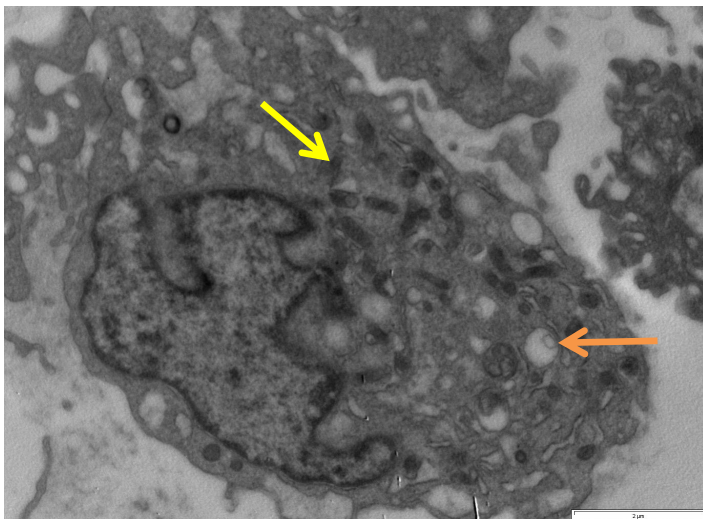
F, P2het
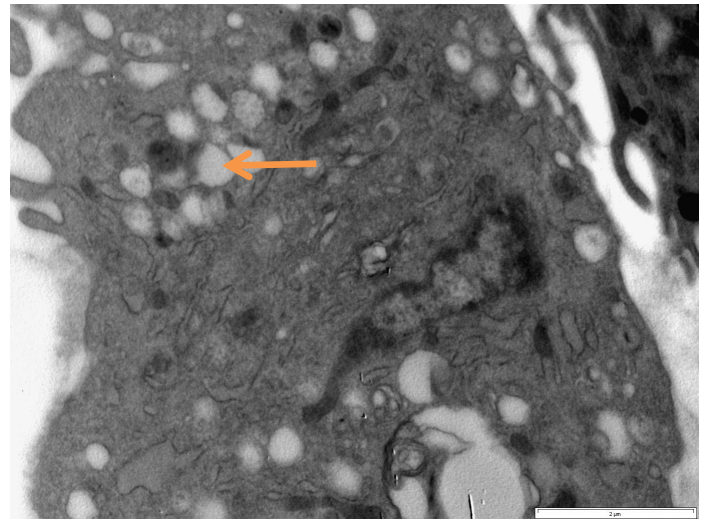
Figure 3.3: **Patient P2 and carrier P2het fibroblasts analysed using transmission electron microscopy.** A & B show well-formed rough endoplasmic reticulum (**red arrow**), nucleus (**blue arrow**), mitochondria (**yellow arrow**) as well as the process of fusion (**green arrow**). C indicates circular, swollen mitochondria (**purple arrow**) and along with D show vacuoles filled with electron dense material not seen in the control or P2het (**orange arrow**). E & F: Rod-shaped mitochondria (**yellow arrow**) with well-formed cristae in carrier P2het. Also, the majority of the vacuoles are white in colour indicating that they are empty (**orange arrow**).

The fibroblasts of patients P3.1 and P3.2 and the heterozygous carrier P3het are shown in Figure 3.4. The mitochondria (Figure 3.4 A, B, and D) of the two patients appear to be normally shaped (not swollen or irregular), and similar to those observed in the control cells (Figure 3.2). Pacelli and colleagues had observed few remaining cristae in patient cells (Pacelli et al., 2011), but this is not apparent in these patients. Although to a lesser degree than patient P2, a large number of electron dense autophagosomes or lysosomal vacuoles with noticeable inclusions were also observed in both patients P3.1 and P3.2 (Figure 3.4 C, D and F). Figure 3.3E from patient P3.2 shows a vacuole situated next to a mitochondrion and it could be speculated that the vacuole is an autophagosome in the process of digesting the mitochondrion. Mitochondrial fusion was also noted in the patient cells (Figure 3.4 C and F), and although the activity of fusion is to a lesser degree than in the control cells, it still suggests that some of the mitochondria are healthy and functional.

TEM images of fibroblasts from P3het are shown in Figure 3.4 G and H. The nucleus and ER are present (Figure 3.4 H) and the mitochondria are rod-shaped and round (Figure 3.4 G), not exhibiting irregularity in shape. The cristae are well formed and mitochondrial fusion is visible (Figure 3.4 H), but the fused mitochondria appear shorter than in the control (Figure 3.2 C). The vacuoles have varying degrees of electron density with inclusions (Figure 3.4 G and H), although less are observed in the carrier than in patients P3.1 and P3.2.

A, P3.1

B, P3.1

C, P3.1

D, P3.2

0.5 µm

E, P3.2

0.5 µm

F, P3.2

2 µm
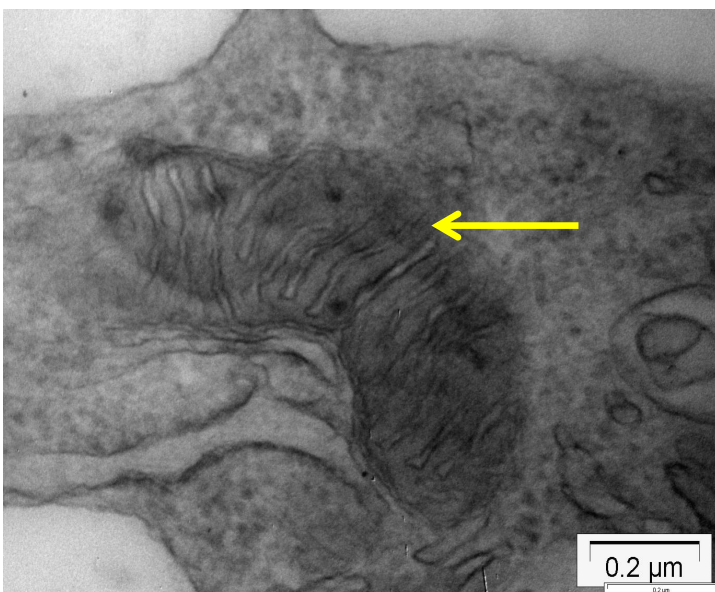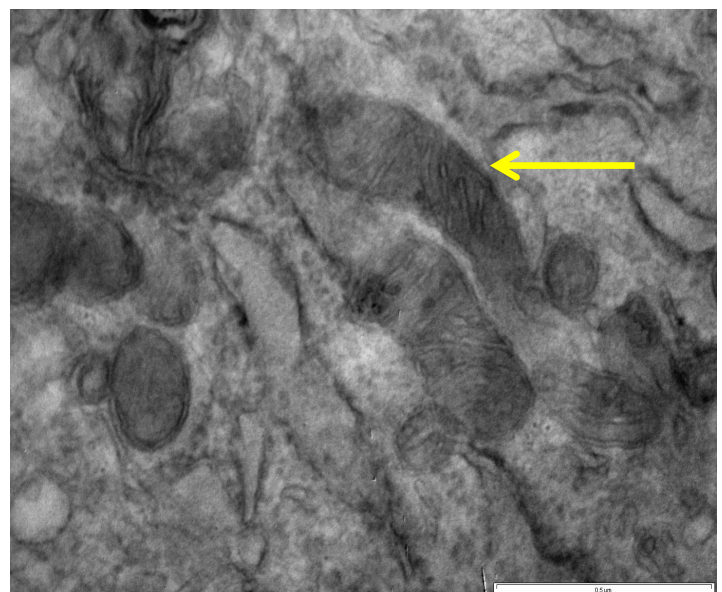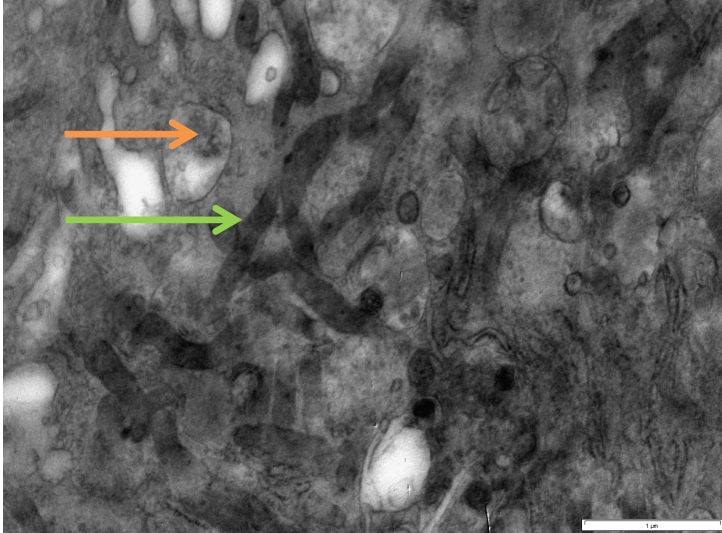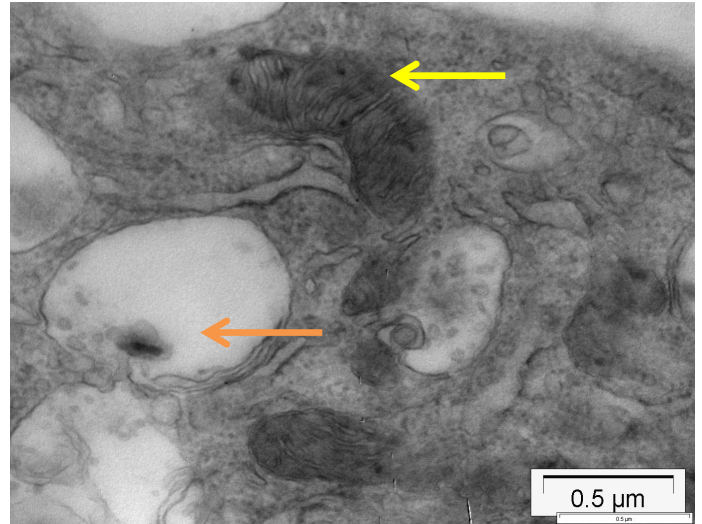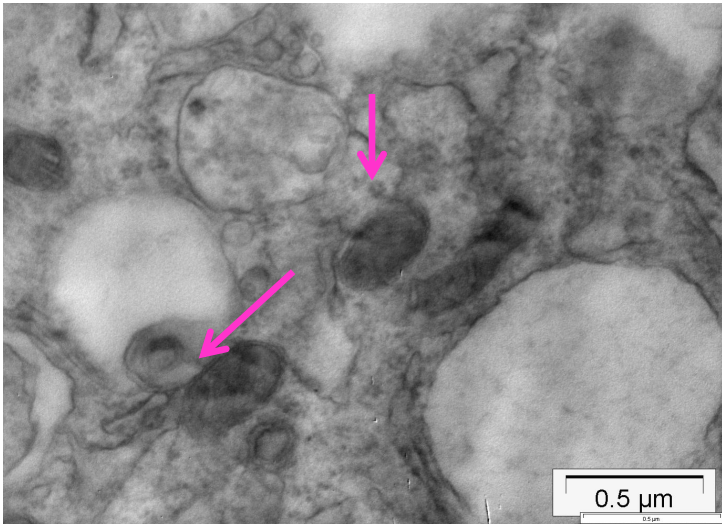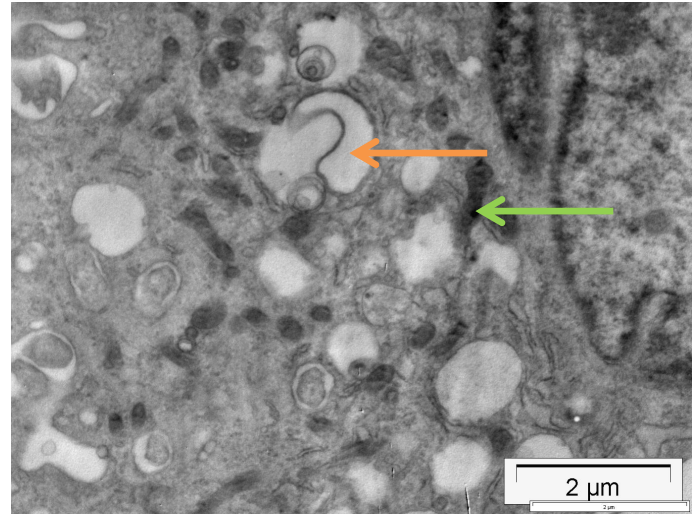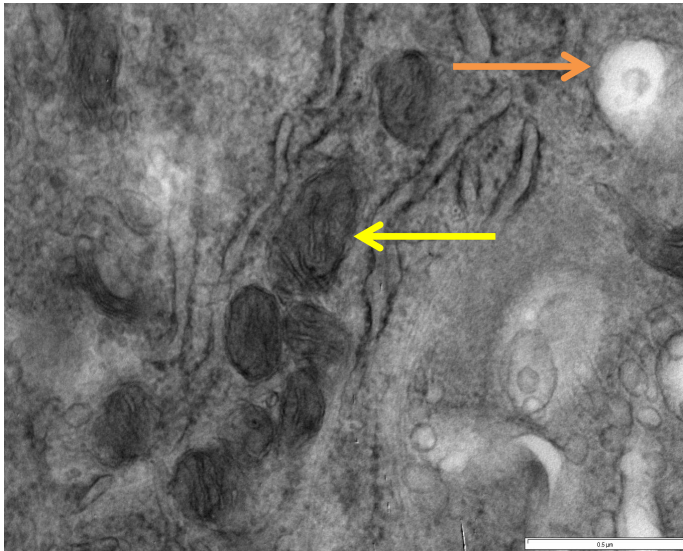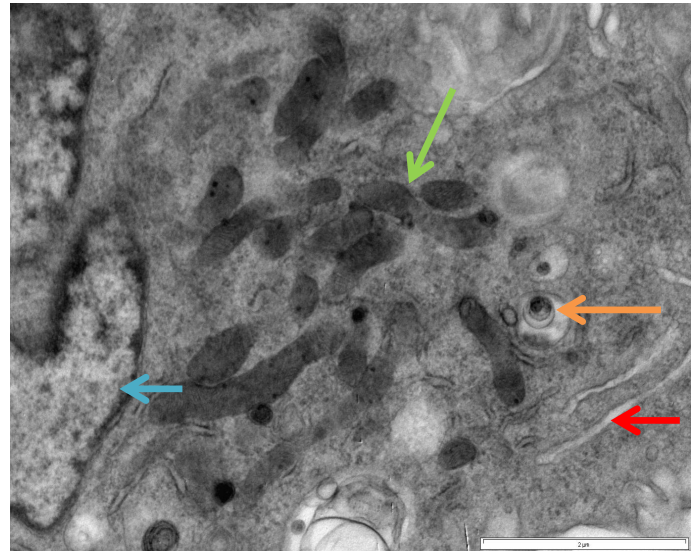
G, P3het

H, P3het

Figure 3.4: **Patients P3.1 and P3.2 and carrier P3het fibroblasts analysed using transmission electron microscopy.** A: Mitochondrion with well-shaped cristae (yellow arrow). B & D: Well shaped mitochondrion (yellow arrow) and autophagosomes with inclusions (orange arrow). C & F: Electron dense vacuoles (orange arrow) and mitochondrial fusion (green arrow). E: Indication of possible mitophagy (pink arrows). G and H: Rod-shaped mitochondria with well-formed cristae in carrier P3het (yellow arrow) and clear vacuoles with some showing slight inclusions (orange arrow). H: Nucleus (blue arrow), endoplasmic reticulum (red arrow) and mitochondrial fusion (green arrow).

3.2.3. Mitochondrial network analysis

The mitochondrial network is highly adaptable and changeable due to the dynamic nature of this organelle. The branches that form this network are responsible for the connectivity of the mitochondria throughout the cytosol of the cell, creating communication with other vital organelles such as the ER and the Golgi apparatus (Anesti & Scorrano, 2006). The more networks observed indicate healthier mitochondria, whereas fragmented and disjointed networks indicate dysfunctional and damaged mitochondria. Fragmentation of these networks has been observed in several studies with fibroblasts from PD patients with *parkin*-null mutations (Grunewald et al., 2010; Pacelli et al., 2011).

The mitochondrial network analysis of patient P2 (Figure 3.5 A), carrier P2het (Figure 3.5 B) and WTC2 (Figure 3.5 C) shows the mitochondrial network (red) and the nucleus (blue) of the fibroblasts. Both patient P2 and carrier P2het's mitochondrial network appear more fragmented compared to the control. The arrows on both images (Figure 3.5 A & B) indicate a dot-like and clustered appearance of the mitochondrial network. In contrast, the control mitochondrial network appears highly connected, suggesting a functional mitochondrial population.
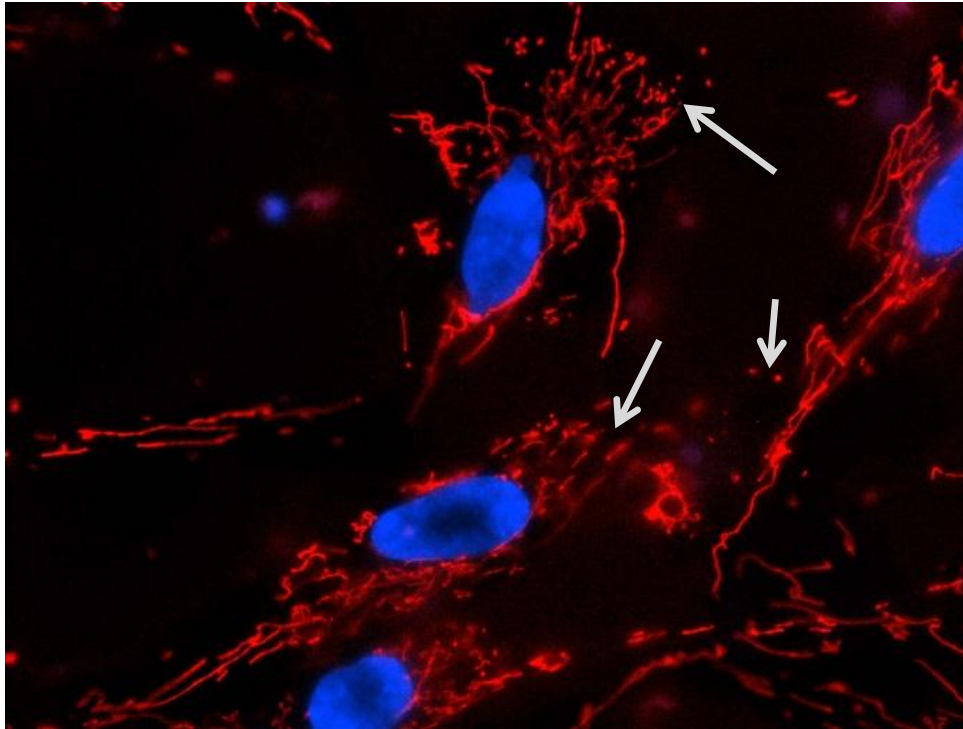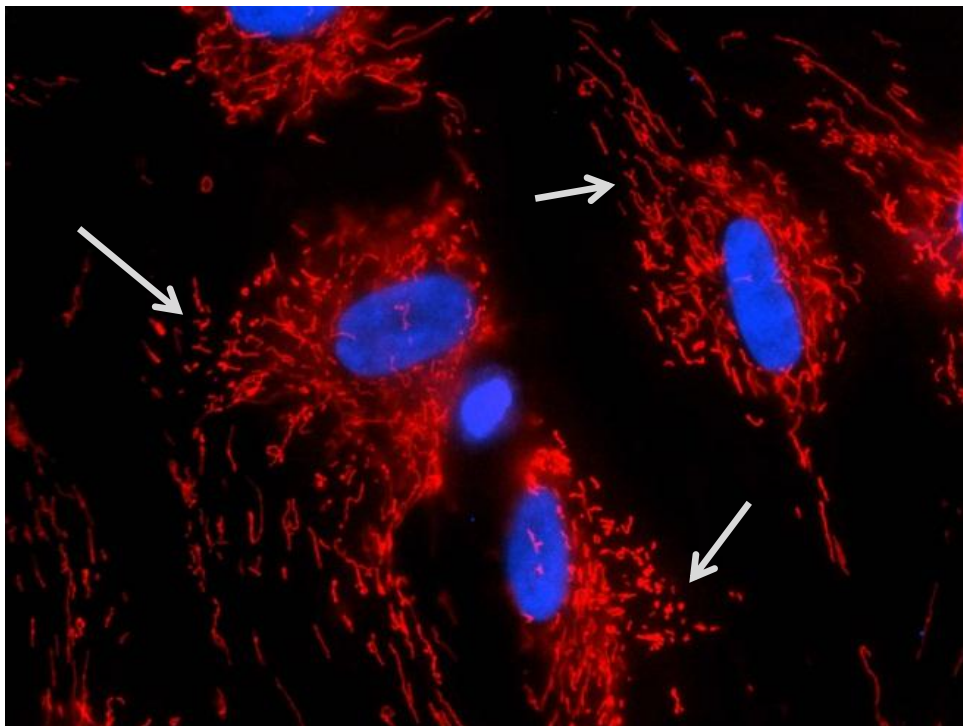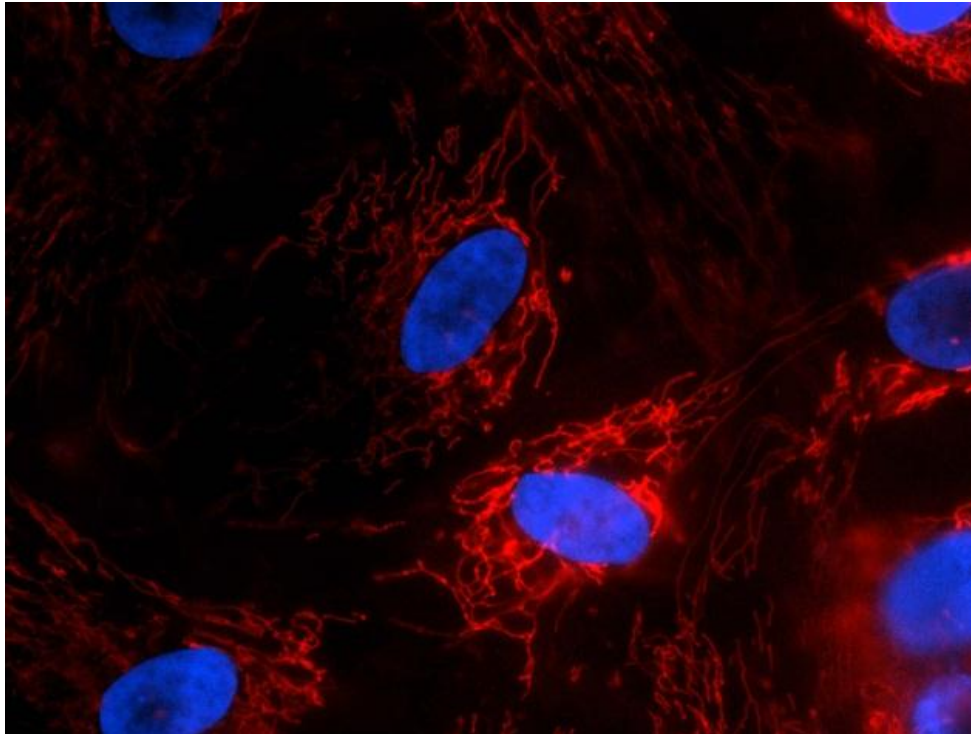
Figure 3.5: **Mitochondrial network analysis of A. patient P2, B. carrier P2het and C. WTC2.** The mitochondrial network is stained in red (MitoTracker Red dye) and the nucleus in blue (Hoescht 3343 dye). Fragmented mitochondria are indicated by the arrows in A and B.

Mitochondrial network analysis of family 3 was also performed (Figure 3.6). Patient P3.1 (Figure 3.6 A) shows very subtle signs of fragmentation of the mitochondrial network in her fibroblasts but not as severe as that of patient P2. In contrast, patient P3.2 does not exhibit these signs of mitochondrial fragmentation, but rather shows interconnectivity between individual mitochondria (Figure 3.6 B). Similarly, the fibroblasts from P3het show clear mitochondrial connection and fusion (Figure 3.6 C).

A

P3.1
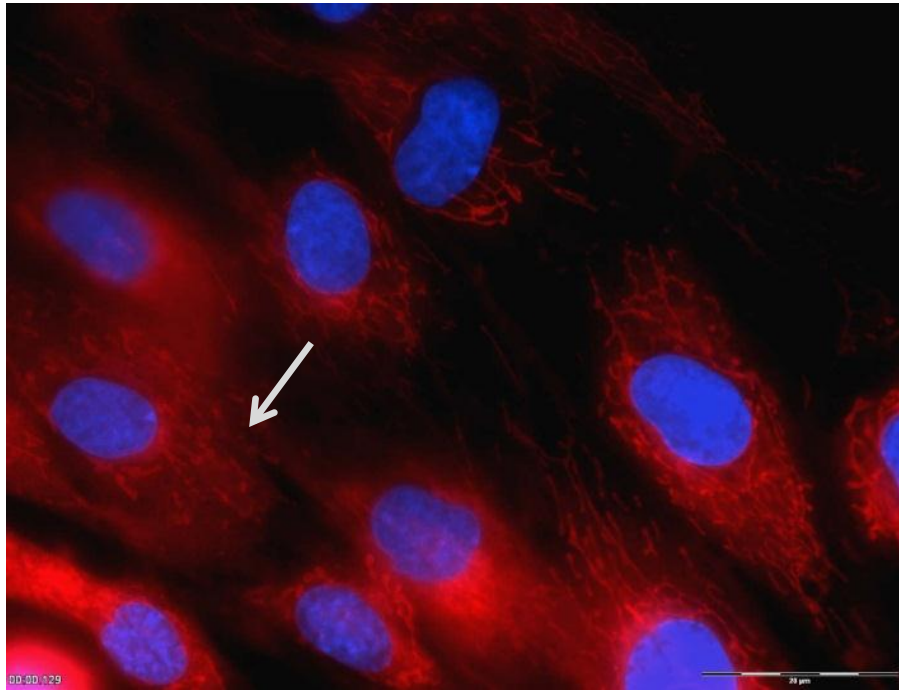
B

P3.2
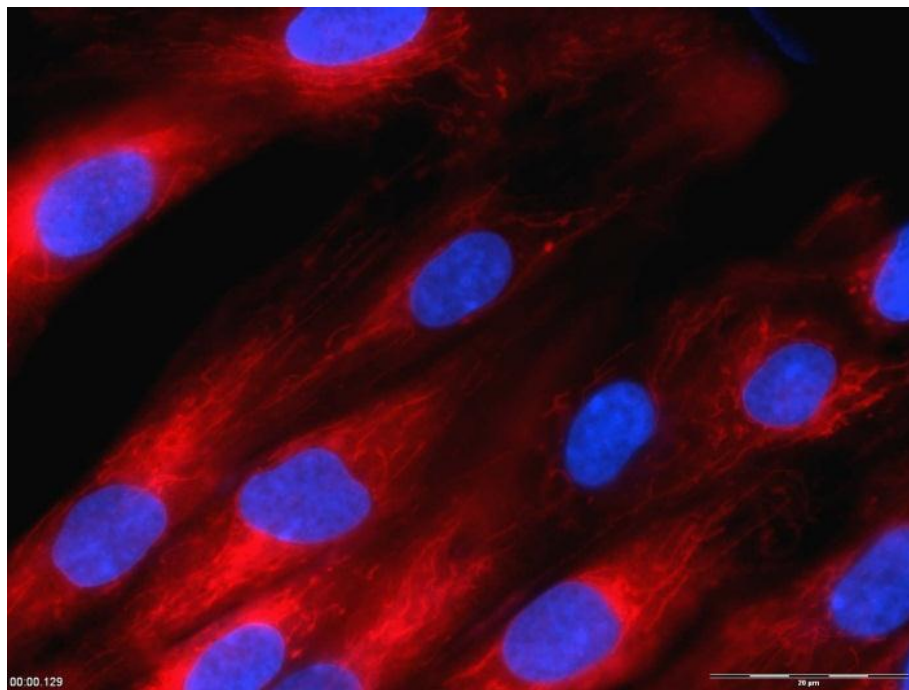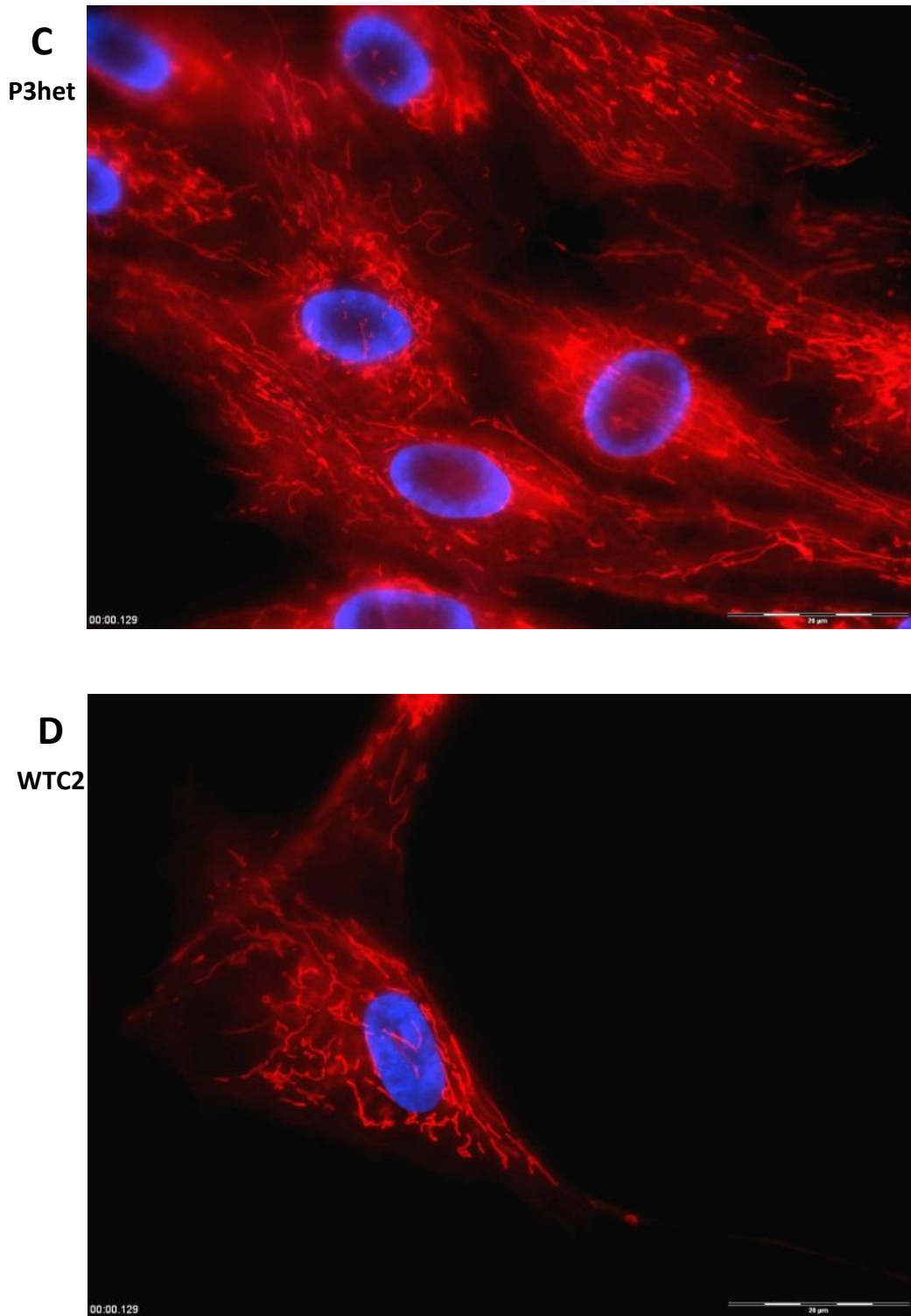
Figure 3.6: Mitochondrial network analysis in fibroblasts from A. patient P3.1, B. patient 3.2, C. heterozygous P3het and D. WTC2. Fragmented mitochondria are indicated by the arrow in A.

3.3. Analysis of mitochondrial function

3.3.1. ROS analysis

One of the main functions of mitochondria is the production of energy in the form of ATP via oxidative phosphorylation. During this process, ROS is released as a by-product and therefore measurement of mitochondrial ROS levels in a cell is an indication of mitochondrial function. In addition to mitochondrial ROS, generic ROS is released from all parts of the cell such as metabolic ROS produced by oxidation and reduction reactions in response to stress within the cell. Generic ROS can also enter the cells from the environment from sources such as radiation, UV light exposure, pesticide use and infection. Further examples of generic ROS sources include peroxisomal oxidases, cytochrome P-450 enzymes and NADPH oxidases (Kregel & Zhang, 2007). In comparison, mitochondrial ROS is produced only from the mitochondria.

The mitochondrial ROS is either produced in normal non-toxic amounts via oxidative phosphorylation, or through a defect in complex I of the electron transport chain, in which case higher levels of ROS are produced, thus resulting in oxidative stress of the cells. It was hypothesized that PD patients release a higher level of mitochondrial ROS compared to the wild-type control. Generic and mitochondrial ROS levels were measured separately in all study participants. For patient P1 and his spouse, the ROS analysis was performed on cultured WBCs, whereas for P2, P2het, P3.1, P3.2, P3het and WTC2 the experiments were performed on fibroblasts. Intensity histograms (example shown in Figure 3.7) were calculated after analysis on the flow cytometer, and the resulting fluorescence intensity signal was measured in terms of the PE and FITC geometric means, respectively.
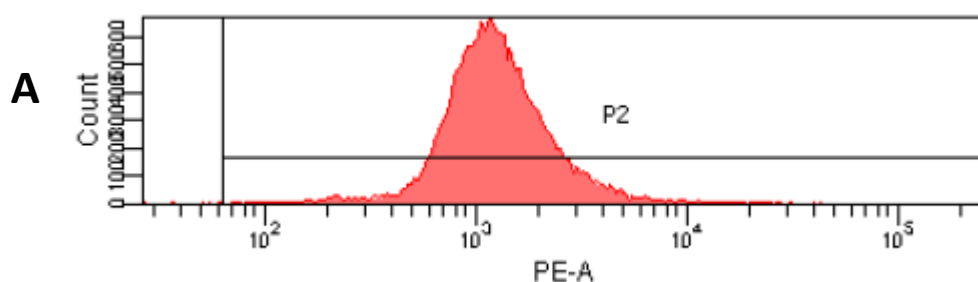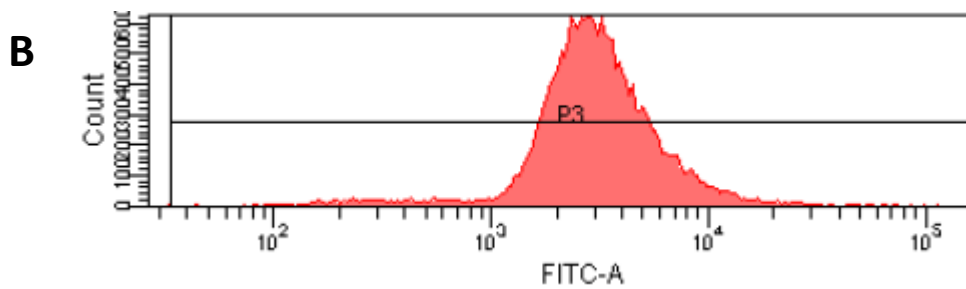
Figure 3.7: **Example of the intensity histograms produced after flow cytometry to measure A. generic ROS measured via the PE geometric mean and B. mitochondrial ROS measured via the FITC geometric mean.**

The raw data for the generic and mitochondrial ROS are shown in Table 3.4. Each run was performed on a separate date; therefore the data cannot be compared across runs as these are independent events. The normalized values are indicated in Table 3.5. Represented graphically, it is apparent that there is no trend in the generic ROS level across the study participants (Figure 3.8 A). Both patients P1 (153.5%) and P3.1 (145.8%) exhibit increased generic ROS compared to the wild-type control WTC2. In contrast, patients P2 (40.6%) and P3.2 (83.8%) have decreased generic ROS levels. Moreover, one heterozygote has decreased levels (P2het; 59.6%) and the other has increased levels (P3het; 115.8%).

Interestingly, for the mitochondrial ROS there is a trend with patients P1 (121.6%), P2 (163.6%) and P3.1 (125.3%) all exhibiting increased levels relative to the wild-type control WTC2. The only exception is patient P3.2 (85.2%) which showed decreased mitochondrial ROS levels. The reason for the different result in this patient is currently unclear, although it is thought that this patient may have a compensatory mechanism at play that alleviates the ROS levels. The findings in the other three patients fit with our hypothesis of increased mitochondrial ROS as a result of dysfunctional mitochondrial in PD patients. Both heterozygotes also exhibited increased mitochondrial ROS (P2het; 104.0% and P3het; 121.3%), although P2het was only marginally higher than the wild-type control WTC2.

Table 3.4: Values of the PE geometric mean measuring generic ROS and the FITC geometric mean measuring mitochondrial ROS in the WBCs of patient P1 and the fibroblasts in patients P2, P3.1 and P3.2, heterozygotes P2het and P3het, and WTC2.

Patient	Generic ROS (PE geometric mean)	Mitochondrial ROS (FITC geometric mean)	Cells	Date of experiment
P1	2586	180	WBCs	
P1 Spouse (wild-type)	1685	148	WBCs	01/03/2011
P2	167	162	Fibroblasts	
P2het	245	103	Fibroblasts	25/07/2012
WTC2	411	99	Fibroblasts	
P3.1	1051	1747	Fibroblasts	
P3.2	604	1188	Fibroblasts	
P3het	835	1691	Fibroblasts	15/03/2012
WTC2	721	1394	Fibroblasts	

*WBCs, white blood cells

Table 3.5: Analysis of generic and mitochondrial ROS measurements in patients and carriers as a percentage of the wild-type control.

	Generic ROS (%) (Normalized to WTC2)	Mitochondrial ROS (%) (Normalized to WTC2)
P1	153.5	121.6
P2	40.6	163.6
P3.1	145.8	125.3
P3.2	83.8	85.2
P2het	59.6	104.0
P3het	115.8	121.3
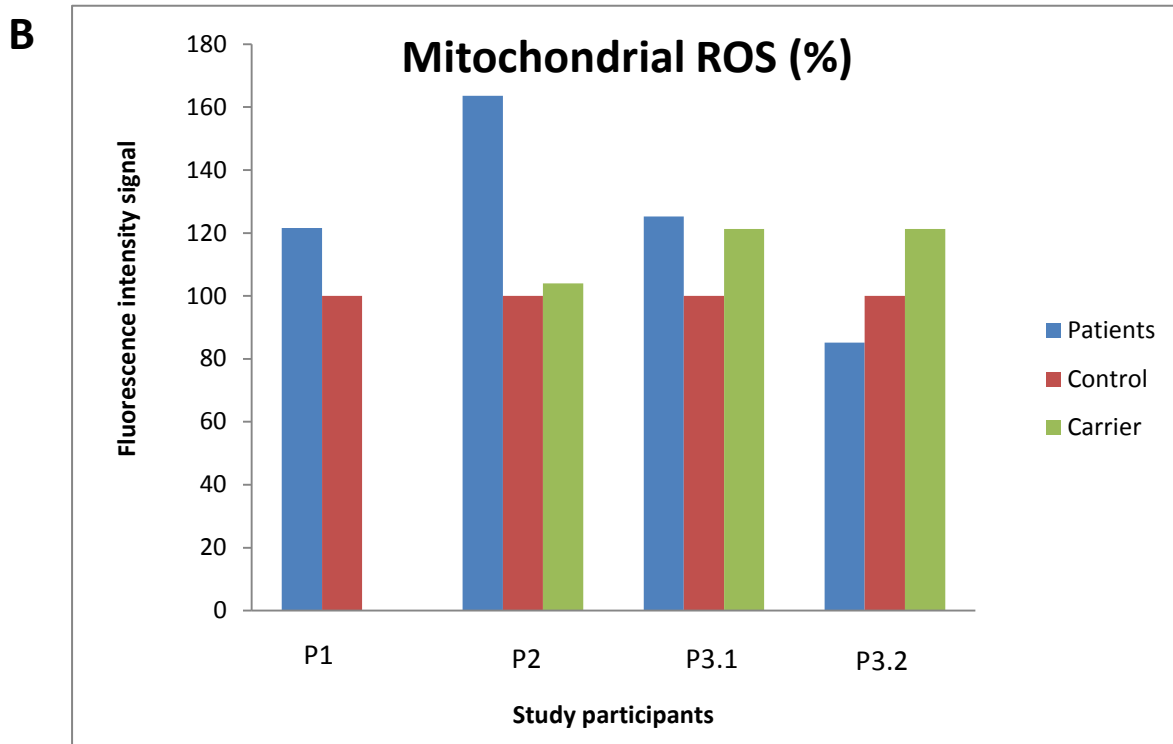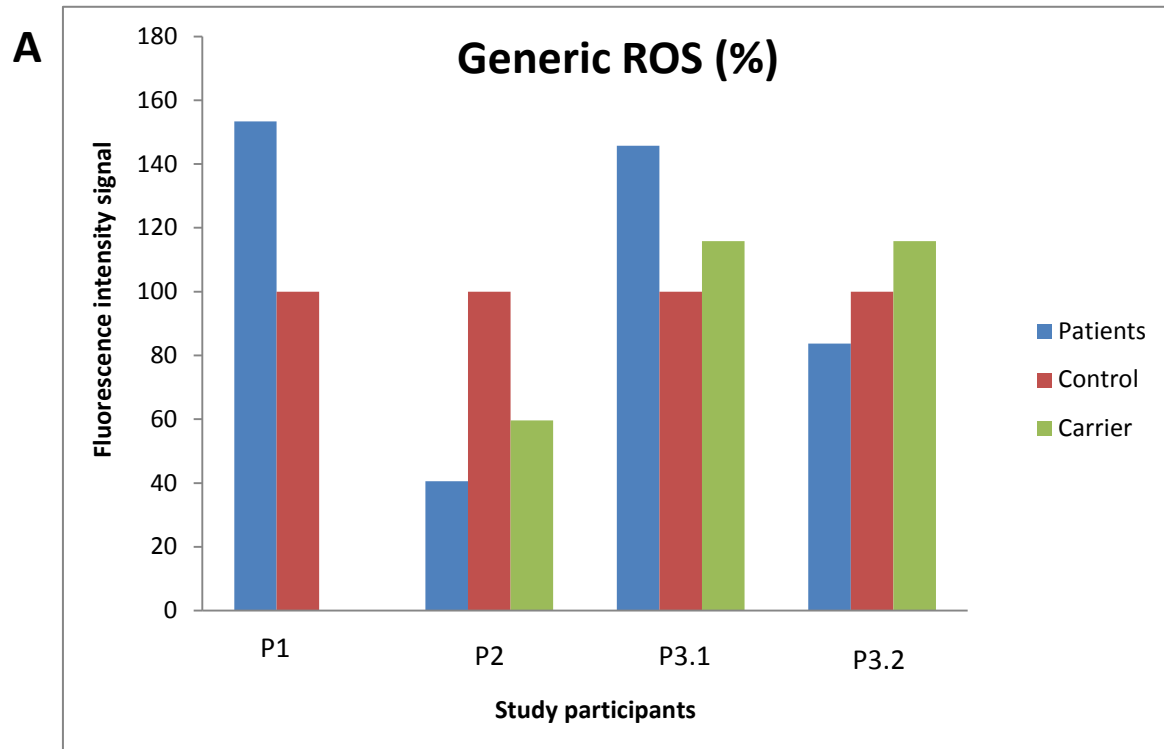
Figure 3.8: **Graphical representation of the reactive oxygen species (ROS) in patients and carriers.**

A. generic and B. mitochondrial ROS.

3.4. Analysis of mitochondrial gene expression

Mitochondrial function may also be affected by the expression levels of the mitochondrial genes. Previous studies have shown down-regulation of the genes involved in mitochondrial electron transport in both brain tissues and blood from PD patients (Zheng et al., 2010). In the present study, peripheral blood samples were used for the gene expression studies due to the fact that expression studies on cultured cells do not produce reproducible results as a result of artifacts induced during the culturing process (Dr. Suzanne Lesage, personal communication).

3.4.1. Determination of quality of extracted RNA

RNA was extracted from peripheral blood samples obtained from patients P1, P2, P3.1, and P3.2 as well as the respective heterozygote family member of each patient, and the wild-type control used in gene expression experiments (WTC1). It is essential to ensure that the isolated RNA is of the highest quality, in other words that there are no contaminants in the sample (a measure of RNA purity), and that the RNA has not been degraded (a measure of RNA integrity). If the RNA is not of a sufficiently high quality, this will result in inhibition of the qRT-PCR process, and may lead to biased data (Taylor et al., 2010). Directly after the extraction, the RNA was pipetted onto the NanoDrop® N1000-UV-Vis Spectrophotometer and the concentration of the RNA was determined using the Beer-Lambert law, which predicts a linear change in absorbance with concentration. A ratio of 260:280 primarily represents the purity of the RNA, and a ratio value of ±2 is accepted as 'pure' RNA. A much lower value may be indicative of possible contamination. The 260:230 ratio is generally accepted at around 1.8 – 2.2 for 'pure' RNA. A lower ratio may also indicate sample contaminants of salts, phenol or protein in the sample.

The concentration of the extracted RNA was within an acceptable range and the samples were relatively pure (Table 3.6). The 260:280 ratio was approximately 2 for all samples, but the 260:230 ratio was <1 for all except P2het, which suggests possible contamination. It could be speculated that column-based extraction methods, such as the one used, may lead to contamination with particles from the column which absorb at 230nm. Both purity and integrity need to be assessed before the

RNA can be used for qRT-PCR experiments, and it is not possible for spectrophotometric readings to produce data on RNA integrity. Therefore a more accurate method of RNA quality determination was performed using the Experion StdSens Analysis Kit (BioRad, USA), which is a microfluidics electrophoresis based system.

Table 3.6: **RNA concentration and quality determination using the NanoDrop® N1000-UV-Vis Spectrophotometer**

Patient	Concentration (ng/µl)	260/280	260/230
P1	77	1.93	0.69
P1het	67	2.1	0.45
P2	98	2.08	0.56
P2het	82	2.06	1.99
P3.1	117	2.04	0.62
P3.2	78	2.16	0.21
P3het	64	2.09	0.39
WTC1	134	2.14	0.74

The parameters measured in an Experion run include RNA concentration, RNA area, 28S/18S RNA ratio and the RNA Quality Indicator (RQI) value. The RQI value standardizes and quantifies RNA integrity, and is able to show the extent of degradation of each RNA sample loaded onto the chip. It is ranked from a value of 1, which indicates highly degraded RNA, to a value of 10, which indicates intact RNA (Drug, Discovery & Development magazine, http://www.dddmag.com/products/2008/12/rna-quality-indicator). The cut-off RQI value used for RNA experiments was taken as 8 or above. With the exception of P1het, all the RNA samples met this standard (Table 3.7) and were thus used in the subsequent gene expression studies. A second quality determining factor is the 28S/18S ratio, which is calculated during the run for each sample. The higher the ratio, the greater the level of intact RNA in the sample, and this will produce a

subsequent higher RQI value. A 28S/18S ratio between 1 and 2 is accepted as good quality RNA. Based on the run and the run images (an example is shown in Figure 3.9), the 28S/18S ratio was indicative of good quality RNA in each of the samples, as two distinct bands were seen that represent 28S and 18S rRNA respectively. The RNA extracted from heterozygous P1het yielded an RQI value of 6.5 and the concentration and 28S/18S ratio were also relatively low in comparison to the RNA values of all other individuals (Table 3.7). Therefore that sample was not used in subsequent experiments. Reasons for the production of a poor quality sample may be contamination of the sample during the RNA extraction procedure, or a degraded blood sample due to a faulty blood collection tube.
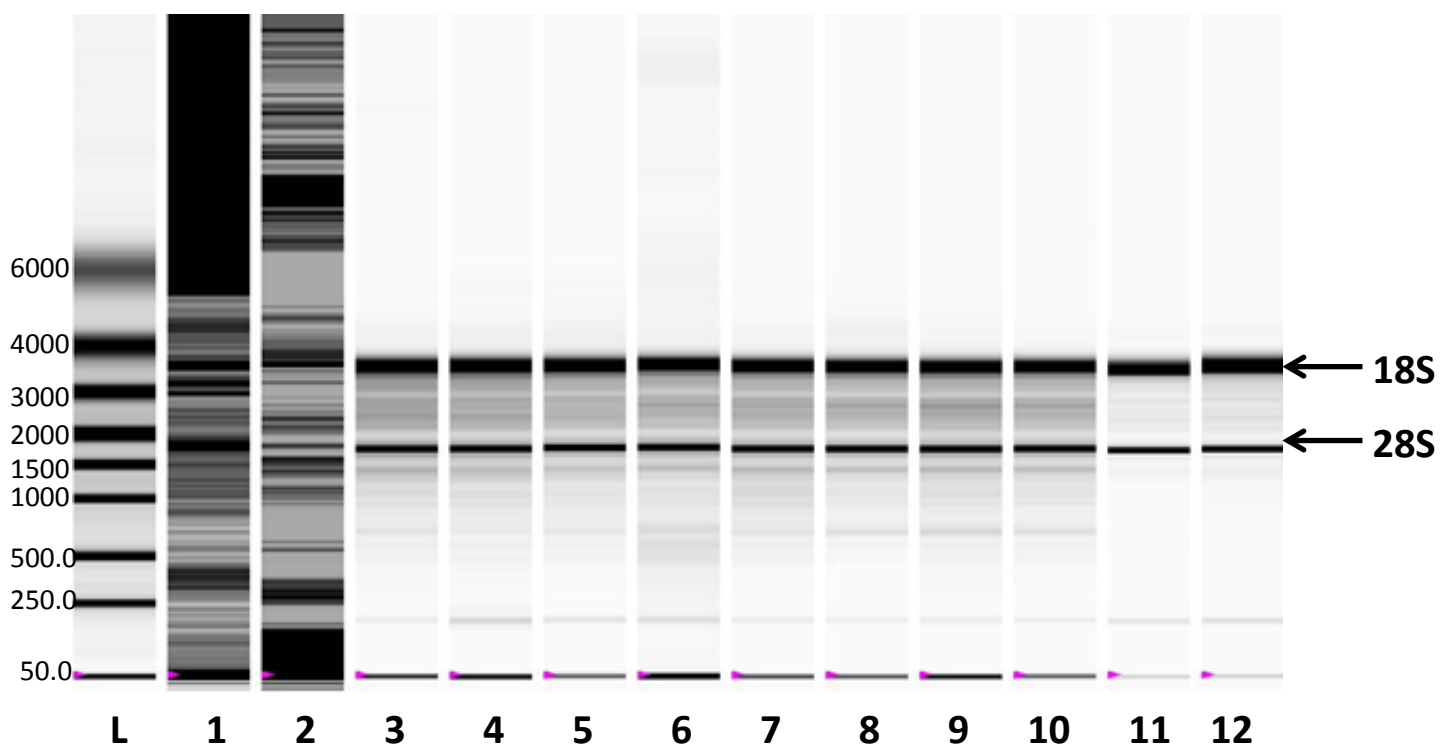
Figure 3.9: Gel picture of an Experion run. Lane L represents the RNA ladder, lanes 1 and 2 represent bad quality RNA (as no 28S and 18S bands are seen) and lanes 3-12 represent good quality RNA (with distinct 28S and 18S bands).

Table 3.7: RNA concentration and quality determination using the Experion StdSens Analysis Kit

Patient	Concentration (ng/µl)	RNA Area	28S/18S	RQI
P1	64.31	315	0.96	8.4
P1het	51.68	253.12	0.63	6.5
P2	111.41	330.67	1.28	9.3
P2het	69.71	206.91	1.4	9.4
P3.1	89.62	221.23	1.59	9.5
P3.2	77.82	214.87	1.51	9.2
P3het	63.37	156.42	1.5	9.3
WTC1	103.41	506.51	1.09	8.8

The RNA extracted from patients P1, P2, P3.1 and the wild-type control WTC1 was converted to cDNA and this was used in qRT-PCR gene expression experiments – namely the RT² Profiler PCR Array (SABiosciences, USA) and the RT² Primer Assay (SABiosciences, USA).

The RT² Profiler PCR Array allows for simultaneous analysis of 84 genes involved in mitochondrial energy metabolism. Up- or down-regulated genes were determined as genes with a fold regulation value of 2 or more compared to WTC1. Thereafter, one of the genes found to be down-regulated genes across all three patients was chosen for independent verification using the Primer Assay, and analysed using REST software. The Primer Assay PCR reactions were performed in triplicate so as to ensure the validity of the results.

3.4.2. RT² Profiler PCR Array and RT² Primer Assay

Table 3.8 summarizes the list of down-regulated genes found across two or more of the patients. The fold difference number shows the fold change for each gene, which was chosen at a minimum value of 2. Each gene is part of one of the five complexes of the mitochondrial electron transport chain, responsible for the production of cellular ATP. Of the 14 down-regulated genes that were found in at least two patients, five form part of complex I, four from complex III, two from complex IV and three from complex V. Notably, no genes from complex II were found to be down-regulated. Of the 14 down-regulated genes, four were found to be down-regulated across all three patients (*NDUFS2, BCS1L, CYC1* and *LHPP*). Only six genes were found to be up-regulated in two or more patients (Table 3.9). Of these, one forms part of complex I, three from complex IV, and two from complex V. No gene was found to be up-regulated across all three patients.

Table 3.8: **List of down-regulated genes common in two or more patients, and resulting fold regulation (i.e. under-expression relative to the control).**

P1	Fold regulation	P2	Fold regulation	P3.1	Fold regulation	Mitochondrial complex
		NDUFA11	-11.01	*NDUFA11*	-3.46	I
		NDUFB7	-6.30	*NDUFB7*	-3.04	I
NDUFS1	-2.09	*NDUFS1*	-18.13			I
*NDUFS2**	-2.47	*NDUFS2*	-65.63	*NDUFS2*	-2.41	I
		NDUFS7	-27.03	*NDUFS7*	-5.85	I
*BCS1L**	-3.68	*BCS1L*	-9.93	*BCS1L*	-2.62	III
*CYC1**	-2.74	*CYC1*	-8.89	*CYC1*	-9.42	III
		UQCRC1	-25.78	*UQCRC1*	-3.22	III
UQCRCQ	-2.48	*UQCRCQ*	-2.32			III
		COX6B1	-6.77	*COX6B1*	-4.12	IV
		COX8A	-11.03	*COX8A*	-2.12	IV
		ATP5G1	-8.18	*ATP5G1*	-2.07	V
ATP5J2	-2.91			*ATP5J2*	-2.01	V
*LHPP**	-2.75	*LHPP*	-6.36	*LHPP*	-2.12	V

*Genes down-regulated across all three patients

Table 3.9: **List of up-regulated genes common in two or more patients, and resulting fold regulation (i.e. over-expression relative to the control).**

P1	Fold regulation	P2	Fold regulation	P3.1	Fold regulation	Mitochondrial complex
NDUFA4	+9.54	*NDUFA4*	+2.35			I
COX7B	+9.46	*COX7B*	+3.05			IV
COX6C	+5.98	*COX6C*	+2.52			IV
COX7A2	+3.87	*COX7A2*	+2.81			IV
		ATP6VOD2	+3.27	*ATP6VOD2*	+2.56	V
ATP50	+3.19	*ATP50*	+2.11			V

It was hypothesized that the majority of the 84 genes analysed would be down-regulated in patients P1, P2 and P3.1. This was, however, not observed in the patients. Also different profiles were observed across these three individuals (Figure 3.10 A-C). Figure 3.10A indicates all genes up- and down-regulated in patient P1. A total of 24 genes showed differences and of these only 30% (8/24) were found to be down-regulated. In comparison, patient P2 had a total of 57 genes with a change in gene expression, of which a 74% majority were down-regulated (42/57; Figure 3.10 B). Patient P3.1 had the least amount of genes with differences in expression (15 genes), however similarly to patient P2, the majority of these genes, 87%, were also down-regulated (13/15; Figure 3.10 C).

A

Up- and down-regulated genes in P1

B

Figure: Up- and down-regulated genes in P2

C

Figure 3.10: Graphs showing all up-and down-regulated genes found in A. patient P1; B. patient P2; C. patient P3.1
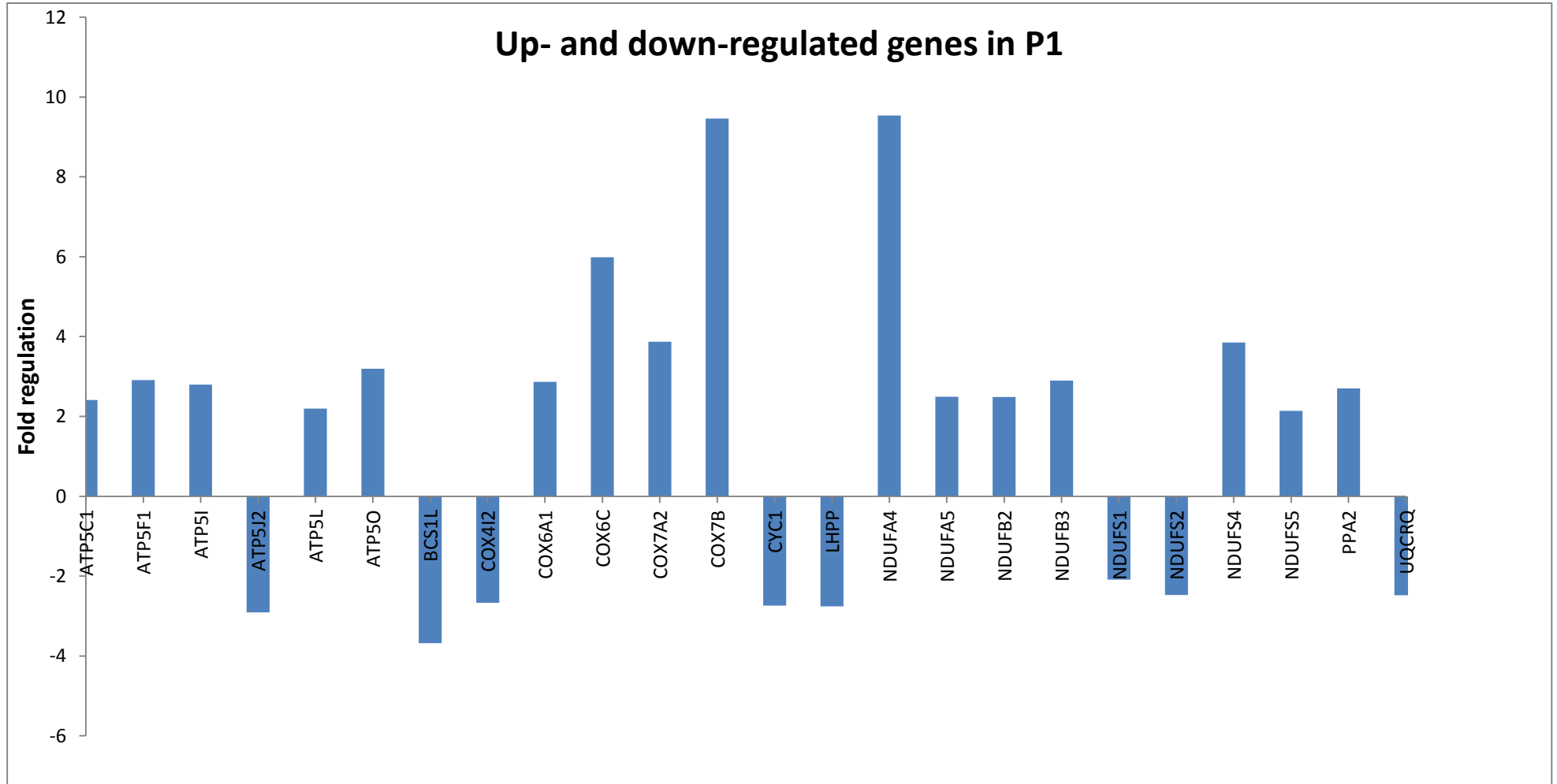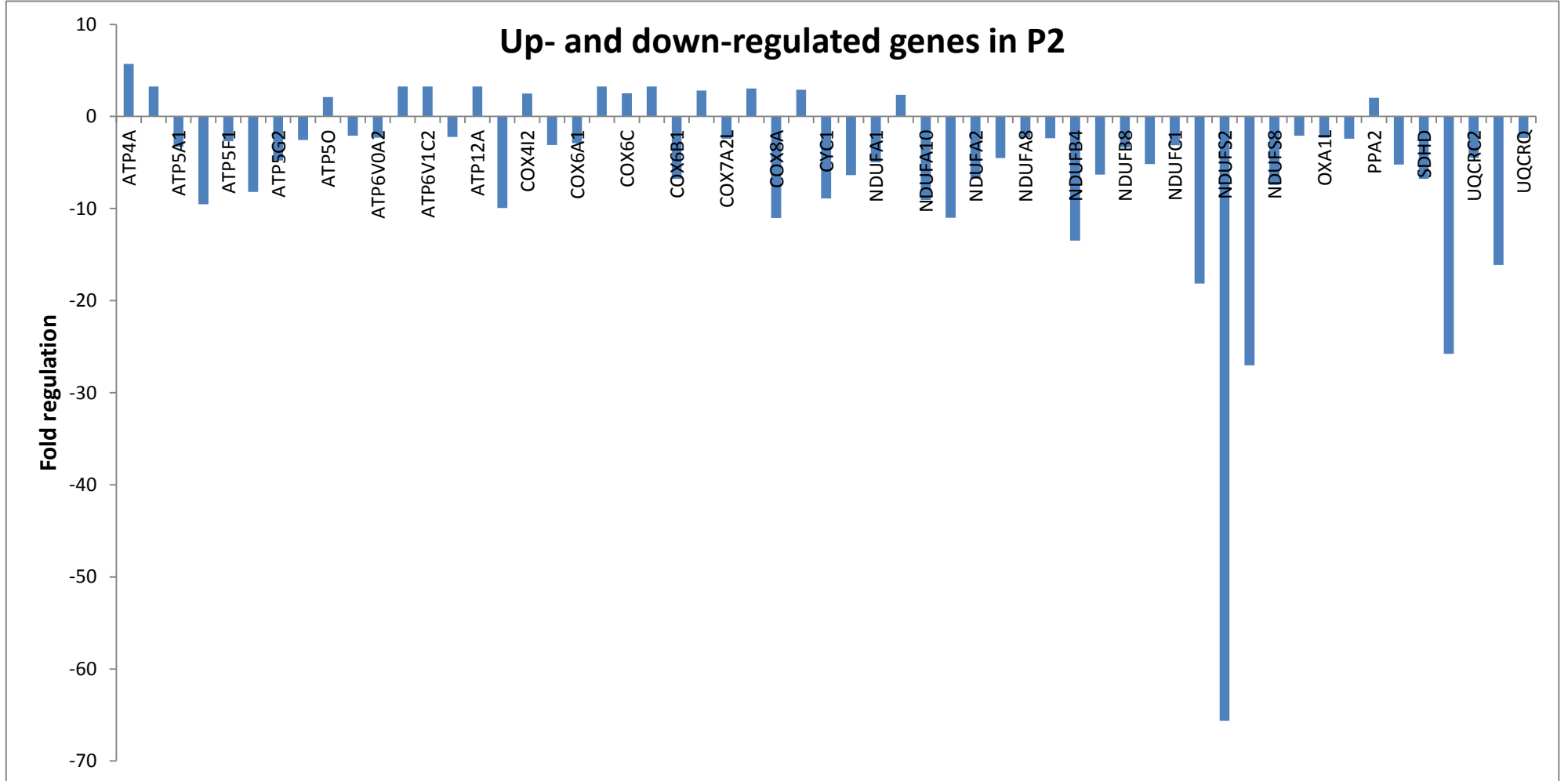
The PCR Primer Assay was performed as a validation step for the results observed in the PCR Array. A gene of interest that was down-regulated across all three patients (*CYC1*) was chosen for the Primer Assay and two housekeeping genes were chosen for normalisation of results – *HPRT1* and *RPL13A*. The *CYC1* gene was chosen as it correlated with down-regulation observed in a previous study (Zheng et al., 2010). The standard curve results for each of the three genes are shown in Appendix V. After normalisation the results indicated that although an increased expression is observed (5.693), *CYC1* expression levels is unchanged in the patient blood samples compared to the wild-type control (p = 0.065; Table 3.10). This contradicts the results observed in the PCR Array, in which down-regulation of *CYC1* was seen for all three patients.

Table 3.10: Relative expression values of the target (TRG) gene *CYC1* normalized to the two housekeeping (REF) genes HPRT1 and RPL13A.

Gene	Type	Reaction Efficiency	Expression	Std. Error	95% C.I	P(H1)
HPRT1	REF	0.9353	0.937			
RPL13A	REF	0.8521	1.067			
CYC1	TRG	0.9818	5.693	1.959 – 34.845	1.461 – 69.694	0.065

3.5.   Analysis of protein expression

Studies have failed to provide a correlation between differences in the levels of mRNA transcripts and levels of protein expression for protein-coding genes (Nie et al., 2007). It is therefore important to also examine the differences between patients and controls at the level of the proteome, as gene expression studies can only provide limited insight into post-transcriptional regulation.

In the present study, we wanted to ensure that no parkin protein was produced in the *parkin*-null patients. In addition, we performed a pilot study to determine whether a sufficient number of

proteins could be extracted from cell lysates of fibroblasts and also to determine whether there were any differences between the proteomes of PD patients and the wild-type control.

3.5.1. Determination of parkin expression in cultured fibroblasts using Western blotting

When an antibody against an epitope of a particular protein is available, western blotting can enable high sensitivity detection of that specific protein in a protein mixture such as a lysate. One of the objectives in this research project was to show, using fibroblasts, that parkin protein is present in a wild-type control, absent in a patient with PD caused by two mutations in the *parkin* gene, and present in a heterozygote carrier of the *parkin* mutation, but to a lesser degree than in the wild-type.

3.5.1.1. *Polyclonal goat antibody*

Initially, the primary antibody used was a polyclonal goat antibody (Abcam, Biocom BioTech, SA) and according to the manufacturer's protocol, a dilution of 1:5000 was recommended. Using this dilution of primary antibody, parkin could not be detected (Figure 3.11). Thereafter, the cell lysate was blotted with different dilutions of antibody – 1:5000, 1:3000 and 1:2000. However, no parkin protein was detected using any of these concentrations, although a possible band was observed at 110kDa using the 1:2000 dilution, but when the procedure was repeated, no bands were visible, suggesting that the 110kDa band was a contaminant.
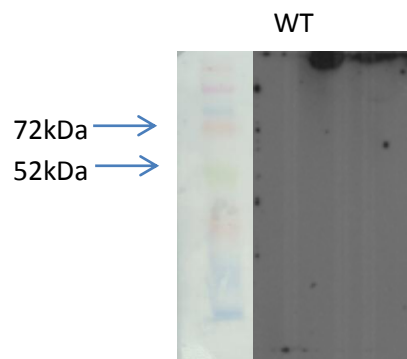
Figure 3.11: **Western blot with no parkin band detected when using a 1:5000 dilution of the primary antibody**

3.5.1.2.   Monoclonal mouse antibody

After several more unsuccessful blots using the polyclonal goat antibody, it was decided that a
monoclonal mouse antibody for parkin should be used (Cell Signalling Technology, USA). A
monoclonal antibody is formed due to a single cell fusion that is grown up into a clonal population,
recognizing only one epitope of the antigen. In contrast, a polyclonal antibody is a mix of different
antibodies that recognize multiple different epitopes on an antigen (Lipman et al., 2005). The
advantage of using a monoclonal antibody is the specificity with which this antibody interacts with
only one target epitope; this could markedly reduce excessive background and non-specific target
binding. The new monoclonal mouse antibody was first tested using lysates of rat hypothalamus
GT17 cells as a positive control. The concentration of the GT17 cells was notably higher (7.3µg/µl)
than that of the fibroblasts (4.3µg/µl). Figure 3.12 indicates the parkin band detected when the GT17
cells and a band of 50kD was seen, which is the expected size according to the manufacturer's
specifications.
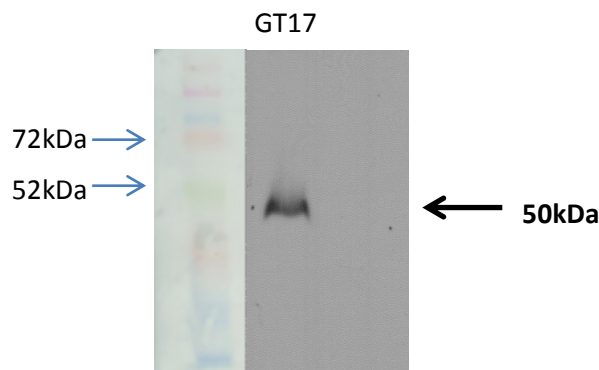
Figure 3.12: **Western blot showing a 50kDa band which represents parkin protein using rat
hypothalamus GT17 cell lysates.**

Thereafter, control, patient and heterozygote fibroblasts were analysed on a western blot using the
monoclonal antibody. After increasing the concentration of the cell lysate (Control = 7.3µg/µl;
patient and carrier = 7.2µg/µl), changing the primary antibody dilution from 1:1000 to 1:500, and
making the gel in a 10% resolving gel solution rather than a 12% solution, the blots were successful
in showing the presence of parkin protein in wild-type control fibroblasts, and the absence in patient

fibroblasts (Figure 3.13). Unexpectedly, no parkin was observed in the carrier, but this may be due to half the amount of parkin protein which was not visible on this blot. Future studies are needed to determine if a band of half the intensity is visible in the carrier.
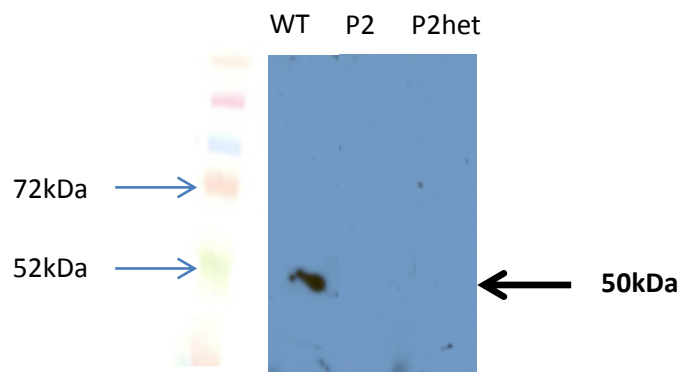
Figure 3.13: Western blot showing a 50kDa band which represents parkin protein in wild-type fibroblasts. No band was observed in patient P2 and carrier P2het.

3.5.2. Investigation of the proteome of cultured fibroblasts

The cell lysates of fibroblasts from the PD patients, a carrier and a control sample were analysed on a mass spectrometer as part of a pilot study to analyse the proteome. To date, this type of study has not been done on *parkin*-null patients, and the ultimate goal is to identify possible biomarkers for the disease.

Patients P3.1 and P3.2, carrier P3het and WTC2 were used for this analysis. Approximately 1000 proteins were identified in each individual: Patient P3.1 – 998 proteins; patient P3.2 – 1023 proteins; carrier P3het – 1143 proteins and WTC2 – 985 proteins. Firstly, the protein products of the eight known PD genes were screened for in these lists and notably parkin was not present in any of the samples (Table 3.11). DJ-1 was present in all except patient P3.1 and EIF4G1 was only present in P3het.

Table 3.11: **List of known PD proteins screened for in the fibroblasts**

Patients	P3.1	P3.2	P3het	WTC2
Parkin	✗	✗	✗	✗
DJ-1	✗	✓	✓	✓
EIF4G1	✗	✗	✓	✗
PINK1	✗	✗	✗	✗
SNCA	✗	✗	✗	✗
LRRK2	✗	✗	✗	✗
ATP13A2	✗	✗	✗	✗
VPS35	✗	✗	✗	✗

✓ , positive detection; ✗, no detection

Moreover, none of the protein products of the down- or up-regulated genes from the PCR Array experiments (Table 3.8 and 3.9) were present in these samples. Possible reasons for this could be the differences in the proteomes between blood samples and fibroblasts or that the method used did not capture the complete fibroblast proteome. Of the 84 genes screened for in the PCR Array, 15 of these protein products were present in the fibroblast proteomes.

Thereafter, we determined which proteins were present in both of the patients and not in the wild-type control, and also which proteins were absent in the patients and present in the control. This revealed a total of 152 proteins that were only in the patients and 688 proteins that were only in the control. The 688 proteins detected in the control (assumed to be absent in the patients) were analysed using IPA software (Ingenuity, USA). Interestingly, the results indicated that some of these proteins belong to the pathway associated with mitochondrial dysfunction in PD, Alzheimers disease and breast cancer (Figure 3.14). Further analysis indicated 14 proteins from this pathway were present in the wild-type control and absent in the combined patient group. These proteins form part of smaller pathways involved in mitochondrial dysfunction such as: apoptosis (CASP3), amyloid β accumulation (NCSTN), complex I (NDUFA9, NDUFS1), complex II (SDHA), complex III (UQCRB), complex IV (COX7A2), complex V (ATP5J), protection of FES cluster containing mitochondrial enzymes (SOD2), oxidative stress (OGDH, PARK7/DJ-1), ageing (CAT) and ROS accumulation (PRDX3, PRDX5). These results should be interpreted with caution as only 1000 proteins were identified.
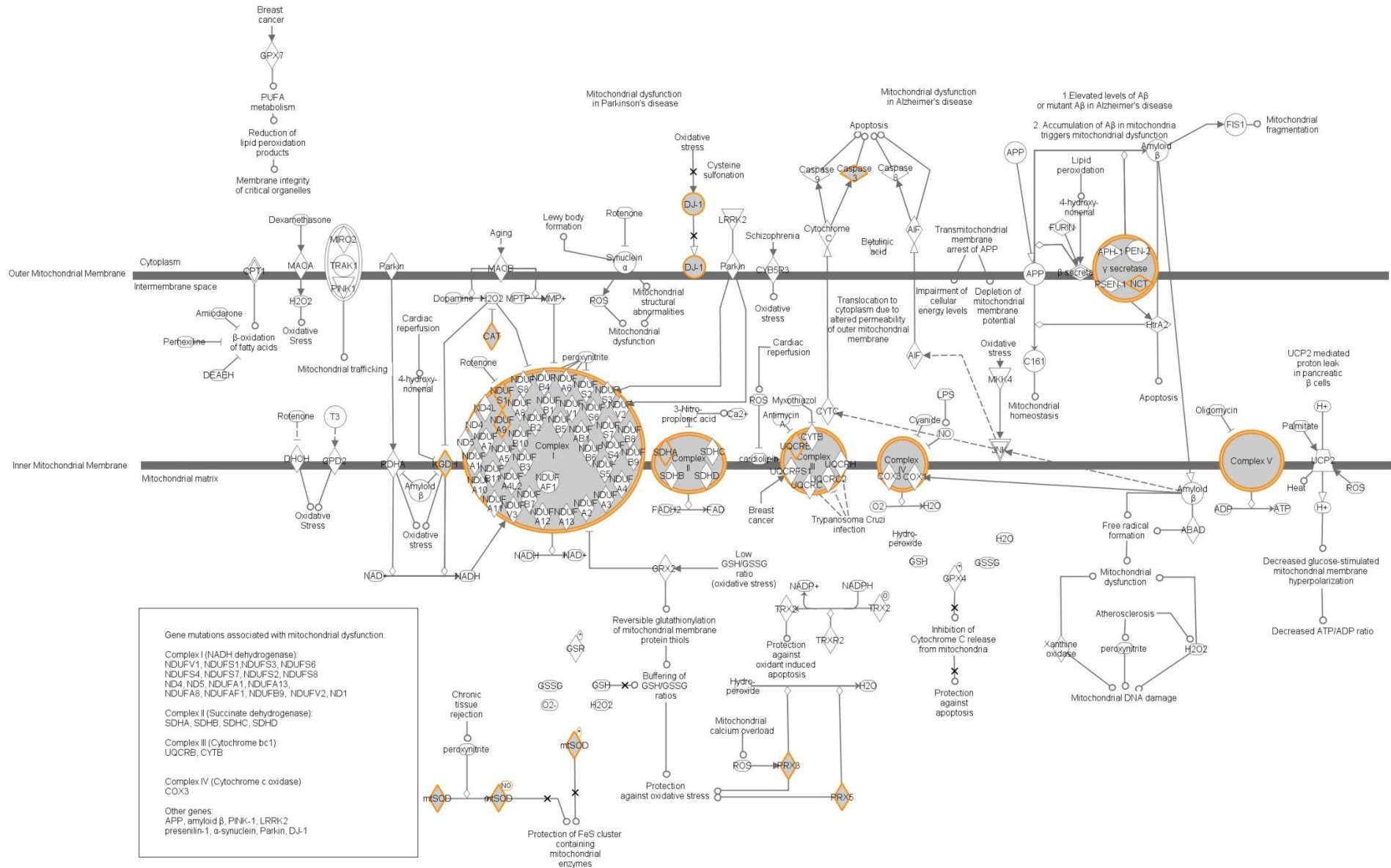
Figure 3.14: Pathway implicated in mitochondrial dysfunction in PD, Alzheimer's disease and breast cancer. The 14 proteins found only in the wild-type control and not in the two PD patients are highlighted in orange.

Chapter 4

DISCUSSION

113

PAGE

In the present study we had hypothesized that mitochondrial dysfunction plays a critical role in our South African PD patients with *parkin* mutations. Using western blots we verified that parkin protein was absent in the patient fibroblasts. We investigated whether there was evidence for mitochondrial dysfunction in these patients using a range of different experimental procedures. The TEM analysis of fibroblasts noted in one patient (patient P2) high levels of electron dense cellular vacuoles surrounding the mitochondria, suggestive of possible mitophagy. Also, the mitochondrial network appeared extensively damaged and fragmented in that particular patient. In muscle cells, subtle defects (accumulation of lipids, wrinkling of the sarcoplasmic membrane, presence of type II fibres and the presence of atrophic fibres) were observed in all three patients but particularly in the oldest patient (patient P3.1). This patient also had slightly more prominent and enlarged mitochondria.

Three of the four patients exhibited increased mitochondrial ROS levels compared to the control. Furthermore, a number of electron transport chain genes were down-regulated, in particular *CYC1*, *BCS1L*, *NDUFS2* and *LHPP* which were found to be down-regulated in all three probands. Lastly, in the pilot study performed on the proteome of fibroblasts a total of 688 proteins were present in the control and not in the patients. IPA analysis revealed that 14 of these proteins were part of the 'mitochondrial dysfunction' pathway which further implicates this process in the pathogenesis of PD.

4.1. Changes in the mitochondrial morphology and network of the patients

Structural analysis of the mitochondrion allows one to identify defects which could impair mitochondrial function, and this could ultimately affect the overall cellular function. Mitochondrial structure assessment should include several parameters, such as the overall size and shape of the mitochondria, the appearance of the cristae and the mitochondrial membrane, the electron density which provides a basic impression of the level of oxidative phosphorylation occurring within the organelle, and the presence of glycogen or lipids in the matrix of the mitochondria. Analysis of the cellular structure can also provide an indication of dysfunctional mitochondria, such as the presence of certain enzymes and lysosomal vacuoles, the fibre type when focusing on muscle cells, as well as the occurrence of mitochondrial fusion and/or fission through analysis of the cellular mitochondrial network.

Animal models are used to investigate a number of aspects of PD, such as cause, treatment or gene expression. Studies on mitochondrial morphology in animal models of *parkin* knockouts have yielded contradicting results – *Drosophila parkin* knockout models show mitochondrial pathology as the earliest manifestation of muscle degeneration (Greene et al., 2003; Pesah et al., 2004), observing an increase in vacuole number, cellular debris, with irregular myofibrillar arrangement of the muscle cells and swollen mitochondria with disintegrated cristae. In comparison, no mitochondrial morphological defects were seen in *parkin* knockout mice models (Palacino et al., 2004), with both knockouts and controls exhibiting well-formed mitochondrial membranes and intact, discernible cristae. A possible reason for the differences observed in these two animal models may be due to the differences in the genome of each species. Approximately 60 percent of genes are conserved between the *Drosophila* and humans (Adams et al., 2000). Comparatively, the mice genome shares approximately 85 percent of the human genome, although there is a high level of variation from gene to gene. Although these models are advantageous in investigating PD, these conflicting findings suggest that human studies are essential in determining the precise mechanisms involved in the disorder. In humans, relatively few morphological studies have been performed to date on tissues obtained from *parkin* patients (who are in essence '*parkin* knockouts'). Although these human studies have provided interesting insights, the findings have also been conflicting (Grünewald et al., 2010; Hanagasi et al. 2009; Mortiboys et al., 2008; Pacelli et al., 2011).

In the present study the results from the analysis of mitochondrial morphology in the muscle biopsies varied between the three patients (Table 3.3) but most obvious were the lack of ragged red fibres (RRFs). RRFs have been observed in various mitochondrial diseases such as MERRF (Berkovic et al., 1989), and are one of the strongest indicators of severe mitochondrial dysfunction in muscle cells. The generation of these fibres indicates abnormal proliferation and sub-sarcolemmal accumulations of mitochondria. Other reports on muscle biopsies of *parkin* patients are rare. One study done on a 53 year old male with a homozygous *parkin* deletion at the exon9/intron9 boundary observed a few ragged red fibres and an abundance of cytochrome oxidase negative fibres (Hanagasi et al. 2009). Although no RRFs were observed in our patients, sub-sarcolemmal aggregates of normal mitochondria associated with increased lipid content were noted. This could suggest that mitochondrial dysfunction is at an initial phase of accumulation, and that RRFs may present in the future in these patients.

Despite the lack of RRFs in the patients' muscle cells, an abundance of type II muscle fibres were observed in patient P3.1, as well as grouping of these fibres in patients P2 and P3.1. Type II fibres are fast twitch muscle fibres that utilize anaerobic metabolism (i.e. glycolysis) to produce energy .The increased presence and grouping of type II fibres suggests that the majority of the ATP produced in these cells is via glycolysis (which occurs outside the mitochondria in the cytoplasm of the cell) and not via oxidative phosphorylation. This could indicate that there is a possible defect in the mitochondrial electron transport chain in these cells and the grouping of the type II fibres may be a compensatory mechanism to produce ATP. Although no work has been published regarding the presence of type II fibres in the muscle of PD patients, previous studies done on fibre type and ageing show increased grouping of type II fibres as the age of the individuals increases (Brunner et al., 2007; Fayet et al., 2001) as well as an increase in lipid droplets in the muscle fibres (Poggi et al., 1987). All studies observed these changes in individuals over the age of 50 years. The patients recruited for this study are 50 years and younger (Table 2.1), so the fibre grouping observed appears to indicate premature ageing possibly due to the *parkin* mutation.

Muscle biopsies that were performed on 13 healthy elderly individuals (66 – 77 years of age) and 15 healthy younger individuals (23-37 years of age) revealed scattered atrophic fibres, collections of lipofuscin, and wrinkling of the sarcolemmal membranes only in the elderly group of patients (Jakobsson et al., 1990). The observation of sarcolemmal membrane wrinkling in patients P1, P2 and P3.1, as well as scattered atrophic fibres in patients P1 and P3.1 and lipofuscin in patient P3.1 is additional evidence of premature ageing of the muscle cells, as all three individuals are aged 38 years, 37 years and 50 years respectively, and show similar muscle morphology to individuals over the age of 66. It would be interesting to examine muscle cells of pre-symptomatic *parkin*-null patients to see whether these individuals also show evidence of premature ageing.

In addition, lipid droplets were also observed in two of our patients (patient P1 and P3.1). The presence of increased lipids in the mitochondria may lead to the process of lipid peroxidation – whereby free radicals such as ROS degrade excess lipids in order to scavenge the electrons from these fatty deposits. Excessive lipid peroxidation could result in cell membrane damage and cell death if toxic end products are produced, possibly contributing to neuronal cell death found in PD. Lipid accumulation and peroxidation have been observed in the brains of patients with PD (Dexter et

al., 1989), however the presence of lipids in cells other than neurons is unreported, and there have been no studies to show the presence of lipids in muscle cells of *parkin*-positive PD patients. Therefore, at this stage it is not certain that lipid peroxidation is occurring in the muscle cells of these patients, although it could be speculated that the subtle mitochondrial structural changes observed may cause altered metabolic reactions that could lead to eventual cellular death.

In the present study, we also investigated mitochondrial morphology and function in fibroblasts cultured from skin biopsies of our patients. Ideally, neurons from the SNc should be chosen as the main cell type for studies on PD; however these cells can only be obtained post mortem. Morphological and functional studies have been performed on skin fibroblasts of PD patients and have noted similar results to that observed in post mortem brain tissue (Wiedemann et al., 1999; Hoepken et al., 2007; Mortiboys et al., 2008; Grünewald et al., 2010; Pacelli et al., 2011). Recently, it has been stated that fibroblasts serve as a useful primary PD cell model (Auburger et al., 2012). Expression levels of both *parkin* and *PINK1* genes are at relevant levels in fibroblasts. Several advantages of using skin fibroblasts as a cell model include the following (Auburger et al., 2012):

- Relative ease of availability (fibroblasts can be easily isolated from a skin biopsy)
- Robustness in culture, storage and transport
- Reflect cumulative cellular damage according to the age of the patient
- Expression of most of the PD genes are at relatively high expression levels
- Fibroblasts can be immortalized (i.e. they avoid apoptosis) and can therefore proliferate faster than primary cells, producing far more cells than any other cell line would in the same amount of time

Disadvantages of fibroblasts use may be the length of culture time (can only culture after passage 3) specifically in older cells, contaminations are frequent, and fibroblasts are resistant to stressors (Auburger et al., 2012). However a study performed on *parkin*-null fibroblasts used paraquat as a stressor and observed relative changes in both control and patient cells (Grünewald et al., 2010).

The TEM results of fibroblasts obtained from patients P3.1 and P3.2 show rod-shaped and round mitochondria with normally arranged cristae. In comparison, several cells from patient P2 exhibited a mixture of rod-shaped and circular mitochondria that appeared swollen. A recent study on *parkin*-null fibroblasts showed swollen mitochondria of an irregular shape, with few remaining cristae (Pacelli et al., 2011). Except for their study, no other studies to date have been performed using TEM to analyse the mitochondrial morphology in *parkin*-null patient fibroblasts.

Interestingly, in patient P2 cells there were numerous autophagic vacuoles filled with dark material of an unknown source. Cellular vacuoles are generally filled with water containing enzymes in solution, and function as exporters of waste in the cell. It can be speculated that these vacuoles (or autophagosomes) are filled with cellular material such as accumulated proteins or damaged mitochondria which are accumulating due to the absence of parkin. An alternative hypothesis is that filled autophagic vacuoles are present as a precursor for cellular apoptosis. The accumulation of these vacuoles is dependent on a receptor-interacting protein that is associated with a death receptor and caspase 8 – which initiate apoptosis (Codogno & Meijer, 2005). Electron dense vacuoles had previously been observed in PD *parkin*-positive patient fibroblasts (Pacelli et al., 2011), similar to that found in patient P2 and P3.1. Pacelli and colleagues speculated that this material degraded mitochondria that have been engorged via the process of mitophagy. However, it cannot be stated unequivocally that mitophagy is occurring in these cells as the electron dense vacuoles observed may also be due to lysosomal digestion of cellular debris, and thus increased autophagy. Further analysis of the material inside these vacuoles is needed before conclusions can be formed.

Subsequent to the observation of mitochondrial fusion in the TEM of the fibroblasts, the cellular mitochondria were stained in order to investigate the mitochondrial network. Tubular networks are formed by the mitochondria in order to promote cell survival and maintain healthy mitochondria. This network is developed through the processes of fusion and fission. Although both processes are vital in maintenance of mitochondrial function, fusion protects function whereas fission isolates damaged mitochondria for autophagy (Chen & Chan, 2009). Therefore, in cells where fission is prominent, damaged mitochondria are in the majority. A study on fibroblasts of two siblings with PD, both with homozygous *parkin* mutations, showed fragmented mitochondria in both patients, which indicates fission and damaged mitochondria (Pacelli et al., 2011). In the present study, patient P2, and to a lesser degree patient P3.1, exhibited a mitochondrial network showing dot-like staining

indicating fission and extensive fragmentation. It could be speculated that the electron dense material observed in this patients autophagosomes are these damaged mitochondria that have been tagged for degradation during fission.

No studies to date have been reported on mitochondrial morphology of unaffected *parkin* heterozygous family members of PD patients. In our study, individual P2het showed high degrees of fragmentation in the mitochondrial network, whereas P3het exhibited a normal mitochondrial network. In recent years, it has been discovered that mitochondrial fragmentation, along with cristae remodelling, plays an important role in the initiation and execution of the death cascade that results in cellular apoptosis (Chang & Blackstone, 2010; Heath-Engel & Shore, 2006; Perfettini et al., 2005). It has also been observed that fragmented mitochondria are removed by mitophagy before apoptosis is induced (Kim et al., 2007). Mitochondrial dysfunction has also been linked to ageing (Lin & Beal, 2006) through various functional aspects such as a decrease in ATP production or an increase in ROS production. It is now thought that control of apoptosis by mitochondria (through mitochondrial fragmentation) can also contribute to the decline in function of long-lived cells, resulting in ageing. We therefore speculate that the fragmentation observed in carrier P2het could be due to her increased age (65 years) compared to P3het (54 years; Table 2.1).

Taken together, our findings suggest that patients with *parkin* –null mutations have an accumulation of damaged mitochondria similar to that seen in the cells of aged individuals. Parkin is known to tag damaged and dysfunctional proteins in the cells for degradation, and therefore a lack of parkin results in accumulation of these proteins. It is possible that parkin acts in the same way on mitochondria, and without parkin, these damaged mitochondria accumulate and result in an increased cellular toxicity possibly through a higher level of ROS production, eventually leading to apoptosis.

4.2.   Increase in mitochondrial ROS levels in three patients

We investigated whether the subtle changes observed in the mitochondrial structure would influence the bioenergetics metabolism. Functional analysis was determined by the measurement of ROS from i) the mitochondria and ii) the cytosol in patient fibroblasts and compared to that of the carriers and the wild-type control. Ideally, mitochondrial complex activity and ATP production should also be measured, however due to unavailability of equipment in our laboratory and the lack of suitable collaborators in the country, only ROS analysis was performed to analyse the mitochondrial function. By staining the mitochondrial ROS and generic ROS with two different fluorochromes these could be distinguished from each other.

The results were inconclusive regarding generic ROS, with patient P3.1 exhibiting levels higher than the control and heterozygote, whereas patients P2 and P3.2 had lower levels compared to the control. Although lymphocytes were used instead of fibroblasts for patient P1, results from generic ROS studies on this patient found higher levels in the patient compared to the control. Therefore in summary, two patients exhibited higher generic ROS levels, and two patients exhibited lower generic ROS levels compared to the wild-type control. Although mitochondrial generation of ROS is one the cell's primary sources of ROS, oxidation and reduction reactions that produce ROS continuously occur in the cytoplasm. There are also various external environmental ROS sources such as exposure to radiation and infections that can also increase the levels of generic ROS (Kregel & Zhang, 2007). This may be a reason why conflicting results were obtained as generic ROS levels are influenced by a number of external factors such as a different genetic make-up, environment and lifestyle. It is therefore more important to specifically analyse mitochondrial ROS levels to assess mitochondrial function.

The results from the mitochondrial ROS analysis showed that three of the patients exhibited higher levels than the control and heterozygotes. This fits in with our hypothesis that the cells are experiencing oxidative stress. Notably, the patient (P2) with the highest level of mitochondrial ROS also exhibited highly electron dense vacuoles and a fragmented mitochondrial network. Previous studies performed on *PINK1* knockout mice and *PINK1*-mutant PD patients have found an increased level of oxidative stress compared to controls (Gautier et al., 2008; Grünewald et al., 2009). Another

study analysing *LRRK2* mutant fibroblasts found a significant increase in intracellular ROS levels in the patients (Wang et al., 2012), although these results have been contradicting (Papkovskaia et al., 2012). Similarly, *parkin*-mutant PD patient fibroblasts have also shown to have a higher level of oxidative stress under basal conditions (Grünewald et al., 2010) when analysing the cells with an OxyBlot. Pacelli and colleagues found a significant increase in generic ROS production in two PD patients with *parkin* mutations by analysing the fluorescence intensity of DCF, the oxidation-sensitive staining dye used to measure generic ROS (Pacelli et al., 2011). Our study was unique in the fact that we measured both generic ROS as well as mitochondrial ROS.

One of our patients P3.2 showed decreased levels of mitochondrial ROS. Interestingly patient P3.2 was also the only patient that did not exhibit any features of mitochondrial network fragmentation. A possible reason for this may be that this patient has an underlying compensatory mechanism that is able to protect the mitochondria in fibroblasts tissue. Further tests need to be performed regarding mitochondrial function, such as determining complex activity and levels of ATP production, before conclusions can be drawn regarding the mitochondrial function in *parkin*-null PD patients. Also, these analyses should be performed in triplicate, as technical repeats as well as biological repeats are necessary for the validation of all results.

In other studies on *parkin*-mutant patients, alterations in mitochondrial function in several categories were detected – namely complex activity, respiration rates, ATP production and cellular content, mitochondrial membrane potential and levels of antioxidants e.g. glutathione reductase, glutathione peroxidase and catalase. Significantly decreased complex I activity and respiration rates, lower mitochondrial membrane potential, and lower antioxidant levels were observed in some patients from previous studies(Mortiboys et al., 2008; Pacelli et al., 2011). However, results were contradictory with regard to ATP cellular levels, with some studies revealing a decrease in ATP synthesis rates and ATP levels (Grünewald et al., 2010; Mortiboys et al., 2008)and others revealing a significantly higher ATP content in patient cells, due to possible compensation by the glycolytic pathway (Pacelli et al., 2011).

4.3.   Down-regulation of genes involved in mitochondrial electron transport

Analysis of gene expression in mRNA allows for the identification of changes in pathways that may provide clues to the pathogenesis of a disease. In PD, the majority of gene expression studies have used dopaminergic neurons or substantia nigra (SNc) post mortem tissue (Grünblatt et al., 2004; Hauser et al., 2005; Simunovic et al., 2009; Zhang et al., 2005). Due to almost selective loss of dopaminergic neurons in the SNc of patients with PD, obtaining brain tissue is essential in assessing the physiological events that cause the disease. Marked expression changes in genes involved in energy metabolism were observed in these studies. Analysis of gene expression levels has also been done in other tissues, including whole blood (Scherzer et al., 2007) and fibroblasts (Pacelli et al., 2011). These two tissue types are far easier to obtain due to the non-invasive procedures of specimen retrieval, however whole blood is preferable as artifacts in gene expression can be induced during cell culturing (Whitney et al., 2003). In the present study, we therefore used whole blood for the gene expression experiments.

For any analysis of gene expression levels, the highest possible quality of RNA is necessary for reproducible results. RNA quality can be measured through two parameters – the purification of the sample and the integrity (or degradation status) of the RNA (Bustin & Nolan, 2009). Based on several analyses of RNA quality determination methods, the spectrophotometric measurement is not a reliable measure of sample quality as it does not reveal a degradation state. Alternatively, the use of an electropherogram (such as the Experion Std Sense Analyser) allows for a more objective measure of RNA quality by the measure of several characteristics which determine the RQI value (Denisov et al., 2008). A RQI value of 8 or higher has been deemed as acceptable for use in gene expression studies (Fleige & Pfaffl, 2006). The RNA samples that were used in the present study all had RQI values of >8. Possible reasons for low RQI values may be due to the presence of inhibitors or contaminants in the sample.

For these experiments we selected a pathway-based gene expression PCR Array (SABiosciences, USA) that included genes which code for parts of each of the five complexes in the electron transport chain. A previous study performed on the same PCR Array on human embryonic stem cells

and induced pluripotent stem cells found similar expression in both cell types, but proved that this array is useful, precise and efficient when analysing gene expression (Prigione & Adjaye, 2010).

Results from our analysis showed that the expression of the majority of genes (76.2%) remained unchanged in the patients. Also, twice the number of genes were down-regulated (16.7%) in patients compared to the number of up-regulated genes (7.1%). The majority of these down-regulated genes code for part of complexes I and III. Six of the 14 down-regulated genes from our PCR Array gene expression analysis correlated with the findings observed in a previous meta-analysis (Zheng et al., 2010) – namely *ATP5G1, ATP5J2, CYC1, NDUFB7, NDUFS1* and *UQCRC1*. Interestingly, two of the 14 genes that our study found to be down-regulated were up-regulated in the meta-analysis (*NDUFS2* and *NDUFS7*), although only slightly (by a fold change of +0.01 and +0.02 respectively). Similarly, the genes that our study found up-regulated in the PD patients were all down-regulated in the meta-analysis. A possible reason for the differences may be that whilst our three patients all had *parkin* mutations, the tissues used in the previous studies were taken from sporadic PD cases.

The Primer Assay (SABiosciences, USA) performed on *CYC1* to validate the PCR Array results showed no change in expression levels across all four patients. This result suggests that gene expression studies using PCR Arrays need to be validated with independent experiments. The use of both biological (different samples) and technical (same sample analysed multiple times) replicates in Primer Assays may produce more reproducible data than that obtained using PCR Arrays. The greater the number of biological and technical repeats, the better the implementation of robust statistical methods to select differentially expressed genes (Tan et al., 2003). However, it is possible that the results for only the *CYC1* gene are not verified in the Primer Assay and analysis of the other down-regulated genes is warranted.

A meta-analysis of 17 independent genome-wide expression studies was recently performed (Zheng et al., 2010). Included in this analysis were the studies that had been performed on either different parts of the brain, the SNc, dopaminergic neurons, and peripheral blood or lymphoblastoid cells. The purpose of this study was to combine the results from individual gene expression studies to increase the statistical power and precision of pathway associations. Across these studies, the consensus appears to be that genes in various processes including mitochondrial electron transport, glucose

utilisation and glucose sensing, were under-expressed in PD patients. This down-regulation was observed in both brain and blood tissue. In particular they noted PGC-1α-responsive genes were under-expressed. PGC-1α is a key regulator of mitochondrial biogenesis and oxidative metabolism. It acts as a transcription co-activator, which is a protein that increases the probability of genes to be transcribed by interactions with transcription factors (such as the PPARs) involved in biological responses (Liang & Ward, 2006). Overexpression of PGC-1α in primary cultures from the midbrain of rats that were overexpressing α-synuclein (a model of PD), activated expression of the genes encoding the mitochondrial respiratory complexes I, II, IV and V, indicating that PGC-1α expression can alleviate the toxic effects of α-synuclein in this cell model (Zheng et al., 2010). Secondly, they also found that overexpression of PGC-1α in cells exposed to rotenone activated the expression of genes for all five of the respiratory complexes. Interestingly PGC-1α halted dopamine neuron loss in both PD models. It can therefore be speculated that the mitochondrial functional loss observed in PD patients, such as complex I activity decrease and ROS production increase, could be due to a transcriptional defect involving PGC-1α. This knowledge is critical for the development of improved therapeutic targets and even prevention of PD.

Pacelli and colleagues investigated regulation of PGC-1α expression in fibroblasts of *parkin*-null patients (Pacelli et al., 2011). Their results showed up-regulation of PGC-1α in both patients compared to the control, as well as an increased PGC-1α protein content in the patients. They then analysed target genes involved in mitochondrial biogenesis that are all situated downstream of PGC-1α and found that the genes were generally unchanged (*ATPaseβ, COX2*) or down-regulated (*NRF1, NRF2, TFAM, MCAD*). This observation suggests that post-translational modifications such as phosphorylation, methylation and acetylation are at play that can modulate the PGC-1α activity and stability (Pacelli et al., 2011).

PGC-1α knockout animal models have shown up to a 44% decrease in mitochondrial content in muscle (Adhihetty et al., 2009) as well as impaired mitochondrial function (Lin et al., 2004). Knockout PGC-1α models have also shown a blunted mitochondrial respiration gene expression levels (Arany et al., 2005). An example of the mechanism of PGC-1α is the increased transcription of nuclear respiratory factor 1 (NRF1) and NRF2, which subsequently leads to increased expression of the complexes in the electron transport chain (Scarpulla, 2002). These are just two examples of thousands of genes that are activated by PGC-1α. PGC-1α has also been observed to induce

antioxidants in response to oxidative stress levels in the cell (St-Pierre et al., 2006), and has also been implicated in playing a role in Huntington's disease when impaired (McGill & Beal, 2006). Therefore, PGC-1α has been the focus of several recent studies as a possible therapeutic target in neurodegenerative disorders such as PD.

In summary, our results and that of others suggest that some of the electron transport genes may be down-regulated in patients with *parkin* mutations. It is possible that parkin regulates, directly or indirectly, the levels of an activator(s) such as PGC-1α, which activates transcription of specific components of the electron transport chain. If these findings are verified it could be speculated that down-regulation of these genes may lead to impaired oxidative phosphorylation and increased mitochondrial ROS ultimately resulting in an accumulation of damaged mitochondria triggering apoptosis.

4.4.   Proteome of fibroblasts

Western blot analysis was performed to verify the absence of parkin protein in patients with two *parkin*-null mutations. The western blot experiments required extensive optimisation in order to identify the correct primary antibody and dilution factor, and fibroblast concentration in these experiments. Eventually, the procedure was successful using a monoclonal primary antibody dilution of 1:500, a cell lysate concentration of 7μg/μl and a 10% resolving gel solution. Parkin was detected at 50kDa in control fibroblasts, but was absent in the patient (with homozygous exon 3 and 4 deletion) and carrier fibroblasts. This observation is supported by the literature whereby an absence of parkin was observed in fibroblasts from patients with similar exonic deletions (Mortiboys et al., 2008; Pacelli et al., 2011). It could be speculated that the parkin band in the carrier (only one functional *parkin* allele) is present, but the intensity is too low to be visible. However this requires further study.

In addition, we analysed the proteome of the fibroblasts in order to answer the following questions: Can the gene and protein expression data in the blood and fibroblast tissue be correlated? Also, can analysis of the proteome identify possible biological pathways implicated in PD?

To answer the first question we compared the gene expression data from the PCR Arrays with the proteome data albeit from two different tissue types, which may be problematic. We expected to observe the down-regulated gene products in wild-type control but not in patient samples, and the up-regulated gene products were expected to be observed in patient samples but not the in control. This was not found possibly due to these two tissue types having different expression profiles or because the entire fibroblast proteome had not been captured. It is thought that the each individual cell contains approximately 10 000 different proteins, such as enzymes, proteins involved in cell maintenance, transport, synthesis and various other cellular functions. Therefore, the approximately 1000 proteins detected in each sample in the present study are likely to be an underestimate. However, despite this limitation, IPA analysis of the 688 proteins that were present only in the wild-type control and not in the two patients identified the 'mitochondrial dysfunction' pathway as possibly playing a role in the disorder.

4.5.   Limitations of study

The current study involves a multi-faceted analysis of *parkin*-null PD patients regarding mitochondrial morphology and function, as well as gene and protein expression. The limitations faced in this research project included not being able to utilize all four patients in every section of the project due to various reasons. One of the major limitations was the inability to grow up fibroblasts from patient P1. This patient was the first of the four to be recruited, and unfortunately his skin biopsy was referred to the incorrect laboratory by the doctor who took the biopsy. This meant that fibroblasts of patient P1 were not available for the TEM, mitochondrial network, ROS and proteome studies, for comparison with the other patients. Although white blood cells from patient P1 were used for ROS measurements, this in itself was a limitation as results should not be compared across different tissue types.

Financial restraints also proved to be a limitation in parts of this study. Due to the cost of the RT² Profiler PCR Array, only the three probands could be used for gene expression analysis. Also, we were unable to perform exon dosage experiments on the controls. Due to financial constraints, the

MLPA kits needed for this procedure were not available. Also, although wild-type controls were age-matched to patients P1 and P2, they were not age-matched to patients P3.1 and P3.2.

The mitochondrial functional studies were limited to the analysis of ROS levels in this study. A better assessment of mitochondrial function should have included respiratory complex activities and mitochondrial ATP production and levels. However, during the course of the study, attempts to find the necessary equipment (oxygraph) and expertise were unsuccessful.

Although the proteome analysis was a pilot study as no previous studies have been reported on the proteome of *parkin*-null patients, this work has also had a number of limitations. Firstly, we did not include technical replicates of the runs on the Orbitrap. Secondly, we did not fractionate the samples on a PAGE gel before analysis on the Orbitrap. Instead we used the cell lysate solution in a single run, and this identified only approximately 1000 proteins, whereas if we had run a fractionated sample then we may have been able to detect up to 5000 proteins. And thirdly, not all four of the patients had been analysed using this technique.

Finally, another shortcoming of this particular study was the use of fibroblasts of the patients to study mechanisms underlying PD. Fibroblasts have been used by numerous groups to study this disorder and has been shown to be a good cell model albeit with some drawbacks (Auburger et al., 2012). This may explain why some of the defects found were not consistent across all four patients as the experiments were not done on the tissue affected by PD – substantia nigral neuronal tissue.

4.6.   Future work

A summary of previous work and recommended future work in relation to the findings of the present study is shown in Table 4.1.

One of the primary aims for future work is to investigate all aspects of mitochondrial function in fibroblasts of all four *parkin*-null patients. This will involve the analysis of all five respiratory chain complex activities through the use of an oxygraph, via collaboration with either a laboratory within South Africa, or an international collaboration where this method has been utilized. In addition, the levels of cellular ATP content should be measured for each patient, heterozygous carrier and control. Subsequently, several other functional aspects can also be investigated in patient fibroblasts. These include: mitochondrial membrane potential, cellular membrane integrity, viability and apoptosis analysis as well as patient and control fibroblasts growth rate in different media e.g. glucose and galactose. It is vital to analysis the apoptotic pathways in greater detail, to identify possible links between PD patients with mitochondrial fragmentation and apoptosis. Furthermore, building on the work on ROS levels, it would be appropriate to perform a study on the antioxidant capacity in these patients. Although several of these experiments have been performed by other groups (Table 4.1), the findings are equivocal, indicating that future work on mitochondrial function of *parkin*-null patients including a large number of biological and technical replicates, are necessary.

On a structural level, this study covered mitochondrial morphological analysis on both muscle and skin biopsies of *parkin*-null patients. Until dopaminergic neurons from SNc of these patients are available to us post-mortem, these TEM results are the best that we can expect to obtain with regards to the effect of parkin on mitochondrial structure. Future work to determine the compositions of the electron dense vacuoles could include ultracryomicrotomy and electron probe x-ray microanalysis, and to determine whether mitophagy is occurring within the cell we could label the mitochondria with live cell imaging. Measurement of mitochondrial length and mass should also be performed on patients and fibroblasts in the future. Also, future work should include quantitative analysis of the mitochondrial network. Other groups have analysed mitochondrial networks by the calculation of a 'form factor' (Table 4.1), whereby mitochondrial area and outline are measured. The form factor allows for quantification of the degree of branching of the mitochondrial network relative to a control.

In terms of future work regarding gene expression levels, other pathway focused PCR Array options include catalogued arrays for Apoptosis, Autophagy, Mitochondria and Oxidative Stress (http://www.sabiosciences.com/). Also, a customized plate can be designed with genes of interest selected to study the effect of parkin on the mitochondria. An interesting approach would be

analysis of the expression level of the genes involved in mitochondrial fusion (*Mfn1*, *Mfn2*, *Opa1*) and fission (*Drp1* and *Fis1*), as well as the expression of the genes that operate upstream from PGC-1α, as was performed by Pacelli and colleagues (Pacelli et al., 2011; Table 4.1). More importantly, however, will be to perform the expression studies with a larger number of biological and technical repeats than were previously used. Proteome expression studies should be extended by performing all of the runs on the LTQ Velos Orbitrap in triplicate at the same time for more accurate results.

Inclusion of stressors is another important factor that should be included in the design of future studies. A study performed by Grunewald and colleagues analysed fibroblasts from *parkin*-null patients and controls under two conditions: i) basal conditions and ii) oxidative stress conditions induced by the herbicide paraquat (Grünewald et al., 2010; Table 4.1). Future work planned should therefore involve the addition of a stressor (such a rotenone, paraquat or H_2O_2) to the cells, to observe the effect on growth rate, cell viability, mitochondrial structure and function and gene and protein expression.

As parkin and PINK1 have been shown to function in a common pathway (Dagda et al., 2009; Park et al., 2006; Silvestri et al., 2005), we had initially planned to include a *PINK1*-null patient in the present study but that had proven unsuccessful as this patient was too ill to travel to Cape Town. For future studies we will attempt to obtain a muscle biopsy, skin biopsy and peripheral blood sample from this patient and her two siblings, who also have *PINK1*-null mutations. With this we can then repeat the experimental approach taken in this study (Table 4.1), and compare the results between these two genes, to gain a better understanding of the disease process. Ideally, the effect of all the PD genes on the mitochondria should be assessed. Continued patient recruitment and mutation screening is necessary to identify PD patients with mutations in a range of different genes. This will facilitate a comprehensive and systematic well-designed study on the pathobiology of PD.

Table 4.1: A comparison of previous, current and recommended future work on *parkin*-null PD patients to investigate mitochondrial dysfunction. Recommended future work on *PINK1*-positive patients in pink font

STRUCTURAL ANALYSIS			
	Previous work	**The present study**	**Recommended future work**
Mitochondrial morphology in muscle	Hanagasi et al. 2009: • Ragged red fibres • Cytochrome oxidase negative fibres	• No ragged red fibres • Increased lipid content • Wrinkling of sarcoplasmic membrane • Atrophic fibres • Type II fibre grouping • Subtle mitochondrial abnormalities	• Measurement of mitochondrial length and mass • *PINK1*-null patients muscle biopsy for histological and TEM analysis
Mitochondrial morphology in fibroblasts	Pacelli et al. 2011: • Swollen mitochondria • Electron dense lysosomal vacuoles • Few remaining cristae • Decreased electron dense mitochondrial matrix	• Normal rod-like shaped mitochondria • Slightly swollen, circular mitochondria in one patient • Electron dense autophagosomes	• Measurement of mitochondrial length and mass • *PINK1*-null patients skin biopsy for TEM analysis
Mitochondrial network analysis	Mortiboys et al. 2008: • Fragmented mitochondria in control, not patients • Analysed by form factor Grunewald et al. 2010: • No change at basal conditions • Fragmentation of patients after induction of oxidative stress • Analysed by form factor Pacelli et al. 2011: • Fragmented mitochondria in patients	• Studied patients and heterozygotes • Fragmented network in two out of three patients • Fragmented network in one out of two heterozygotes	• Analyse network results via calculation of form factor • Perform network analysis and form factor calculations on *PINK1*-null patient fibroblasts
FUNCTIONAL ANALYSIS			
	Previous work	**The present study**	**Recommended future work**
ROS measurements	Grunewald et al. 2010: • Higher level of oxidative stress in patient cells under basal conditions Pacelli et al. 2011: • Increased generic ROS in patients • Lower antioxidant levels in patients	• Higher mitochondrial ROS levels in three out of four patients • No correlation with generic ROS levels	• Analyse antioxidant capacity in patient fibroblasts • Perform ROS and antioxidant studies on *PINK1*-null fibroblasts

	Previous work	The present study	Recommended future work
Complex activity	Mortiboys et al. 2008: • Decrease in complex I in patients • No change in other complexes Grunewald et al. 2010: • No change in complex activity Pacelli et al. 2011: • Decrease in complex's I & IV in patients	Not done	• Analyse activity levels of all five complexes in parkin-positive and **PINK1-null patients** using an oxygraph
ATP levels	Mortiboys et al. 2008: • Decrease in ATP synthesis rates & ATP levels in patients Grunewald et al. 2010: • Decrease in ATP synthesis rates & ATP levels in patients Pacelli et al. 2011: • Decrease in ATP content in patients	Not done	• Analyse ATP synthesis rates and ATP content in parkin-positive and *PINK1*-null patients
Mitochondrial membrane potential	Mortiboys et al. 2008: • Decrease in patients Grunewald et al. 2010: • Decrease in patients AFTER oxidative stress insult	Not done	• Analyse mitochondrial membrane potential in parkin-positive and *PINK1*-null patients
EXPRESSION STUDIES			
	Previous work	**The present study**	**Recommended future work**
Gene expression analysis	Zheng et al. 2010: • Down-regulation of electron transport genes Pacelli et al. 2011: • Up-regulation of PGC-1α • Down-regulation of genes situated upstream of PGC-1α	• Up – and Down-regulation of mitochondrial energy metabolism genes in three patients • More genes down-regulated than up-regulated	• Analysis of expression levels in genes associated with mitochondria, oxidative stress, apoptosis and autophagy • **Analysis of mitochondrial energy metabolism genes in *PINK1*-nullpatients**
Proteome analysis	Not done	• A total of 688 proteins found only in control and not in two PD patients • Mitochondrial dysfunction pathway implicated	• **Analyse proteome of *PINK1*-null patients**

4.7.   Concluding remarks

In conclusion, the present study has elucidated on possible disease mechanisms in *parkin*-null PD patients. Increased levels of mitochondrial-produced ROS, as well as subtle changes in the mitochondrial structure such as type II fibre grouping, indicate a dysfunctional oxidative phosphorylation system, and a possible compensation for ATP production via glycolysis. This conclusion is further supported by the observation of down-regulation of electron transport genes in four of the five complexes. This work also supports and builds on the observations in several other studies of the effect of *parkin* mutations on the mitochondria, and although these studies appear contradicting, it can be concluded that parkin is vital in the correct functioning of the mitochondria.

Based on the results obtained in the present study, a model of the disease process is proposed and this is shown in Figure 4.1. Figure 4.1A represents the cell with wild-type parkin and Figure 4.1B when *parkin* is mutated. We speculate that *parkin*-null mutations lead to no parkin protein being produced. This leads to down-regulation of the mitochondrial electron transport genes which in turn causes a decrease in ATP and concomitant increased mitochondrial ROS levels. Increased ROS damages the mitochondria, which initially is cleared by mitophagy. Eventually, these and other compensatory mechanisms fail as more and more damaged mitochondria accumulate and this triggers the apoptotic pathway, eventually resulting in cell death. Future work will be vital in continuing the quest to understand the mechanisms underlying this debilitating disorder. By piecing together all the parts of the puzzle it is hoped that this will lead to development of neuroprotective strategies or ultimately a cure for not only PD but also many other neurodegenerative disorders.

Cell death via apoptosis

B: PD patients with two *parkin*-null mutations

Deletions in *parkin*

No parkin protein

Wrinkling of cell membrane & premature ageing of the cell

Down-regulation of mitochondrial electron transport chain genes

Slightly enlarged, swollen mitochondria

Fragmented mitochondrial network

Numerous electron dense autolysosomes removing damaged mitochondria from cell

Increased presence of lipids

Increased levels of mitochondrial ROS

Figure 4.1: Proposed model of the effects of parkin in a fibroblast or muscle cell in A: wild-type control and B: *parkin*-null PD patients

APPENDICES
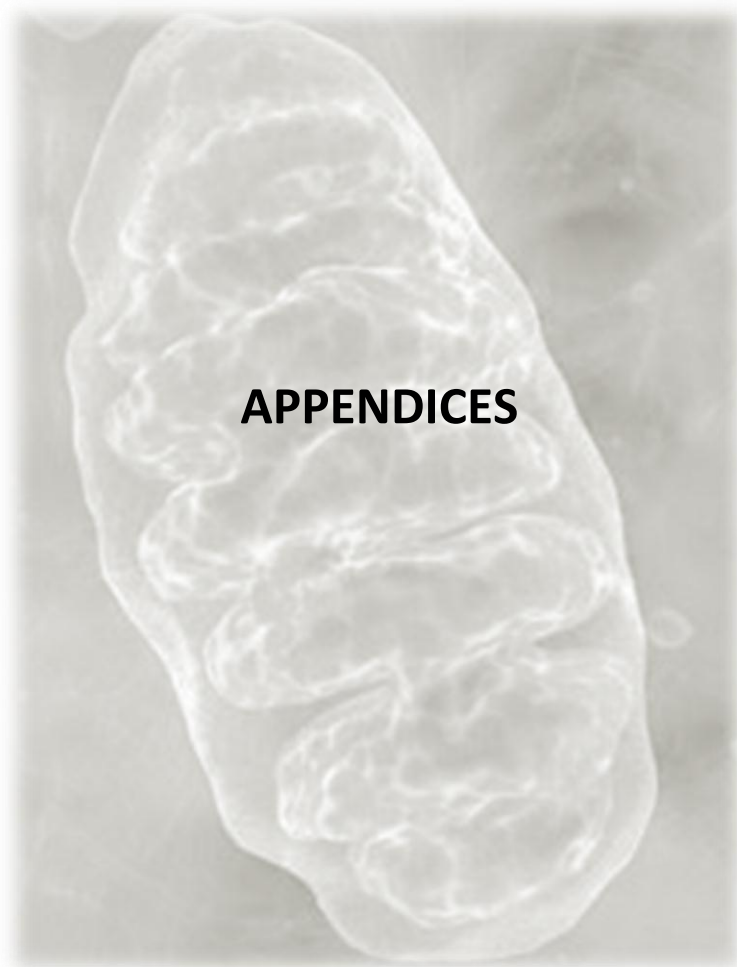
APPENDIX I

Figures of genes known to cause PD

A: *SNCA*
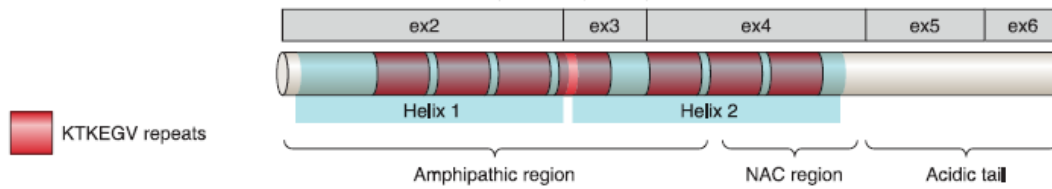
B: *LRRK2*
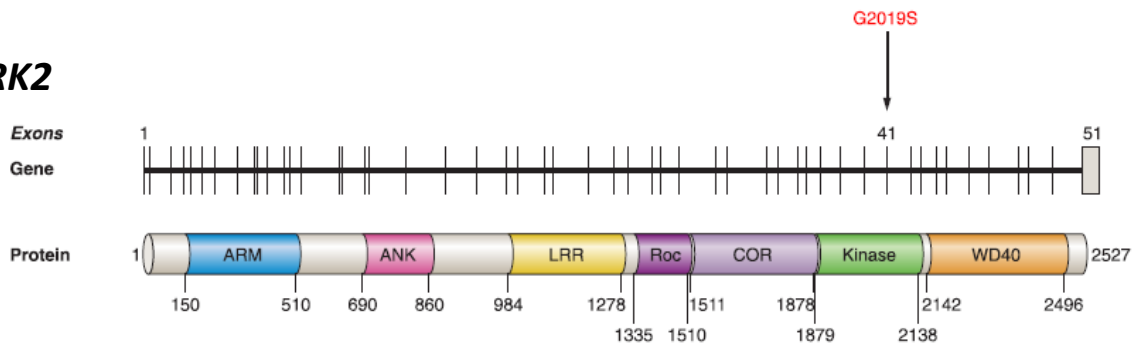
C: *parkin*

D: *PINK1*

E: *DJ-1*
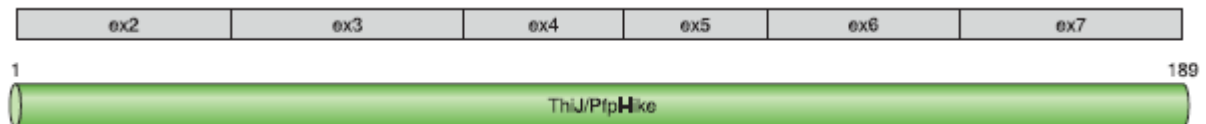
F: *ATP13A2*
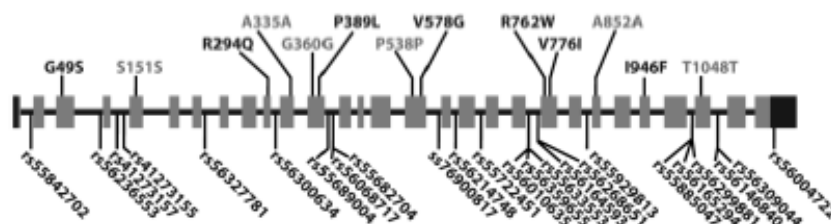
APPENDIX II

Solutions for various techniques used in the present study

Sodium Borate (SB) buffer (20x stock)

38.137g $Na_2B_4O_7$ (di-sodium tetraborate decahydrate) dissolved in 1L distilled water

- 1x SB running buffer (Agarose gel electrophoresis):

Dilute 100ml of 20x SB buffer in 2L distilled water

Bromophenol Blue Loading Dye

0.2% (w/v) bromophenol blue

50% glycerol

10mM TRIS

Add all above reagents and place on magnetic stirrer until properly mixed

10x TBE

216g Trizma Base

110g Boric Acid

18.6g Sodium-EDTA

- 1x TBE Buffer (PAGE)
Dilute 50ml of 10x TBE Buffer in 450ml distilled water

Lysis of fibroblasts and Bradford protein concentration determination

PBS (Phosphate Buffer Saline)

1 PBS tablet (Sigma, Germany)

200ml ddH_2O

Dissolve tablet in ddH_2O

Store solution at 0-5°C

IGFIR lysis buffer

50mM Hepes

100mM NaCl

10mM EDTA

1% Triton X-100

4mM NaPPi

2mM Na_3VO_4

H_2O

pH 7.5

Cell lysis buffer

5ml IGFIR lysis buffer

100µl 50mM PMSF

¼ protease inhibitor tablet (Roche diagnostics, Germany).

Bradford reagent

100mg Coomassie Brilliant Blue

100ml Phosphoric acid

50ml 95% ethanol

Dilute Coomassie Brilliant Blue in phosphoric acid and then add ethanol.

Make up to 1L with ddH_2O, stir.

Filter 2-5X until solution has light brown colour.

Store at room temperature in light proof container.

Western Blot gel preparation

Resolving gel

100µl 10% SDS

1.25ml Resolving buffer

3ml 40% acrylamide (Promega, Madison Wisconsin, USA)

75µl 10% APS (Ammonium-Perox-disulphate)

5µl TEMED (Tertramethylethylenediamine) (Sigma, Germany)

5.57ml ddH$_2$O

Stacking gel

40µl 10% SDS

1ml Stacking buffer

0.39ml 40% acrylamide (Promega, Madison Wisconsin, USA)

30µl 10% APS (Ammonium-Perox-Disulfate)

6µl TEMED (Tertramethylethylenediamine) (Sigma, Germany)

2.56ml ddH$_2$O

Resolving Gel Buffer (4X)

109.2g Tris base

330ml ddH$_2$O

24ml 10% SDS

pH to 8.8 using 1M HCl

Make up to 600ml using ddH$_2$O

Stacking Gel Buffer (4X)

36.3g Tris base

330ml ddH$_2$O

24ml 10% SDS

pH to 6.8 using 1M HCl

Make up to 600ml using ddH$_2$O

10x SDS Running Buffer

30g Tris base

144g Glycine

100ml 10% SDS

ddH₂O to a final volume of 1L

- 1x SDS Running Buffer

Dilute 100ml 10x SDS Running Buffer in 900ml distilled water

SDS loading dye

1M Tris-HCl (50mM, pH 6.8)

100mM DTT

2% SDS

0.1% Bromophenol Blue

10% Glycerol

Transfer Buffer

3.03g Tris base

14.4g Glycine (192mM)

200ml Methanol

ddH₂O to a final volume of 1L

Milk for membrane blocking

10g milk powder

200ml TBST

Mixed together and placed on magnetic stirrer until powder dissolved

TBST

8g NaCl

20ml 1M Tris-HCl (pH 7.6)

1ml Tween 20

pH 7.6

ddH₂O to a final volume of 1L

APPENDIX III

Laboratory protocols

A. DNA isolation from blood

Four 5ml blood samples in EDTA tubes were aliquoted into 2 sterile 50ml tubes. These were then filled to the 45ml mark with cold cell lysis buffer. Each tube was then well shaken and left on ice for 10 minutes. The tubes were shaken again, after which cells were pelleted by spinning at 3000rpm for 10 minutes. The supernatant was then poured off.

The wash with the cell lysis buffer was repeated. A volume of 900µl sodium acetate (3M solution) and 100µl of 10% sodium dodecyl sulfate (SDS) should then be added to each pellet. The pellet was resuspended in this solution and 100µl of proteinase K was added to each tube. The mixture was then incubated at 37°C overnight.

The following day, 2ml of distilled water and 500µl of 3M Na-acetate was added to each tube, after which the solution was mixed. A volume of 2,5ml of phenol-chloroform was added to each tube and the mixture shaken on a shaking platform at room temperature. The mixture was then transferred to a 10ml glass Corex tube and spun at 7000rpm for 12 minutes at a temperature of between 4 °C and 10 °C. The supernatant was then transferred to a clean Corex tube without disturbing the interphase. Thereafter, 2,5 ml octanol-chloroform was added to each tube. The tubes were sealed tightly and slowly mixed by inversion until the mixture turned milky. The tubes were then centrifuged without lids at 7000 rpm for 10 minutes in a Sorval centrifuge at a temperature of between 4°C and 10 °C. The supernatant was poured into a 12ml plastic tube, and 5-7ml ethanol was slowly added. The tube was then closed and mixed until the DNA precipitated.

The DNA was transferred to a 1,5ml Eppendorf tube, which was filled with 70% ethanol and centrifuged at 14000rpm for 3 minutes. The supernatant was poured off and the wash was repeated. The pellet was then dried at room temperature for 30 minutes, after which 500µl of a 1x Tris-EDTA solution was added to each tube. The tubes were incubated overnight at 37°C. Thereafter, the solutions were mixed for three days on a rotating wheel at 30rpm. The concentration of the DNA solution was read by the Nanodrop and the sample was diluted to a concentration of 0,1-0,2µg/µl.

B. Culturing of fibroblasts (Unistel Medical Laboratories (Pty) Ltd.)

1. **Set up of tissue specimen**
   - Flasks were labelled correctly and the work bench was prepared to ensure no contamination

2. **Collagenase treatment**

- A volume of 0.3ml Collagenase + 0.3ml medium was added to the 1ml medium and biopsy in a falcon tube.
- This was incubated for 20-30 min at 37˚C and shaken twice by hand during incubation
- Incubation continued for a further 30 min.
- The tube was centrifuged for 10 min at 1200rpm

3. **Set up cultures from biopsy**

- The collagenase solution was pipetted with a sterile Pasteur pipette until 3ml remained and the supernatant was discarded.
- Using the pellet of the cell suspension, 2 cultures were set up in 50ml tissue culture flasks.
- A volume of 1-2ml of medium and three drops of NEAA was added (with a Pasteur pipette) to each flask.
- Incubation followed in two separate incubators.

4. **Medium change**

- Every second day cultures were fed with 1.5ml medium.
- On day four, cultures were evaluated using an inverted microscope, with a phase contrast objective. Nest-like colonies of fibroblastic cells should be present.
- After four days of incubation, the medium of the tissue culture was decanted and changed with the mixture medium (50:50 Chang D and Amniochrome II) and 1ml NEAA
- Flasks were incubated at 37˚C and cell growth checked.

5. **Trypsinization:**

- The culture was rinsed 1x with trypsin solution (1ml + 58ml Hanks solution).
- It was rinsed a second time and the solution was left in the flask on the warm plate for 7 -10 min and regularly shaken
- Using a Pasteur pipette, the monolayer of fibroblasts was bought to suspension.
- A volume of 1ml medium was added to the culture to stop the action of the trypsin.
- Cells were divided according, to growth, in 2 – 4 culture flasks.
- A volume of 3ml of culture medium was added.
- Each flask was gassed with 5% CO_2 in air and incubated at 37˚C.

C. Freezing down procedure

Two 75cm² confluent flasks were trypsinized, and the cells were pooled and transferred into a 15ml sterile conical tube, that was topped up with culture medium. Thereafter, centrifugation occured for 10mins at 1000rpm. The medium was discarded, and 5ml culture medium was added and re-centrifuged as above. The medium was again discarded and the resulting cell pellet was resuspended in 7ml of freezing medium.

A volume of 1ml of cell suspension was aliquoted into 7 x 2ml sterile cryotubes.

Thereafter, a drop of the cell suspension was placed into two 35mm Petri dishes containing a sterile cover slip, and 2.5ml of culture medium without antibiotics was added. The plates were then incubated for two to three days for mycoplasma testing.

The 2ml cryotubes were placed in the Nalgene freezing container, containing 250ml Propyl alcohol and then placed in the -80°C freezer for a minimum of 4hrs. The tubes were then carried in liquid nitrogen to the liquid nitrogen storage containers and placed in the boxes. The location of boxes were immediately noted and on return to the lab entered in the Cell Bank database. One vial was thawed, put into a 25cm² flask containing 5ml culture medium and incubated for three days as a control to check for viability and exclude contamination (Freshney, 2010).

APPENDIX IV

List of 84 genes from the mitochondrial energy metabolism PCR Array

Gene Table

Position	Unigene	GeneBank	Symbol	Description	Gene Name
A01	Hs.147111	NM_001676	ATP12A	ATPase, H+/K+ transporting, nongastric, alpha polypeptide	ATP1AL1
A02	Hs.36992	NM_000704	ATP4A	ATPase, H+/K+ exchanging, alpha polypeptide	ATP6A
A03	Hs.434202	NM_000705	ATP4B	ATPase, H+/K+ exchanging, beta polypeptide	ATP6B
A04	Hs.298280	NM_004046	ATP5A1	ATP synthase, H+ transporting, mitochondrial F1 complex, alpha subunit 1, cardiac muscle	ATP5A, ATP5AL2, ATPM, MOM2, OMR, ORM, hATP1
A05	Hs.406510	NM_001686	ATP5B	ATP synthase, H+ transporting, mitochondrial F1 complex, beta polypeptide	ATPMB, ATPSB, MGC5231
A06	Hs.271135	NM_005174	ATP5C1	ATP synthase, H+ transporting, mitochondrial F1 complex, gamma polypeptide 1	ATP5C, ATP5CL1
A07	Hs.514870	NM_001688	ATP5F1	ATP synthase, H+ transporting, mitochondrial F0 complex, subunit B1	MGC24431, PIG47
A08	Hs.80986	NM_005175	ATP5G1	ATP synthase, H+ transporting, mitochondrial F0 complex, subunit C1 (subunit 9)	ATP5A, ATP5G
A09	Hs.524464	NM_001002031	ATP5G2	ATP synthase, H+ transporting, mitochondrial F0 complex, subunit C2 (subunit 9)	-
A10	Hs.429	NM_001689	ATP5G3	ATP synthase, H+ transporting, mitochondrial F0 complex, subunit C3 (subunit 9)	MGC125738, P3
A11	Hs.514465	NM_006356	ATP5H	ATP synthase, H+ transporting, mitochondrial F0 complex, subunit d	ATP5JD, ATPQ
A12	Hs.85539	NM_007100	ATP5I	ATP synthase, H+ transporting, mitochondrial F0 complex, subunit e	ATP5K, MGC12532
B01	Hs.246310	NM_001685	ATP5J	ATP synthase, H+ transporting, mitochondrial F0 complex, subunit F6	ATP5, ATP5A, ATPM, CF6, F6
B02	Hs.521056	NM_004889	ATP5J2	ATP synthase, H+ transporting, mitochondrial F0 complex, subunit F2	ATP5JL
B03	Hs.486360	NM_006476	ATP5L	ATP synthase, H+ transporting, mitochondrial F0 complex, subunit g	ATP5JG
B04	Hs.409140	NM_001697	ATP5O	ATP synthase, H+ transporting, mitochondrial F1 complex, O subunit	ATPO, OSCP
B05	Hs.201939	NM_012463	ATP6V0A2	ATPase, H+ transporting, lysosomal V0 subunit a2	ARCL, ATP6N1D, ATP6a2, J6B7, Stv1, TJ6, TJ6M, TJ6s, Vph1, WSS, a2
B06	Hs.436360	NM_152565	ATP6V0D2	ATPase, H+ transporting, lysosomal 38kDa, V0 subunit d2	ATP6D2, FLJ38708, VMA6
B07	Hs.580464	NM_144583	ATP6V1C2	ATPase, H+ transporting, lysosomal 42kDa, V1 subunit C2	ATP6C2, VMA5
B08	Hs.437691	NM_080653	ATP6V1E2	ATPase, H+ transporting, lysosomal 31kDa, V1 subunit E2	ATP6E1, ATP6EL2, ATP6V1EL2, MGC9341, VMA4
B09	Hs.127743	NM_133262	ATP6V1G3	ATPase, H+ transporting, lysosomal 13kDa, V1 subunit G3	ATP6G3, MGC119810, MGC119813, Vma10
B10	Hs.471401	NM_004328	BCS1L	BCS1-like (yeast)	BCS, BCS1, BJS, FLNMS, GRACILE, Hs.6719, PTD, h-BCS
B11	Hs.433419	NM_001861	COX4I1	Cytochrome c oxidase subunit IV isoform 1	COX4, COXIV, MGC72016
B12	Hs.277101	NM_032609	COX4I2	Cytochrome c oxidase subunit IV isoform 2 (lung)	COX4, COX4-2, COX4B, COX4L2, COXIV-2, dJ857M17.2
C01	Hs.401903	NM_004255	COX5A	Cytochrome c oxidase subunit Va	COX, COX-VA, VA
C02	Hs.1342	NM_001862	COX5B	Cytochrome c oxidase subunit Vb	COXVB
C03	Hs.497118	NM_004373	COX6A1	Cytochrome c oxidase subunit VIa polypeptide 1	COX6A, COX6AL, MGC104500
C04	Hs.250760	NM_005205	COX6A2	Cytochrome c oxidase subunit VIa polypeptide 2	COX6AH, COXVIAH
C05	Hs.431668	NM_001863	COX6B1	Cytochrome c oxidase subunit VIb polypeptide 1 (ubiquitous)	COX6B, COXG
C06	Hs.550544	NM_144613	COX6B2	Cytochrome c oxidase subunit VIb polypeptide 2 (testis)	COXVIB2, CT59, MGC119094

C07	Hs.351875	NM_004374	COX6C	Cytochrome c oxidase subunit VIc	-
C08	Hs.70312	NM_001865	COX7A2	Cytochrome c oxidase subunit VIIa polypeptide 2 (liver)	COX7AL, COX7AL1, COXVIIa-L, MGC118950, MGC118951, MGC118952, MGC126875, MGC126877
C09	Hs.339639	NM_004718	COX7A2L	Cytochrome c oxidase subunit VIIa polypeptide 2 like	COX7AR, COX7RP, EB1, SIG81
C10	Hs.522699	NM_001866	COX7B	Cytochrome c oxidase subunit VIIb	-
C11	Hs.433901	NM_004074	COX8A	Cytochrome c oxidase subunit 8A (ubiquitous)	COX, COX8, COX8-2, COX8L, VIII, VIII-L
C12	Hs.666459	NM_182971	COX8C	Cytochrome c oxidase subunit 8C	COX8-3, MGC119774, MGC119775
D01	Hs.289271	NM_001916	CYC1	Cytochrome c-1	UQCR4
D02	Hs.527748	NM_022126	LHPP	Phospholysine phosphohistidine inorganic pyrophosphate phosphatase	MGC117251, MGC142189, MGC142191
D03	Hs.534168	NM_004541	NDUFA1	NADH dehydrogenase (ubiquinone) 1 alpha subcomplex, 1, 7.5kDa	CI-MWFE, MWFE, ZNF183
D04	Hs.277677	NM_004544	NDUFA10	NADH dehydrogenase (ubiquinone) 1 alpha subcomplex, 10, 42kDa	CI-42KD, MGC5103
D05	Hs.406062	NM_175614	NDUFA11	NADH dehydrogenase (ubiquinone) 1 alpha subcomplex, 11, 14.7kDa	B14.7
D06	Hs.534333	NM_002488	NDUFA2	NADH dehydrogenase (ubiquinone) 1 alpha subcomplex, 2, 8kDa	B8, CD14
D07	Hs.198269	NM_004542	NDUFA3	NADH dehydrogenase (ubiquinone) 1 alpha subcomplex, 3, 9kDa	B9
D08	Hs.50098	NM_002489	NDUFA4	NADH dehydrogenase (ubiquinone) 1 alpha subcomplex, 4, 9kDa	CI-MLRQ, FLJ27440, MGC104422, MGC126843, MGC126845, MLRQ
D09	Hs.651219	NM_005000	NDUFA5	NADH dehydrogenase (ubiquinone) 1 alpha subcomplex, 5, 13kDa	B13, CI-13KD-B, DKFZp781K1356, FLJ12147, NUFM, UQOR13
D10	Hs.274416	NM_002490	NDUFA6	NADH dehydrogenase (ubiquinone) 1 alpha subcomplex, 6, 14kDa	B14, CI-B14, LYRM6, NADHB14
D11	Hs.333427	NM_005001	NDUFA7	NADH dehydrogenase (ubiquinone) 1 alpha subcomplex, 7, 14.5kDa	B14.5a
D12	Hs.495039	NM_014222	NDUFA8	NADH dehydrogenase (ubiquinone) 1 alpha subcomplex, 8, 19kDa	CI-19KD, CI-PGIV, MGC793, PGIV
E01	Hs.189716	NM_005003	NDUFAB1	NADH dehydrogenase (ubiquinone) 1, alpha/beta subcomplex, 1, 8kDa	ACP, FASN2A, MGC65095, SDAP
E02	Hs.513266	NM_004548	NDUFB10	NADH dehydrogenase (ubiquinone) 1 beta subcomplex, 10, 22kDa	PDSW
E03	Hs.655788	NM_004546	NDUFB2	NADH dehydrogenase (ubiquinone) 1 beta subcomplex, 2, 8kDa	AGGG, CI-AGGG, MGC70788
E04	Hs.109760	NM_002491	NDUFB3	NADH dehydrogenase (ubiquinone) 1 beta subcomplex, 3, 12kDa	B12
E05	Hs.304613	NM_004547	NDUFB4	NADH dehydrogenase (ubiquinone) 1 beta subcomplex, 4, 15kDa	B15, CI-B15, MGC5105
E06	Hs.718447	NM_002492	NDUFB5	NADH dehydrogenase (ubiquinone) 1 beta subcomplex, 5, 16kDa	CI-SGDH, DKFZp686N02262, FLJ30597, MGC111204, MGC12314, SGDH
E07	Hs.493668	NM_182739	NDUFB6	NADH dehydrogenase (ubiquinone) 1 beta subcomplex, 6, 17kDa	B17, CI, MGC13675
E08	Hs.532853	NM_004146	NDUFB7	NADH dehydrogenase (ubiquinone) 1 beta subcomplex, 7, 18kDa	B18, CI-B18, MGC2480
E09	Hs.523215	NM_005004	NDUFB8	NADH dehydrogenase (ubiquinone) 1 beta subcomplex, 8, 19kDa	ASHI, CI-ASHI
E10	Hs.15977	NM_005005	NDUFB9	NADH dehydrogenase (ubiquinone) 1 beta subcomplex, 9, 22kDa	B22, DKFZp566O173, FLJ22885, LYRM3, UQOR22

E11	Hs.84549	NM_002494	NDUFC1	NADH dehydrogenase (ubiquinone) 1, subcomplex unknown, 1, 6kDa	KFYI, MGC117464, MGC126847, MGC138266
E12	Hs.407860	NM_004549	NDUFC2	NADH dehydrogenase (ubiquinone) 1, subcomplex unknown, 2, 14.5kDa	B14.5b, NADHDH2
F01	Hs.471207	NM_005006	NDUFS1	NADH dehydrogenase (ubiquinone) Fe-S protein 1, 75kDa (NADH-coenzyme Q reductase)	CI-75Kd, MGC26839, PRO1304
F02	Hs.173611	NM_004550	NDUFS2	NADH dehydrogenase (ubiquinone) Fe-S protein 2, 49kDa (NADH-coenzyme Q reductase)	-
F03	Hs.502528	NM_004551	NDUFS3	NADH dehydrogenase (ubiquinone) Fe-S protein 3, 30kDa (NADH-coenzyme Q reductase)	-
F04	Hs.528222	NM_002495	NDUFS4	NADH dehydrogenase (ubiquinone) Fe-S protein 4, 18kDa (NADH-coenzyme Q reductase)	AQDQ
F05	Hs.632385	NM_004552	NDUFS5	NADH dehydrogenase (ubiquinone) Fe-S protein 5, 15kDa (NADH-coenzyme Q reductase)	-
F06	Hs.408257	NM_004553	NDUFS6	NADH dehydrogenase (ubiquinone) Fe-S protein 6, 13kDa (NADH-coenzyme Q reductase)	-
F07	Hs.211914	NM_024407	NDUFS7	NADH dehydrogenase (ubiquinone) Fe-S protein 7, 20kDa (NADH-coenzyme Q reductase)	CI-20KD, FLJ45860, FLJ46880, MGC120002, MY017, PSST
F08	Hs.90443	NM_002496	NDUFS8	NADH dehydrogenase (ubiquinone) Fe-S protein 8, 23kDa (NADH-coenzyme Q reductase)	TYKY
F09	Hs.7744	NM_007103	NDUFV1	NADH dehydrogenase (ubiquinone) flavoprotein 1, 51kDa	CI-51kD, UQOR1
F10	Hs.464572	NM_021074	NDUFV2	NADH dehydrogenase (ubiquinone) flavoprotein 2, 24kDa	-
F11	Hs.473937	NM_021075	NDUFV3	NADH dehydrogenase (ubiquinone) flavoprotein 3, 10kDa	CI-9KD
F12	Hs.151134	NM_005015	OXA1L	Oxidase (cytochrome c) assembly 1-like	MGC133129

G01	Hs.437403	NM_021129	PPA1	Pyrophosphatase (inorganic) 1	IOPPP, MGC111556, PP, PP1, SID6-8061
G02	Hs.654957	NM_176869	PPA2	Pyrophosphatase (inorganic) 2	FLJ20459, HSPC124, MGC49850, SID6-306
G03	Hs.440475	NM_004168	SDHA	Succinate dehydrogenase complex, subunit A, flavoprotein (Fp)	FP, SDH2, SDHF
G04	Hs.465924	NM_003000	SDHB	Succinate dehydrogenase complex, subunit B, iron sulfur (Ip)	FLJ92337, IP, PGL4, SDH, SDH1, SDHIP
G05	Hs.444472	NM_003001	SDHC	Succinate dehydrogenase complex, subunit C, integral membrane protein, 15kDa	CYB560, CYBL, PGL3, QPS1, SDH3
G06	Hs.356270	NM_003002	SDHD	Succinate dehydrogenase complex, subunit D, integral membrane protein	CBT1, PGL, PGL1, SDH4
G07	Hs.8372	NM_006830	UQCR	Ubiquinol-cytochrome c reductase, 6.4kDa subunit	0710008D09Rik, QCR10
G08	Hs.119251	NM_003365	UQCRC1	Ubiquinol-cytochrome c reductase core protein I	D3S3191, QCR1, UQCR1
G09	Hs.528803	NM_003366	UQCRC2	Ubiquinol-cytochrome c reductase core protein II	QCR2, UQCR2
G10	Hs.170107	NM_006003	UQCRFS1	Ubiquinol-cytochrome c reductase, Rieske iron-sulfur polypeptide 1	RIP1, RIS1, RISP, UQCR5
G11	Hs.481571	NM_006004	UQCRH	Ubiquinol-cytochrome c reductase hinge protein	MGC111572, QCR6
G12	Hs.146602	NM_014402	UQCRQ	Ubiquinol-cytochrome c reductase, complex III subunit VII, 9.5kDa	QCR8, QP-C, QPC
H01	Hs.534255	NM_004048	B2M	Beta-2-microglobulin	-
H02	Hs.412707	NM_000194	HPRT1	Hypoxanthine phosphoribosyltransferase 1	HGPRT, HPRT
H03	Hs.523185	NM_012423	RPL13A	Ribosomal protein L13a	-
H04	Hs.592355	NM_002046	GAPDH	Glyceraldehyde-3-phosphate dehydrogenase	G3PD, GAPD, MGC88685
H05	Hs.520640	NM_001101	ACTB	Actin, beta	PS1TP5BP1
H06	N/A	SA_00105	HGDC	Human Genomic DNA Contamination	HIGX1A
H07	N/A	SA_00104	RTC	Reverse Transcription Control	RTC
H08	N/A	SA_00104	RTC	Reverse Transcription Control	RTC
H09	N/A	SA_00104	RTC	Reverse Transcription Control	RTC
H10	N/A	SA_00103	PPC	Positive PCR Control	PPC
H11	N/A	SA_00103	PPC	Positive PCR Control	PPC
H12	N/A	SA_00103	PPC	Positive PCR Control	PPC

APPENDIX V

Standard curves for real-time qPCR

A. Standard curve: *HPRT1*

$y = -3.4165x + 41.849$
$R^2 = 0.9057$

B. Standard curve: *RPL13A*

$y = -3.2561x + 34.175$
$R^2 = 0.9426$

C. Standard curve: *CYC1*

y = -3.1578x + 40.087
R² = 0.981
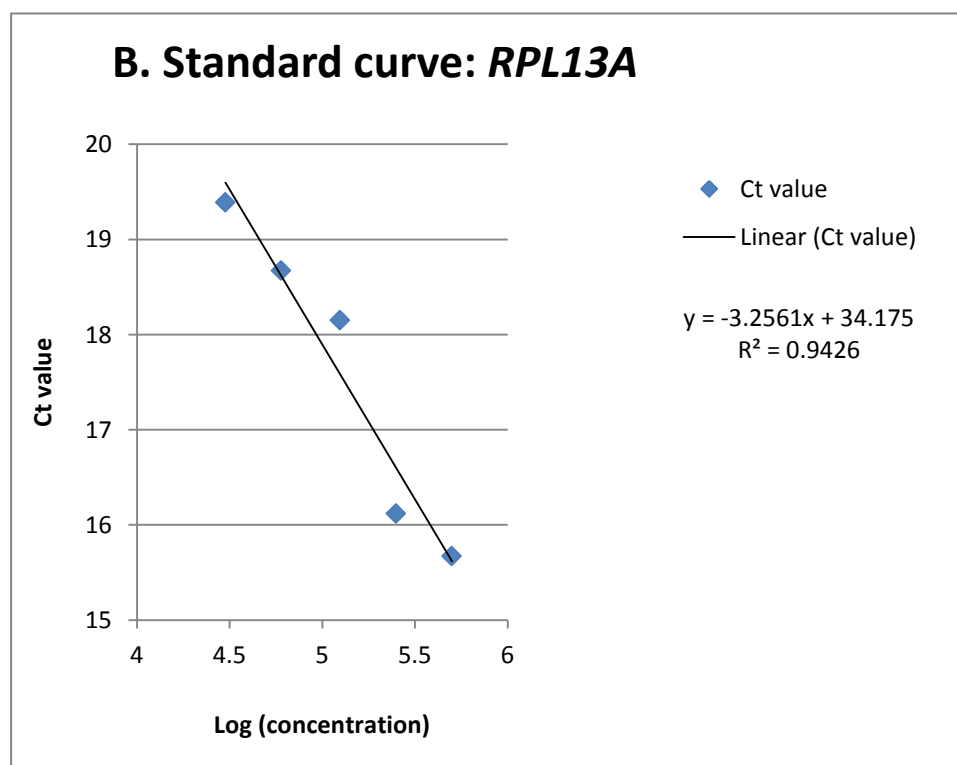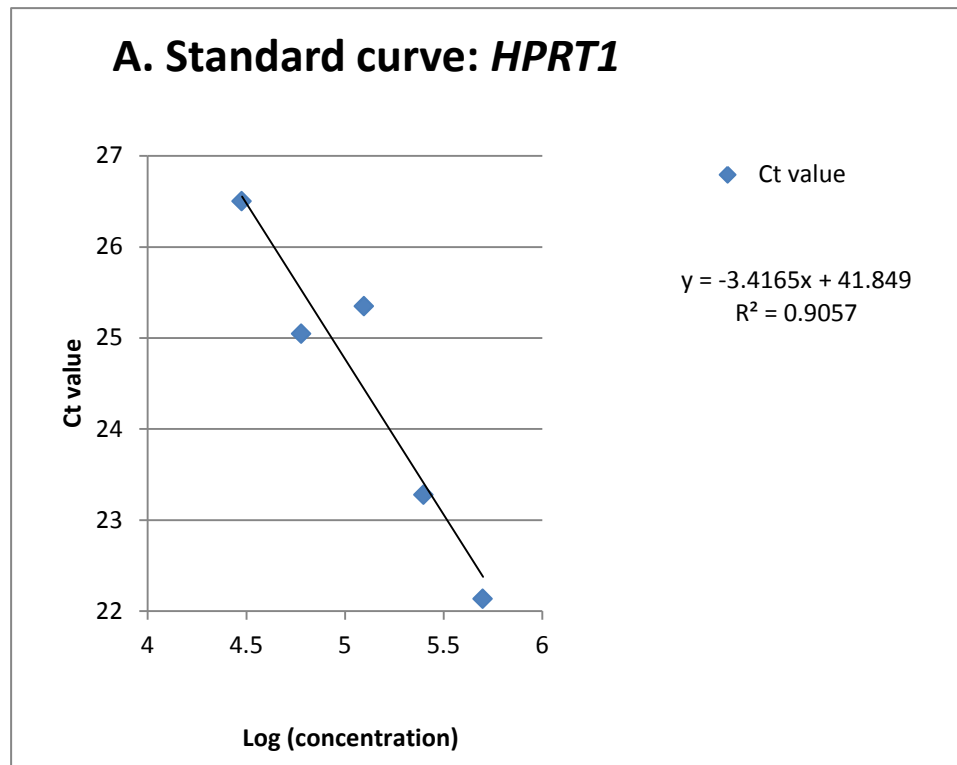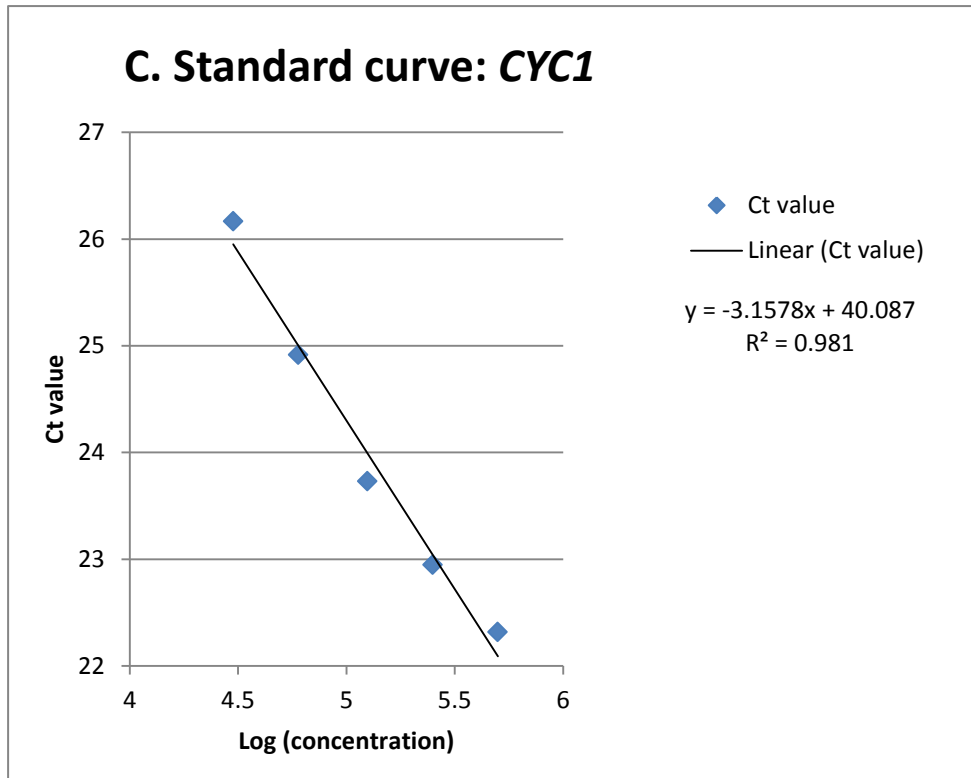
APPENDIX VI

List of conferences where this work has been or will be presented

1. **Van der Merwe C**, Blanckenberg J, Loos B, Henning F, Lombard D, Carr J, Kinnear C, Bardien S. Investigation into the role of mitochondrial dysfunction in Parkinson's disease in patients with mutations in the *parkin* gene. The 55th Annual Academic Year Day, Stellenbosch University. August 2011. Poster presentation

2. **Van der Merwe C**, Blanckenberg J, Loos B, Henning F, Lombard D, Carr J, Kinnear C, Bardien S. Investigation into the role of mitochondrial dysfunction in Parkinson's disease in patients with mutations in the *parkin* gene. Movement Disorder Society 16th International Congress, Dublin, Ireland. 17th-21st June 2012. Poster presentation

3. **Van der Merwe C**, Blanckenberg J, Loos B, Henning F, Lombard D, Carr J, Kinnear C, Bardien S. Investigation into the role of mitochondrial dysfunction in Parkinson's disease in patients with mutations in the *parkin* gene. The 56th Annual Academic Year Day, Stellenbosch University. August 2012. Poster presentation

4. **Van der Merwe C**, Blanckenberg J, Loos B, Henning F, Lombard D, Carr J, Kinnear C, Bardien S. Investigation into the role of mitochondrial dysfunction in Parkinson's disease in patients with mutations in the *parkin* gene. MRC Early Career Scientist Conference, MRC Conference Centre, Cape Town. October 2012. Poster presentation
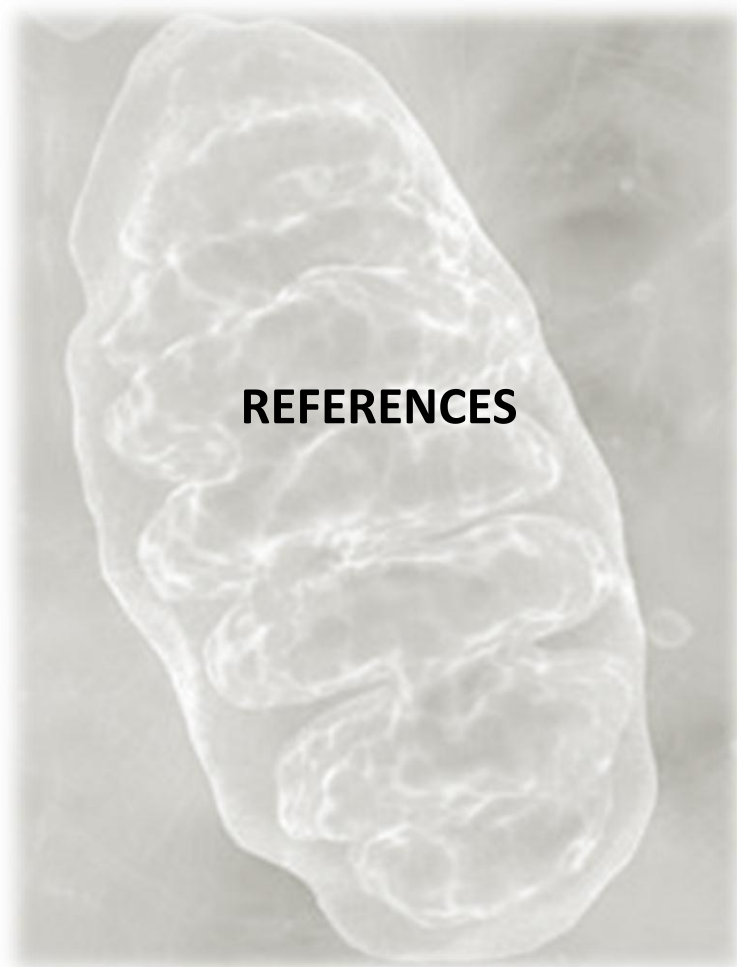
REFERENCES

Electronic references:

dbSNP: http://www.ncbi.nlm.nih.gov/snp

Ensembl: http://www.ensembl.org

Genbank database: http://www.ncbi.nlm.nih.gov/Entrez

REST gene quantification: http://www.gene-quantification.de/rest.html

SABiosciences: http://sabiosciences.com/pcrarraydataanalysis.php

Journal & Book references:

Abeliovich, A. & Flint Beal, M. (2006). Parkinsonism genes: Culprits and clues. *Journal of Neurochemistry,* 99(4): 1062-1072.

Adams, M.D., Celniker, S.E., Holt, R.A., Evans, C.A., Gocayne, J.D., Amanatides, P.G. et al (2000). The genome sequence of drosophila melanogaster. *Science,* 287(5461): 2185-2195.

Adhihetty, P.J., Uguccioni, G., Leick, L., Hidalgo, J., Pilegaard, H. & Hood, D.A. (2009). The role of PGC-1α on mitochondrial function and apoptotic susceptibility in muscle. *American Journal of Physiology-Cell Physiology,* 297(1): C217-C225.

Alam, Z., Jenner, A., Daniel, S.E., Lees, A.J., Cairns, N., Marsden, C.D. et al (1997). Oxidative DNA damage in the parkinsonian brain: An apparent selective increase in 8-Hydroxyguanine levels in substantia nigra. *Journal of Neurochemistry,* 69(3): 1196-1203.

Anesti, V. & Scorrano, L. (2006). The relationship between mitochondrial shape and function and the cytoskeleton. *Biochimica Et Biophysica Acta (BBA)-Bioenergetics,* 1757(5): 692-699.

Arany, Z., He, H., Lin, J., Hoyer, K., Handschin, C., Toka, O. et al (2005). Transcriptional coactivator PGC-1α controls the energy state and contractile function of cardiac muscle. *Cell Metabolism,* 1(4): 259-271.

Auburger, G., Klinkenberg, M., Drost, J., Marcus, K., Morales-Gordo, B., Kunz, W.S. et al (2012). Primary skin fibroblasts as a model of Parkinson's disease. *Molecular Neurobiology,* 1-8.

Autere, J., Moilanen, J.S., Finnila, S., Soininen, H., Mannermaa, A., Hartikainen, P. et al (2004). Mitochondrial DNA polymorphisms as risk factors for Parkinson's disease and Parkinson's disease dementia. *Human Genetics,* 115(1): 29-35.

Bardien, S., Keyser, R., Yako, Y., Lombard, D. & Carr, J. (2009). Molecular analysis of the parkin gene in South African patients diagnosed with Parkinson's disease. *Parkinsonism & Related Disorders,* 15(2): 116-121.

Basso, M., Giraudo, S., Corpillo, D., Bergamasco, B., Lopiano, L. & Fasano, M. (2004). Proteome analysis of human substantia nigra in Parkinson's disease. *Proteomics,* 4(12): 3943-3952.

Beal, M.F. (2003). Mitochondria, oxidative damage, and inflammation in Parkinson's disease. *Annals of the New York Academy of Sciences,* 991(1): 120-131.

Beal, M.F. (1995). Ageing, energy, and oxidative stress in neurodegenerative diseases. *Annals of Neurology*, 38(3): 357-366

Bender, A., Krishnan, K.J., Morris, C.M., Taylor, G.A., Reeve, A.K., Perry, R.H. (2006). High levels of mitochondrial DNA deletions in substantia nigra neurons in aging and Parkinson disease. *Nature Genetics,* 38(5): 515-517.

Berardelli, A., Rothwell, J., Thompson, P.D. & Hallett, M. (2001). Pathophysiology of bradykinesia in Parkinson's disease. *Brain,* 124(11): 2131-2146.

Berkovic, S., Carpenter, S., Evans, A., Karpati, G., Shoubridge, E.A., Anderman, F. et al (1989). Myoclonus epilepsy and ragged-red fibres (MERRF). *Brain,* 112(5): 1231-1260.

Berman, S., Pineda, F. & Hardwick, J. (2008). Mitochondrial fission and fusion dynamics: The long and short of it. *Cell Death & Differentiation,* 15(7): 1147-1152.

Betarbet, R., Sherer, T.B., MacKenzie, G., Garcia-Osuna, M., Panov, A.V. & Greenamyre, J.T. (2000). Chronic systemic pesticide exposure reproduces features of Parkinson's disease. *Nature Neuroscience,* 3(12): 1301-1306.

Bonifati, V., Roche, C.F., Breedveld, G.J., Fabrizio, E., De Mari, M., Tassorelli, C. et al (2005). Early-onset parkinsonism associated with PINK1 mutations. *Neurology,* 65(1): 87-95.

Bower, N.I., Moser, R.J., Hill, J.R. & Lehnert, S.A. (2007). Universal reference method for real-time PCR gene expression analysis of preimplantation embryos. *BioTechniques,* 42(2): 199.

Braak, H., Tredici, K.D., de Vos, R.A.I., Jansen Steur, E.N.H. & Braak, E. (2003). Staging of brain pathology related to sporadic Parkinson's disease. *Neurobiology of Aging,* 24(2): 197-211.

Brunner, F., Schmid, A., Sheikhzadeh, A., Nordin, M., Yoon, J. & Frankel, V. (2007). Effects of aging on type II muscle fibers: A systematic review of the literature. *Journal of Aging and Physical Activity,* 15(3): 336-348.

Burbulla, L.F., Krebiehl, G. & Krüger, R. (2010). Balance is the challenge–The impact of mitochondrial dynamics in Parkinson's disease. *European Journal of Clinical Investigation,* 40(11): 1048-1060.

Burns, R.S., LeWitt, P.A., Ebert, M.H., Pakkenberg, H. & Kopin, I.J. (1985). The clinical syndrome of striatal dopamine deficiency. *New England Journal of Medicine,* 312(22): 1418-1421.

Bustin, S.A. & Nolan, T. (2009). Analysis of mRNA expression by real-time PCR. *Real-Time PCR: Current Technology and Applications,* 111.

Bustin, S., Benes, V., Nolan, T. & Pfaffl, M. (2005). Quantitative real-time RT-PCR–a perspective. *Journal of Molecular Endocrinology,* 34(3): 597-601.

Butterfield, P., Valanis, B., Spencer, P., Lindeman, C. & Nutt, J. (1993). Environmental antecedents of young-onset Parkinson's disease. *Neurology,* 43(6): 1150-1150.

Chan, N.C., Salazar, A.M., Pham, A.H., Sweredoski, M.J., Kolawa, N.J., Graham, R.L.J. et al (2011). Broad activation of the ubiquitin–proteasome system by parkin is critical for mitophagy. *Human Molecular Genetics,* 20(9): 1726-1737.

Chang, C.R. & Blackstone, C. (2010). Dynamic regulation of mitochondrial fission through modification of the dynamin-related protein Drp1. *Annals of the New York Academy of Sciences,* 1201(1): 34-39.

Chartier-Harlin, M.C., Dachsel, J.C., Vilarino-Guell, C., Lincoln, S.J., Lepretre, F., Huilhan, M.M. et al (2011). Translation initiator EIF4G1 mutations in familial Parkinson disease. *The American Journal of Human Genetics,* 89(3): 398-406.

Chaudhuri, K., Healy, D.G. & Schapira, A.H.V. (2006). Non-motor symptoms of Parkinson's disease: Diagnosis and management. *The Lancet Neurology,* 5(3): 235-245.

Checkoway, H., Powers, K., Smith-Weller, T., Franklin, G.M., Longstreth Jr, W. & Swanson, P.D. (2002). Parkinson's disease risks associated with cigarette smoking, alcohol consumption, and caffeine intake. *American Journal of Epidemiology,* 155(8): 732-738.

Chen, H. & Chan, D.C. (2009). Mitochondrial dynamics–fusion, fission, movement, and mitophagy–in neurodegenerative diseases. *Human Molecular Genetics,* 18(R2): R169-R176.

Chien, H.F., Roche, C.F., Costa, M.D.L., Breedveld, G.J., Oostra, B.A., Barbosa, E.R. et al (2006). Early-onset Parkinson's disease caused by a novel parkin mutation in a genetic isolate from north-eastern brazil. *Neurogenetics,* 7(1): 13-19.

Chishti, M.A., Bohlega, S., Ahmed, M., Loualich, A., Carrol, P., Sato, C. et al (2006). T313M PINK1 mutation in an extended highly consanguineous saudi family with early-onset Parkinson disease. *Archives of Neurology,* 63(10): 1483.

Clark, I.E., Dodson, M.W., Jiang, C., Cao, J.H., Huh, J.R., Seol, J.H. et al (2006). Drosophila pink1 is required for mitochondrial function and interacts genetically with parkin. *Nature,* 441(7097): 1162-1166.

Codogno, P. & Meijer, A. (2005). Autophagy and signaling: Their role in cell survival and cell death. *Cell Death & Differentiation,* 121509-1518.

Cookson, M.R. & Bandmann, O. (2010). Parkinson's disease: Insights from pathways. *Human Molecular Genetics,* 19(R1): R21-R27.

Corti, O., Lesage, S. & Brice, A. (2011). What genetics tells us about the causes and mechanisms of Parkinson's disease. *Physiological Reviews,* 91(4): 1161-1218.

Dächsel, J.C., Taylor, J.P., Mok, S.S., Ross, O.A., Hinkle, K.M., Bailey, R.M. et al (2007). Identification of potential protein interactors of Lrrk2. *Parkinsonism & Related Disorders,* 13(7): 382-385.

Dagda, R.K., Cherra, S.J., Kulich, S.M., Tandon, A., Park, D. & Chu, C.T. (2009). Loss of PINK1 function promotes mitophagy through effects on oxidative stress and mitochondrial fission. *Journal of Biological Chemistry,* 284(20): 13843.

Dawson, T.M. & Dawson, V.L. (2003). Molecular pathways of neurodegeneration in Parkinson's disease. *Science's STKE,* 302(5646): 819.

Dawson, T.M. & Dawson, V.L. (2002). Neuroprotective and neurorestorative strategies for Parkinson's disease. *Nature Neuroscience,* 5(supp): 1058-1061.

de Lau, L.M.L. & Breteler, M. (2006). Epidemiology of Parkinson's disease. *The Lancet Neurology,* 5(6): 525-535.

del Hoyo Pilar, G.R.A., de Bustos Fernando, M.J., Sayed Youssef, A.N.H., Caballero Luis, A.J. & Agúndez José, J.J.F. (2012). Oxidative stress in skin fibroblasts cultures from patients with Parkinson's disease. *BMC Neurology,* 10

Deng, H., Dodson, M.W., Huang, H. & Guo, M. (2008). The Parkinson's disease genes pink1 and parkin promote mitochondrial fission and/or inhibit fusion in drosophila. *Proceedings of the National Academy of Sciences,* 105(38): 14503.

Denisov, V., Strong, W., Walder, M., Gingrich, J. & Wintz, H. (2008). Development and validation of RQI: An RNA quality indicator for the experion automated electrophoresis system. *Bio-Rad Bulletin,* 5761

Detmer, S.A. & Chan, D.C. (2007). Functions and dysfunctions of mitochondrial dynamics. *Nature Reviews Molecular Cell Biology,* 8(11): 870-879.

Deuschl, G., Schade-Brittinger, C., Krack, P., Volkmann, J., Schafer, H., Botzel, K. et al (2006). A randomized trial of deep-brain stimulation for Parkinson's disease. *New England Journal of Medicine,* 355(9): 896-908.

Dexter, D., Carter, C.J., Wells, F.R., Javoy-Agid, F., Agid, Y., Lees, A. et al (1989). Basal lipid peroxidation in substantia nigra is increased in Parkinson's disease. *Journal of Neurochemistry,* 52(2): 381-389.

Dheda, K., Huggett, J.F., Bustin, S.A., Johnson, M.A., Rook, G. & Zumla, A. (2004). Validation of housekeeping genes for normalizing RNA expression in real-time PCR. *BioTechniques,* 37112-119.

Domínguez-Garrido, E., Martinez-Redondo, D., Martin-Ruiz, C., Gomez-Duran, A., Ruiz-Pesini, E., Madero, P. et al (2009). Association of mitochondrial haplogroup J and mtDNA oxidative damage in two different north spain elderly populations. *Biogerontology,* 10(4): 435-442.

Dorsey, E., Constantinescu, R., Thompson, J.P., Biglan, K.M., Holloway, R.G., Kieburtz, K. et al (2007). Projected number of people with Parkinson disease in the most populous nations, 2005 through 2030. *Neurology,* 68(5): 384-386.

Exner, N., Treske, B., Paquet, D., Homstrom, K., Schiesling, C., Gispert, S. et al (2007). Loss-of-function of human PINK1 results in mitochondrial pathology and can be rescued by parkin. *The Journal of Neuroscience,* 27(45): 12413-12418.

Fayet, G., Rouche, A., Hogrel, J.Y., Tomé, F.M.S. & Fardeau, M. (2001). Age-related morphological changes of the deltoid muscle from 50 to 79 years of age. *Acta Neuropathologica,* 101(4): 358-366.

Finsterer, J. (2004). Mitochondriopathies. *European Journal of Neurology,* 11(3): 163-186.

Fleige, S. & Pfaffl, M.W. (2006). RNA integrity and the effect on the real-time qRT-PCR performance. *Molecular Aspects of Medicine,* 27(2-3): 126-139.

Follett, K.A., Weaver, F.M., Stern, M., Hur, K., Harris, C.L., Luo, P. et al (2010). Pallidal versus subthalamic deep-brain stimulation for Parkinson's disease. *New England Journal of Medicine,* 362(22): 2077-2091.

Freshney, R.I. (2010). *Culture of animal cells: A manual of basic technique and specialized applications.* Wiley-Blackwell

Gautier, C.A., Kitada, T. & Shen, J. (2008). Loss of PINK1 causes mitochondrial functional defects and increased sensitivity to oxidative stress. *Proceedings of the National Academy of Sciences,* 105(32): 11364.

Gelb, D.J., Oliver, E. & Gilman, S. (1999). Diagnostic criteria for Parkinson disease. *Archives of Neurology,* 56(1): 33.

Gibb, W. & Lees, A. (1988). The relevance of the lewy body to the pathogenesis of idiopathic Parkinson's disease. *Journal of Neurology, Neurosurgery & Psychiatry,* 51(6): 745-752.

Gorell, J., Johnson, C., Rybicki, B., Peterson, E. & Richardson, R. (1998). The risk of Parkinson's disease with exposure to pesticides, farming, well water, and rural living. *Neurology,* 50(5): 1346-1350.

Greene, J.C., Whitworth, A.J., Kuo, I., Andrews, L.A., Feany, M.B. & Pallanck, L.J. (2003). Mitochondrial pathology and apoptotic muscle degeneration in drosophila parkin mutants. *Proceedings of the National Academy of Sciences,* 100(7): 4078.

Grünblatt, E., Mandel, S., Jacob-Hirsch, J., Zeligson, S., Amariglo, N., Rechavi, G. et al (2004). Gene expression profiling of parkinsonian substantia nigra pars compacta; alterations in ubiquitin-proteasome, heat shock protein, iron and oxidative stress regulated proteins, cell adhesion/cellular matrix and vesicle trafficking genes. *Journal of Neural Transmission,* 111(12): 1543-1573.

Grünewald, A., Gegg, M.E., Taanman, J.W., King, R.H., Kock, N., Klein, C. et al (2009). Differential effects of PINK1 nonsense and missense mutations on mitochondrial function and morphology. *Experimental Neurology,* 219(1): 266-273.

Grünewald, A., Gegg, M.E., Taanman, J.W., King, R.H., Kock, N., Klein, C. et al (2010). Mutant parkin impairs mitochondrial function and morphology in human fibroblasts. *PloS One,* 5(9): e12962.

Gulati, A., Forbes, A., Stegie, F., Kelly, L., Clough, C. & Chaudhuri, K. (2004). A clinical observational study of the pattern and occurrence of non-motor symptoms in Parkinson's disease ranging from early to advanced disease. *Mov Disord,* 19(Suppl 9): S406.

Guttmacher, A.E., Collins, F.S., Nussbaum, R.L. & Ellis, C.E. (2003). Alzheimer's disease and Parkinson's disease. *New England Journal of Medicine,* 348(14): 1356-1364.

Hall, T.A. (1999). BioEdit: A User-Friendly Biological Sequence Alignment Editor and Analysis Program for Windows 95/98/NT. Paper presented at Nucleic acids symposium series.

Hanagasi, H.A., Serdaroglu, P., Ozansoy, M., Basak, N., Tasli, H. & Emre, M. (2009). Mitochondrial pathology in muscle of a patient with a novel parkin mutation. *International Journal of Neuroscience,* 119(10): 1572-1583.

Hauser, M.A., li, Y.J., Xu, H., Noureddine, M.A., Shao, Y.S., Gullans, S.R. et al (2005). Expression profiling of substantia nigra in Parkinson disease, progressive supranuclear palsy, and frontotemporal dementia with parkinsonism. *Archives of Neurology,* 62(6): 917.

Haylett, W.L., Keyser, R.J., du Plessis, M.C., van der Merwe, C., Blanckenberg, J., Lombard, D. et al (2011). Mutations in the parkin gene are a minor cause of Parkinson's disease in the south african population. *Parkinsonism & Related Disorders,*

Heath-Engel, H.M. & Shore, G.C. (2006). Mitochondrial membrane dynamics, cristae remodelling and apoptosis. *Biochimica Et Biophysica Acta (BBA)-Molecular Cell Research,* 1763(5): 549-560.

Hedrich, K., Djarmati, A., Schafer, N., Hering, R., Wellenbrook, C., Weiss, P.H. et al (2004). DJ-1 (PARK7) mutations are less frequent than parkin (PARK2) mutations in early-onset Parkinson disease. *Neurology,* 62(3): 389-394.

Hedrich, K., Hagennah, J., Djarmati, A., Hiller, A., Lohnau, T., Lasek, K. et al (2006). Clinical spectrum of homozygous and heterozygous PINK1 mutations in a large german family with Parkinson disease: Role of a single hit? *Archives of Neurology,* 63(6): 833.

Hernán, M.A., Takkouche, B., Caamaño-Isorna, F. & Gestal-Otero, J.J. (2002). A meta-analysis of coffee drinking, cigarette smoking, and the risk of Parkinson's disease. *Annals of Neurology,* 52(3): 276-284.

Hoepken, H.H., Gispert, S., Azizov, M., Klinkenberg, M., Ricciardi, F., Kurz, A. et al (2007). Mitochondrial dysfunction, peroxidation damage and changes in glutathione metabolism in PARK6. *Neurobiology of Disease,* 25(2): 401-411.

Hu, Q., Noll, R.J., Li, H., Makarov, A., Hardman, M. & Graham Cooks, R. (2005). The orbitrap: A new mass spectrometer. *Journal of Mass Spectrometry,* 40(4): 430-443.

Jakobsson, F., Borg, K. & Edström, L. (1990). Fibre-type composition, structure and cytoskeletal protein location of fibres in anterior tibial muscle. *Acta Neuropathologica,* 80(5): 459-468.

Jenner, P. (2003). The contribution of the MPTP-treated primate model to the development of new treatment strategies for Parkinson's disease. *Parkinsonism & Related Disorders,* 9(3): 131-137.

Kahle, P.J. & Haass, C. (2004). How does parkin ligate ubiquitin to Parkinson's disease? *EMBO Reports,* 5(7): 681-685.

Keyser, R.J., Lombard, D., Veikondis, R., Carr, J. & Bardien, S. (2010). Analysis of exon dosage using MLPA in south african Parkinson's disease patients. *Neurogenetics,* 11(3): 305-312.

Kim, I., Rodriguez-Enriquez, S. & Lemasters, J.J. (2007). Selective degradation of mitochondria by mitophagy. *Archives of Biochemistry and Biophysics,* 462(2): 245-253.

Kösel, S., Grasbon-Frodl, E.M., Hagenah, J.M., Graeber, M.B. & Vieregge, P. (2000). Parkinson disease: Analysis of mitochondrial DNA in monozygotic twins. *Neurogenetics,* 2(4): 227-230.

Kregel, K.C. & Zhang, H.J. (2007). An integrated view of oxidative stress in aging: Basic mechanisms, functional effects, and pathological considerations. *American Journal of Physiology-Regulatory, Integrative and Comparative Physiology,* 292(1): R18-R36.

Kubista, M., Andrade, J.M., Bengtsson, M., Forootan, A., Jonak, J., Lind, K. et al (2006). The real-time polymerase chain reaction. *Molecular Aspects of Medicine,* 27(2-3): 95-125.

Küttner, V., Biniossek, M.L., Gretzmeier, C., Boerries, M., Mack, C., Has, C. et al (2010). Comparative quantitation of proteome alterations induced by aging or immortalization in primary human fibroblasts and keratinocytes for clinical applications. *Molecular BioSystems,* 6(9): 1579-1582.

Langston, J.W. (1985). The case of the tainted heroin. *Science,* 2534-40.

Legros, F., Lombès, A., Frachon, P. & Rojo, M. (2002). Mitochondrial fusion in human cells is efficient, requires the inner membrane potential, and is mediated by mitofusins. *Molecular Biology of the Cell,* 13(12): 4343-4354.

Lemasters, J.J., Nieminen, A.L., Qian, T., Trost, L.C., Elmore, S.P., Nishimura, Y. et al (1998). The mitochondrial permeability transition in cell death: A common mechanism in necrosis, apoptosis and autophagy. *Biochimica Et Biophysica Acta,* 1366(1-2): 177.

Lesage, S. & Brice, A. (2009). Parkinson's disease: From monogenic forms to genetic susceptibility factors. *Human Molecular Genetics,* 18(R1): R48-R59.

Lesage, S., Durr, A., Tazir, M., Lohmann, E., Leutenegger, A.L., Janin, S. et al (2006). LRRK2 G2019S as a cause of Parkinson's disease in north african arabs. *New England Journal of Medicine,* 354(4): 422-423.

Lesage, S., Ibanez, P., Lohmann, E., Pollak, P.M., Tison, F., Tazir, M. et al (2005). G2019S LRRK2 mutation in french and north african families with Parkinson's disease. *Annals of Neurology,* 58(5): 784-787.

Liang, H. & Ward, W.F. (2006). PGC-1α: A key regulator of energy metabolism. *Advances in Physiology Education,* 30(4): 145-151.

Lin, J., Wu, P.H., Tarr, P.T., Lindenberg, K.S., St-Pierre, J., Zhang, C. et al (2004). Defects in adaptive energy metabolism with CNS-linked hyperactivity in PGC-1α null mice. *Cell,* 119(1): 121-135.

Lin, M.T. & Beal, M.F. (2006). Mitochondrial dysfunction and oxidative stress in neurodegenerative diseases. *Nature,* 443(7113): 787-795.

Lin, X., Parisiadou, L., Gu, X.L., Wang, L., Shim, H., Sun, L. et al (2009). Leucine-rich repeat kinase 2 regulates the progression of neuropathology induced by Parkinson's-disease-related mutant [alpha]-synuclein. *Neuron,* 64(6): 807-827.

Lipman, N.S., Jackson, L.R., Trudel, L.J. & Weis-Garcia, F. (2005). Monoclonal versus polyclonal antibodies: Distinguishing characteristics, applications, and information resources. *ILAR JOURNAL,* 46(3): 258.

Livak, K.J. & Schmittgen, T.D. (2001). Analysis of relative gene expression data using real-time quantitative PCR and the 2-[delta][delta] CT method. *Methods,* 25(4): 402-408.

Lozano, A.M. (2012). Deep brain stimulation therapy. *BMJ,* 344

Lucking, C., Durr, A., Bonifati, V., Vaughan, J., De Michele, G., Gasser, T. et al (2000). Association between early-onset Parkinson's disease and mutations in the parkin gene. *New England Journal of Medicine,* 342(21): 1560-1567.

Mandel, S., Grunblatt, E., Riederer, P., Amariglio, N., Hirsch, J.J., Rechavi, G. et al (2005). Gene expression profiling of sporadic Parkinson's disease substantia nigra pars compacta reveals impairment of Ubiquitin-Proteasome subunits, SKP1A, aldehyde dehydrogenase, and chaperone HSC-70. *Annals of the New York Academy of Sciences,* 1053(1): 356-375.

Mattson, M.P., Gleichmann, M. & Cheng, A. (2008). Mitochondria in neuroplasticity and neurological disorders. *Neuron,* 60(5): 748-766.

McBride, H.M., Neuspiel, M. & Wasiak, S. (2006). Mitochondria: More than just a powerhouse. *Current Biology,* 16(14): R551-R560.

McCormack, A.L., Thiruchelvam, M., Manning-Bog, A.B., Thiffault, C., Langston, J.W., Cory-Slechta, D.A. et al (2002). Environmental risk factors and Parkinson's disease: Selective degeneration of nigral dopaminergic neurons caused by the herbicide paraquat. *Neurobiology of Disease,* 10(2): 119-127.

McGill, J.K. & Beal, M.F. (2006). PGC-1α, a new therapeutic target in huntington's disease? *Cell,* 127(3): 465-468.

Moran, L., Duke, D., Deprez, M., Dexter, D., Pearce, R.K.B. & Graeber, M. (2006). Whole genome expression profiling of the medial and lateral substantia nigra in Parkinson's disease. *Neurogenetics,* 7(1): 1-11.

Mortiboys, H., Thomas, K.J., Koopman, W.J.H., Klaffke, S., Abou-Sleiman, P., Oplin, S. et al (2008). Mitochondrial function and morphology are impaired in parkin-mutant fibroblasts. *Annals of Neurology,* 64(5): 555-565.

Müftüoglu, M., Elibol, B., Dalmizrak, O., Ercan, A., Kulaksiz, G.M., Ogus, H. et al (2004). Mitochondrial complex I and IV activities in leukocytes from patients with parkin mutations. *Movement Disorders,* 19(5): 544-548.

Narendra, D., Tanaka, A., Suen, D.F. & Youle, R.J. (2008). Parkin is recruited selectively to impaired mitochondria and promotes their autophagy. *Science's STKE,* 183(5): 795.

Narendra, D.P., Jin, S.M., Tanaka, A., Suen, D.F., Gautier, C.A., Shen, J. et al (2010). PINK1 is selectively stabilized on impaired mitochondria to activate parkin. *PLoS Biology,* 8(1): e1000298.

Nie, L., Wu, G., Culley, D.E., Scholten, J.C.M., Zhang, W. (2007). Integrative analysis of transcriptomic and proteomic data: challenges, solutions and applications. Critical Reviews in Biotechnology, 27(2): 63-75.

Ossowska, K., Wardas, L., Smialowska, M., Kuter, K., Lenda, T., Wieronska, J.M. et al (2005). A slowly developing dysfunction of dopaminergic nigrostriatal neurons induced by long-term paraquat administration in rats: An animal model of preclinical stages of Parkinson's disease? *European Journal of Neuroscience,* 22(6): 1294-1304.

Ozelius, L.J., Senthill, G., Saunders-Pullma, R., Ohmann, E., Deligtisch, A., Tagliati, M. et al (2006). LRRK2 G2019S as a cause of Parkinson's disease in ashkenazi jews. *New England Journal of Medicine,* 354(4): 424-425.

Pacelli, C., De Rasmo, D., Signorile, A., Grattagliano, I., Di Tullio, G., D'Orazio, A. et al (2011). Mitochondrial defect and PGC-1 [alpha] dysfunction in parkin-associated familial Parkinson's disease. *Biochimica Et Biophysica Acta (BBA)-Molecular Basis of Disease,* doi: 10.1016/j.bbadis.2010.12.022

Paisán-Ruíz, C., Nath, P., Washecka, N., Gibbs, J.R. & Singleton, A.B. 2(008). Comprehensive analysis of LRRK2 in publicly available Parkinson's disease cases and neurologically normal controls. *Human Mutation,* 29(4): 485-490.

Palacino, J.J., Sagi, D., Goldberg, M.S., Krauss, S., Motz, C., Wacker, M. et al (2004). Mitochondrial dysfunction and oxidative damage in parkin-deficient mice. *Journal of Biological Chemistry,* 279(18): 18614.

Palmfeldt, J., Vang, S., Stenbroen, V., Pedersen, C.B., Christensen, J.H., Bross, P. (2009). Mitochondrial proteomics on human fibroblasts for identification of metabolic imbalance and cellular stress. *Proteome Sci,* 720.

Papkovskaia, T.D., Chau, K.Y., Inesta-Vaguera, F., Papkovsky, D.B., Healy, D.G., Nishio, K. et al (2012). G2019S leucine rich repeat kinase 2 causes uncoupling protein mediated mitochondrial depolarisation. *Human Molecular Genetics,* doi: 10.1093/hmg/dds244

Park, J., Lee, S.B., Lee, S., Kim, Y., Song, S., Kim, S. et al (2006). Mitochondrial dysfunction in drosophila PINK1 mutants is complemented by parkin. *Nature,* 441(7097): 1157-1161.

Parkinson, J. (1817). *An essay on the shaking palsy.* Printed by Whittingham and Rowland for Sherwood, Neely, and Jones

Perfettini, J.L., Roumier, T. & Kroemer, G. (2005). Mitochondrial fusion and fission in the control of apoptosis. *Trends in Cell Biology,* 15(4): 179-183.

Pesah, Y., Pham, T., Burgess, H., Middlebrooks, B., Verstreken, P., Zhou, Y et al (2004). Drosophila parkin mutants have decreased mass and cell size and increased sensitivity to oxygen radical stress. *Development,* 131(9): 2183-2194.

Petit, A., Kawarai, T., Paitel, E., Sanjo, N., Maj, M., Scheid, M. et al (2005). Wild-type PINK1 prevents basal and induced neuronal apoptosis, a protective effect abrogated by Parkinson disease-related mutations. *Journal of Biological Chemistry,* 280(40): 34025.

Piccoli, C., Sardanelli, A., Scrima, R., Ripoli, M., Quarato, G., D'Aprile, A. et al (2008). Mitochondrial respiratory dysfunction in familiar parkinsonism associated with PINK1 mutation. *Neurochemical Research,* 33(12): 2565-2574.

Poggi, P., Marchetti, C. & Scelsi, R. (1987). Automatic morphometric analysis of skeletal muscle fibers in the aging man. *The Anatomical Record,* 217(1): 30-34.

Polymeropoulos, M.H., Higgins, J.J., Golbe, l.I., Johnson, W.G., Ide, S.E., Iorio, G.D. et al (1996). Mapping of a gene for Parkinson's disease to chromosome 4q21-q23. *Science,* 274(5290): 1197.

Polymeropoulos, M.H., Lavedan, C., Leroy, E., Ide, S.E., Dehejia, A., Dutra, A. et al (1997). Mutation in the α-synuclein gene identified in families with Parkinson's disease. *Science,* 276(5321): 2045.

Poole, A.C., Thomas, R.E., Andrews, L.A., McBride, H.M., Whitworth, A.J. & Pallanck, L.J. (2008). The PINK1/Parkin pathway regulates mitochondrial morphology. *Proceedings of the National Academy of Sciences,* 105(5): 1638.

Prigione, A. & Adjaye, J. (2010). Modulation of mitochondrial biogenesis and bioenergetic metabolism upon in vitro and in vivo differentiation of human ES and iPS cells. *International Journal of Developmental Biology,* 54(11): 1729.

Priyadarshi, A., Khuder, S.A., Schaub, E.A. & Priyadarshi, S.S. (2001). Environmental risk factors and Parkinson's disease: A metaanalysis. *Environmental Research,* 86(2): 122-127.

Przedborski, S., Tieu, K., Perier, C. & Vila, M. (2004). MPTP as a mitochondrial neurotoxic model of Parkinson's disease. *Journal of Bioenergetics and Biomembranes,* 36(4): 375-379.

Ramirez, A., Heimbach, A., Grundemann, J., Stiller, B., Hampshire, D., Cid, L.P. et al (2006). Hereditary parkinsonism with dementia is caused by mutations in ATP13A2, encoding a lysosomal type 5 P-type ATPase. *Nature Genetics,* 38(10): 1184-1191.

Rascol, O., Brooks, D.J., Korczyn, A.D., De Deyn, P.P., Clarke, C.E. & Lang, A.E. (2000). A five-year study of the incidence of dyskinesia in patients with early Parkinson's disease who were treated with ropinirole or levodopa. *New England Journal of Medicine,* 342(20): 1484-1491.

Ross, O.A., Braithwaite, A.T., Skipper, L.M., Kachergus, J., Hulihan, M.M., Middleton, F.A. et al (2008). Genomic investigation of α-synuclein multiplication and parkinsonism. *Annals of Neurology,* 63(6): 743-750.

Ross, O.A., McCormack, R., Maxwell, L.D., Duguid, R.A., Quinn, D.J., Barnett, Y.A. et al (2003). mt4216C variant in linkage with the mtDNA TJ cluster may confer a susceptibility to mitochondrial dysfunction resulting in an increased risk of Parkinson's disease in the irish. *Experimental Gerontology,* 38(4): 397-405.

Rozen, S. & Skaletsky, H. (2000). Primer3 on the WWW for general users and for biologist programmers. *Methods Mol Biol,* 132(3): 365-386.

Russ, H., Mihatsch, W., Gerlach, M., Riederer, P. & Przuntek, H. (1991). Neurochemical and behavioural features induced by chronic low dose treatment with 1-methyl-4-phenyl-1, 2, 3, 6-tetrahydropyridine (MPTP) in the common marmoset: Implications for Parkinson's disease? *Neuroscience Letters,* 123(1): 115-118.

Sanchez-Ramos, J., Overvik, E. & Ames, B. (1994). A marker of oxyradical-mediated DNA damage (8-hydroxy-2'-deoxyguanosine) is increased in nigro-striatum of Parkinson's disease brain. *Neurodegeneration,* 3(3): 197-204.

Santel, A. & Frank, S. (2008). Shaping mitochondria: The complex posttranslational regulation of the mitochondrial fission protein DRP1. *IUBMB Life,* 60(7): 448-455.

Scarpulla, R.C. (2002). Transcriptional activators and coactivators in the nuclear control of mitochondrial function in mammalian cells. *Gene,* 286(1): 81-89.

Scherzer, C.R., Eklund, A.C., Morse, L.J., Liao, Z., Locascio, J.J., Fefer, D. et al (2007.) Molecular markers of early Parkinson's disease based on gene expression in blood. *Proceedings of the National Academy of Sciences,* 104(3): 955.

Seidler, A., Hellenbrand, W., Robra, B.P., Vieragge, P., Nischan, P., Joerg, J et al (1996). Possible environmental, occupational, and other etiologic factors for Parkinson's disease. *Neurology,* 46(5): 1275-1275.

Sherer, T.B., Betarbet, R. & Greenamyre, J.T. (2002). Environment, mitochondria, and Parkinson's disease. *The Neuroscientist,* 8(3): 192-197.

Sherwood, L. (2012). *Human physiology: From cells to systems.* Brooks/Cole Pub Co

Shimura, H., Hattori, N., Kubo. S.I., Yoshikawa, M., Kitada, T., Matsumine, H. et al (1999). Immunohistochemical and subcellular localization of parkin protein: Absence of protein in autosomal recessive juvenile parkinsonism patients. *Annals of Neurology,* 45(5): 668-672.

Shoffner, J.M., Brown, M.D., Torroni, A., Lott, M.T., Cabell, M.F., Mirra, S.S. et al (1993). Mitochondrial DNA variants observed in alzheimer disease and Parkinson disease patients. *Genomics,* 17(1): 171.

Silvestri, L., Caputo, V., Bellacchio, E., Atorino, L., Dallapiccola, B., Valente, E.M. et al (2005). Mitochondrial import and enzymatic activity of PINK1 mutants associated to recessive parkinsonism. *Human Molecular Genetics,* 14(22): 3477-3492.

Simunovic, F., Yi, M., Wang, Y., Macey, L., Brown, L.T., Krichevsky, A.M. et al (2009). Gene expression profiling of substantia nigra dopamine neurons: Further insights into Parkinson's disease pathology. *Brain,* 132(7): 1795-1809.

Spillantini, M.G., Schmidt, M.L., Lee, V.M.Y., Trojanowski, J.Q., Jakes, R. & Goedert, M. (1997). α-Synuclein in lewy bodies. *Nature,* 388(6645): 839-840.

St-Pierre, J., Drori, S., Uldry, M., Silvaggi, J.M., Rhee, J., Jager, S. et al (2006). Suppression of reactive oxygen species and neurodegeneration by the PGC-1 transcriptional coactivators. *Cell,* 127(2): 397-408.

Sundal, C., Fujioka, S., Uitti, R.J. & Wszolek, Z.K. (2012). Autosomal dominant Parkinson's disease. *Parkinsonism & Related Disorders,* 18S7-S10.

Tan, P.K., Downey, T.J., Spitznagel Jr, E.L., Xu, P., Fu, D., Dimitrov, D.S. et al (2003). Evaluation of gene expression measurements from commercial microarray platforms. *Nucleic Acids Research,* 31(19): 5676-5684.

Taylor, C., Saint-Hilaire, M.H., Cupples, L.A., Thomas, C.A., Burchard, A.E., Feldman, R.G. et al (1999). Environmental, medical, and family history risk factors for Parkinson's disease: A new England-based case control study. *American Journal of Medical Genetics,* 88(6): 742-749.

Taylor, R.W. & Turnbull, D.M. (2005). Mitochondrial DNA mutations in human disease. *Nature Reviews Genetics,* 6(5): 389-402.

Taylor, S., Wakem, M., Dijkman, G., Alsarraj, M. & Nguyen, M. (2010). A practical approach to RT-qPCR-- publishing data that conform to the MIQE guidelines. *Methods,* 50(4): S1-S5.

Tipton, K.F. & Singer, T.P. (1993). Advances in our understanding of the mechanisms of the neurotoxicity of MPTP and related compounds. *Journal of Neurochemistry,* 61(4): 1191-1206.

Tucci, A., Charlesworth, G., Sheerin, U.M., Plagnol, V., Wood, N. & Hardy, J. (2012). Study of the genetic variability in a Parkinson's disease gene: EIF4G1. *Neuroscience Letters,*

Twelves, D., Perkins, K.S.M. & Counsell, C. (2003). Systematic review of incidence studies of Parkinson's disease. *Movement Disorders,* 18(1): 19-31.

Uversky, V.N. (2004). Neurotoxicant-induced animal models of Parkinson's disease: Understanding the role of rotenone, maneb and paraquat in neurodegeneration. *Cell and Tissue Research,* 318(1): 225-241.

Van Den Eeden, S.K., Tanner, C.M., Bernstein, A.L., Fross, R.D., Leimpeter, A., Bloch, D.A. et al (2003). Incidence of Parkinson's disease: Variation by age, gender, and race/ethnicity. *American Journal of Epidemiology,* 157(11): 1015-1022.

Van der Walt, J.M., Nicodemus, K.K., Martin, E.R., Scott, W.K., Nance, M.A., Watts, R.L. et al (2003). Mitochondrial polymorphisms significantly reduce the risk of Parkinson disease. *American Journal of Human Genetics,* 72(4): 804.

Vilariño-Güell, C., Wider, C., Ross, O.A., Dachsel, J.C., Kachergus, J.M., Lincoln. S.J. et al (2011). VPS35 mutations in Parkinson disease. *The American Journal of Human Genetics,* 89(1): 162-167.

Vives-Bauza, C., Andreu, A.L., Manfredi, G., Beal, M.F., Janetzky, B., Grunewald, T.H. et al (2002). Sequence analysis of the entire mitochondrial genome in Parkinson's disease. *Biochemical and Biophysical Research Communications,* 290(5): 1593-1601.

Wang, X., Yan, M.H., Fujioka, H., Liu, J., Wilson-Delfosse, A., Chen, S.G. et al (2012). LRRK2 regulates mitochondrial dynamics and function through direct interaction with DLP1. *Human Molecular Genetics,*

Werner, C.J., Heyny-von Haussen, R., Mall, G. & Wolf, S. (2008). Proteome analysis of human substantia nigra in Parkinson's disease. *Proteome Sci,* 6(8):

West, A., Periquet, M., Lincoln, S., Lucking, C.B., Nicholl, D., Bonifati, V. et al (2002). Complex relationship between parkin mutations and Parkinson disease. *American Journal of Medical Genetics,* 114(5): 584-591.

Whetten-Goldstein, K., Sloan, F., Kulas, E. & Cutson, T. (1997). The burden of Parkinson's disease on society, family, and the individual. *Journal of the American Geriatrics Society; Journal of the American Geriatrics Society,*

Whitney, A.R., Diehn, M., Popper, S.J., Alizadeh, A.A., Boldrick, J.C., Relman, D.A. et al (2003). Individuality and variation in gene expression patterns in human blood. *Proceedings of the National Academy of Sciences,* 100(4): 1896.

Wiedemann, F.R., Winkler, K., Lins, H., WALLESCH, C.W. & Kunz, W.S. (1999). Detection of respiratory chain defects in cultivated skin fibroblasts and skeletal muscle of patients with Parkinson's disease. *Annals of the New York Academy of Sciences,* 893(1): 426-429.

Winkler-Stuck, K., Wiedemann, F.R., Wallesch, C.W. & Kunz, W.S. (2004). Effect of coenzyme Q on the mitochondrial function of skin fibroblasts from Parkinson patients. *Journal of the Neurological Sciences,* 220(1): 41-48.

Wooten, G. (1997). Neurochemistry and neuropharmacology of Parkinson's disease. *Movement Disorders: Neurologic Principles and Practice.New York: McGraw-Hill,* 153-160.

Yakes, F.M. & Van Houten, B. (1997). Mitochondrial DNA damage is more extensive and persists longer than nuclear DNA damage in human cells following oxidative stress. *Proceedings of the National Academy of Sciences,* 94(2): 514.

Yang, Y., Gehrke, S., Imai, Y., Huang, Z., Ouyang, Y., Wang, J.W. et al (2006). Mitochondrial pathology and muscle and dopaminergic neuron degeneration caused by inactivation of drosophila Pink1 is rescued by parkin. *Proceedings of the National Academy of Sciences,* 103(28): 10793-10798.

Ye, Y. & Rape, M. (2009). Building ubiquitin chains: E2 enzymes at work. *Nature Reviews Molecular Cell Biology,* 10(11): 755-764.

Zarranz, J.J., Alegre, J., Gomez-Esteban, J.C., Lexcano, E., Ros, R., Ampeuro, I. et al (2004). The new mutation, E46K, of α-synuclein causes parkinson and lewy body dementia. *Annals of Neurology,* 55(2): 164-173.

Zhang, Y., James, M., Middleton, F.A. & Davis, R.L. (2005). Transcriptional analysis of multiple brain regions in Parkinson's disease supports the involvement of specific protein processing, energy metabolism, and signaling pathways, and suggests novel disease mechanisms. *American Journal of Medical Genetics Part B: Neuropsychiatric Genetics,* 137(1): 5-16.

Zheng, B., Liao, Z., Locascio, J.J., Lesniak, K.A., Roderick, S.S., Watt, M.L. et al (2010). PGC-1α, a potential therapeutic target for early intervention in Parkinson's disease. *Science Translational Medicine,* 2(52): 52ra73.

Zimprich, A., Benet-Pagcs, A., Struhal, W., Graf, E., Eck, S.H., Offman, M.N. et al (2011). A mutation in VPS35, encoding a subunit of the retromer complex, causes late-onset Parkinson disease. *The American Journal of Human Genetics,* 89(1): 168-175.

Ziviani, E., Tao, R.N. & Whitworth, A.J. (2010). Drosophila parkin requires PINK1 for mitochondrial translocation and ubiquitinates mitofusin. *Proceedings of the National Academy of Sciences,* 107(11): 5018.